CISM International Centre for Mechanical Sciences 562
Courses and Lectures

Davide Bigoni *Editor*

Extremely Deformable Structures

Engineering
ISSN 0254-1971
ISBN 978-3-7091-1876-4

▶ springer.com

International Centre
for Mechanical Sciences

CISM 562 Bigoni *Ed.*
Extremely Deformable Structures

CISM International Centre for Mechanical Sciences 562
Courses and Lectures

Davide Bigoni
Editor

Extremely Deformable Structures

International Centre
for Mechanical Sciences

Springer

PREFACE

Structures have traditionally been designed to work below their critical load, because any instability was normally identified as connected to failure or loss of functionality. Instability and bifurcation were viewed simply as potentially dangerous phenomena and hence structural deformations under load were required to be small. Recently, a variety of soft structures have been considered in mechanics. These are structures that work in a large deformation regime, where elastic elements are subject to extreme deformations and loads well beyond the critical values for buckling. Examples of structures that exhibit excellent mechanical performance even under severe deformation conditions are found in biological systems, deployable space structures, and a variety of devices in everyday use.

The lesson from nature is that the possibility of exploiting highly deformable structures, made for instance of rubber or gel, may open new and unexpected technological possibilities.

The exploration of these possibilities is the focus of this volume and of the so-called Extreme Mechanics, an emerging branch of the instability of solids and structures. This branch is aimed at the investigation of instabilities as related to pattern formation and the subsequent nonlinear behaviour of large deformations.

Here the challenge is the design of deformable and bi-stable mechanisms, which can give superior mechanical performance and which will have an impact on many high tech applications such as stretchable electronics, nanotube serpentines, deployable structures for aerospace engineering, cable deployment in the ocean, as well as on sensors and flexible actuators and vibration absorbers.

This monograph is the collection of the Lecture Notes for the Advanced School 'Extremely Deformable Structures' held at the International Centre for Mechanical Sciences (CISM) in Udine, Italy, June 2-6 2014. The course was given by six lecturers and attended by nearly fifty participants from eight European and four extra European countries. The chapters are devoted to an introduction to the methods used in the study of the stability of elastic structures in the finite dimensional case (A. Lazarus, C. Maurini and S. Neukirch), in the infinite dimensional case for the Euler elastica (D. Bigoni, F. Bosi, D. Misseroni, F. Dal Corso, and G. Noselli), and to the advanced problem

of the dynamics of a naturally curved elastica (B. Audoly, A. Callan-Jones, and P.-T. Brun). Two-dimensional problems are introduced with the purpose of analyzing the mechanics of two-dimensional periodic and highly deformable cellular structures (K. Bertoldi) and of the folding and deployment of thin-shells (S. Pellegrino). Structural concepts are linked to the modelling of growth processes occurring in biology (A. Erlich, Th. Lessinnes, D. E. Moulton, and A. Goriely). It is believed that the volume can represent a valid introduction to the field of extreme mechanics.

I wish to thank the Rectors of the CISM Professors E. Guazzelli, F. Pfeiffer, and F.G. Rammerstorfer, the Secretary General Professor B.A. Schrefler and all the staff for the warm hospitality and kind assistance during the course. Finally, I would like to gratefully acknowledge support from the FP7-PEOPLE-IDEAS-ERC-2013-ADG-340561-INSTABILITIES.

Davide Bigoni

CONTENTS

In *CISM Lecture Notes No. 562*
"Extremely Deformable Structures" D. Bigoni
Ed. Springer, Wien–New York, 2015
ISBN 978-3-7091-1876-4 doi 10.1007/978-3-7091-1877-1

New phenomena in nonlinear elastic structures: from tensile buckling to configurational forces

D. Bigoni*, F. Bosi*, D. Misseroni*, F. Dal Corso* and G. Noselli†
* DICAM, University of Trento, Trento, IT
† SISSA-International School for Advanced Studies, Trieste, IT

Abstract The theory of the planar elastica is presented in detail and is used to illustrate problems of buckling of a slender structure under tensile dead loading, of buckling as related to constraint's curvature, and of configurational forces. These problems are important tools in the design of compliant mechanisms, in the emergent field of soft robotics and for the understanding of snake and fish locomotion.

1 Introduction

The problem of the planar elastica has a long history, leading back to Jacob Bernoulli (1654-1705), Daniel Bernoulli (1700-1782), Leonhard Euler (1707-1783), and Pieter van Musschenbroek (1692-1761), but is still relevant and rich with applications at times quite unexpected ones. The elastica has attracted a great interest in the past and has involved contributions from first-class scientists, including Kirchhoff, Love, and Born. Research on the elastica marked the initiation of the calculus of variations and promoted the development of the theory of elliptic functions. Nowadays the elastica represents a useful introduction to the theory of nonlinear bifurcation and stability, but is also an important tool in the field of soft robotics and in the design of compliant mechanisms. Moreover, the elastica can be effectively used to explain snake or fish locomotion and to design snake-like robots.

The theory of the Euler elastica is addressed in detail in Section 2 and includes an analysis of the instability of equilibrium configurations. The elastica theory is applied to the problem of tensile buckling, in which an elastic rod bifurcates under tensile dead loading, due to the presence of an internal slider constraint, see Section 3. This problem opens a new perspective on buckling problems, which were usually believed to occur only for compressive loads. The influence of the constraint's curvature on

In *CISM Lecture Notes No. 562*
"Extremely Deformable Structures" D. Bigoni
Ed. Springer, Wien–New York, 2015
ISBN 978-3-7091-1876-4 doi 10.1007/978-3-7091-1877-1

buckling and post-critical behaviour is analyzed in Section 4, with reference to elastic systems representing examples of compliant mechanisms. The concept of 'Eshelby-like' or 'configurational' forces in elastic structures is introduced in Section 5, and this represents the key to the understanding of snake locomotion. In fact, roughly speaking, a snake can be idealized as an elastic rod whose propulsion arises from the release of elastic energy that is responsible of an Eshelby-like force. It is shown that this force strongly affects the bifurcation and stability of elastic rods, as explained in Section 6, and that it can be used in the design of a new elastic arm weighing device, Section 7.

2 The Euler elastica

The purpose of this section is to introduce the theory of the Euler's elastica with reference to an elastic, inextensible rod subject to large deflections and with different types of constraints at its ends. When a rectilinear (in its undeformed, reference state) elastic rod is compressed, the determination of the critical load and of the post-critical behaviour provides a beautiful example of linear and nonlinear eigenvalue problems. We will follow and generalize the treatment of Bigoni (2012). Classical references are Timoshenko and Gere (1961), Love (1927), and Reiss (1969), whereas recent work has been presented by Wang (1997), Vaz (2003), Mikata (2007) and by O'Reilly and Peters (2011, 2012). The stability of the equilibrium configurations will also be addressed, which has been previously treated by Maddocks (1984), Manning et al. (1998), Hoffman et al. (2002), Manning (2009, 2014), Kuznetsov and Levyakov (1999, 2002), and by Levyakov and Kuznetsov (2010).

2.1 The kinematics of an inextensible planar rod

We consider an inextensible planar rod of length l, rectilinear in its reference configuration and smoothly deformed into the current configuration as shown in Fig. 1. In the deformed configuration, a generic point can be picked up using a curvilinear coordinate $s \in [0, l]$ (corresponding to $x_0 \in [0, l]$ in the undeformed, straight configuration), such that the inextensibility of the rod implies that $x_0 = s$ and thereby $\mathrm{d}x_0 = \mathrm{d}s$.

If we write $\mathbf{e}_1$ and $\mathbf{e}_2$ as unit vectors, see Fig. 1, then the *displacement* $\mathbf{u}$ of point $\mathbf{x}_0$ from the reference configuration is given by

$$\mathbf{u} = u_1(\mathbf{x}_0)\mathbf{e}_1 + u_2(\mathbf{x}_0)\mathbf{e}_2 = \mathbf{x} - \mathbf{x}_0, \tag{1}$$

which, by introducing the (twice-continuously differentiable) deformation function

$$\mathbf{x} = \mathbf{g}(\mathbf{x}_0), \tag{2}$$

In *CISM Lecture Notes No. 562*
"Extremely Deformable Structures" D. Bigoni
Ed. Springer, Wien–New York, 2015
ISBN 978-3-7091-1876-4 doi 10.1007/978-3-7091-1877-1

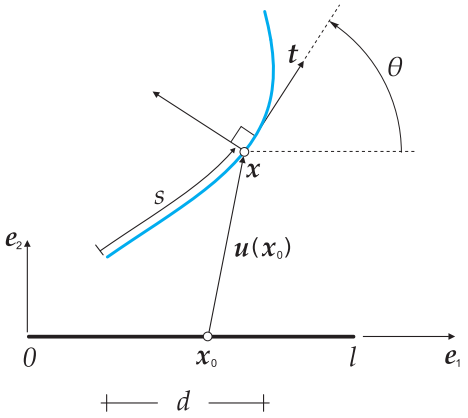

Figure 1. The kinematics of an elastic inextensible rod of length l, rectilinear in the reference configuration. The displacement of a generic point $\mathbf{x}_0$ of coordinate x_0 is $\mathbf{u}(x_0) = \mathbf{x} - \mathbf{x}_0$. Note that inextensibility implies that the curvilinear coordinate s is equal to the coordinate x_0, namely, $s = x_0$.

and noting that the point $\mathbf{x}_0$ has coordinate $x_0\mathbf{e}_1$, becomes

$$\mathbf{u} = \mathbf{g}(x_0\mathbf{e}_1) - x_0\mathbf{e}_1. \tag{3}$$

Since $\mathbf{e}_1$ is fixed, the dependence of function $\mathbf{g}$ on the unit vector can be omitted, so that equation (2) becomes the parametric representation of the curve describing the elastica.

Let us consider now two neighbouring points of the reference configuration at coordinates x_0 and $x_0 + \omega_0$, defining the vector $\mathbf{t}_0 = \omega_0\mathbf{e}_1$. This vector is mapped into

$$\mathbf{g}(\mathbf{x}_0 + \omega_0\mathbf{e}_1) - \mathbf{g}(\mathbf{x}_0), \tag{4}$$

so that, assuming ω_0 to be small, a Taylor series expansion of the deformation around $\omega_0 = 0$ yields the transformed vector (tangent to the deformed line at $\mathbf{x}$)

$$\mathbf{F}(\omega_0\mathbf{e}_1), \tag{5}$$

where

$$\mathbf{F} = \frac{\partial \mathbf{g}}{\partial \mathbf{x}_0} = \left(u_1' + 1\right)\mathbf{e}_1 \otimes \mathbf{e}_1 + u_2'\mathbf{e}_2 \otimes \mathbf{e}_1 + \mathbf{e}_2 \otimes \mathbf{e}_2, \tag{6}$$

in which a prime denotes differentiation with respect to the coordinate $x_0 = s$ and the symbol '$\otimes$' denotes the dyadic product.

In *CISM Lecture Notes No. 562*
"Extremely Deformable Structures" D. Bigoni
Ed. Springer, Wien–New York, 2015
ISBN 978-3-7091-1876-4 doi 10.1007/978-3-7091-1877-1

Since the elastica is assumed *inextensible*, the length of the transformed vector $\mathbf{F}(\omega_0\mathbf{e}_1)$ must remain equal to the length of the initial vector $\mathbf{t}_0 = \omega_0\mathbf{e}_1$, therefore from equation (5) we obtain

$$|\mathbf{F}\mathbf{e}_1| = 1, \tag{7}$$

which, using equation (6) yields

$$u_1^{'} + 1 = \pm\sqrt{1-(u_2^{'})^2}. \tag{8}$$

Differentiation of equation (8) finally provides the inextensibility constraint in the form

$$u_1^{''} = \mp\frac{u_2^{'}u_2^{''}}{\sqrt{1-(u_2^{'})^2}}. \tag{9}$$

Since the inextensibility constraint is enforced and the tangent to the elastica at $\mathbf{x}$ is given by the unit vector $\mathbf{t}$

$$\mathbf{t} = \left(u_1^{'}+1\right)\mathbf{e}_1 + u_2^{'}e_2 = \pm\sqrt{1-(u_2^{'})^2}\,\mathbf{e}_1 + u_2^{'}\mathbf{e}_2, \tag{10}$$

the angle θ of inclination of the tangent $\mathbf{t}$ to the elastica at $\mathbf{x}$ can be introduced to satisfy

$$\sin\theta = x_2^{'} = u_2^{'}, \quad \cos\theta = x_1^{'} = \pm\sqrt{1-(u_2^{'})^2}. \tag{11}$$

Equation $(11)_2$ shows that the '+' sign in equation (8) refers to moderate deflection, for which $\cos\theta$ remains positive. Furthermore, the length d of the projection of the elastica onto the $\mathbf{e}_1$-axis can be written as

$$d = \int_0^l \cos\theta \mathrm{d}s = \pm\int_0^l \sqrt{1-(u_2^{'})^2}\,\mathrm{d}s. \tag{12}$$

The unit vector $\mathbf{n}$ normal to the elastica at $\mathbf{x}$ can be obtained through differentiation (with respect to s) of the scalar product $\mathbf{t}\cdot\mathbf{t}$, so that $\mathbf{t}^{'}$ is found normal to $\mathbf{t}$ in the form

$$\mathbf{t}^{'} = \mp\frac{u_2^{'}u_2^{''}}{\sqrt{1-(u_2^{'})^2}}\mathbf{e}_1 + u_2^{''}\mathbf{e}_2, \tag{13}$$

or, equivalently, in the form

$$\mathbf{t}^{'} = -\theta^{'}\sin\theta\mathbf{e}_1 + \theta^{'}\cos\theta\mathbf{e}_2. \tag{14}$$

In *CISM Lecture Notes No. 562*
"Extremely Deformable Structures" D. Bigoni
Ed. Springer, Wien–New York, 2015
ISBN 978-3-7091-1876-4 doi 10.1007/978-3-7091-1877-1

The unit normal $\mathbf{n}$ can therefore be obtained from $\mathbf{t}^{'}$ through division by its modulus $|\mathbf{t}^{'}|$, that is, the so-called 'curvature'

$$|\mathbf{t}^{'}| = \frac{|u_2^{''}|}{\sqrt{1-(u_2^{'})^2}} = |\theta^{'}|, \tag{15}$$

thus obtaining

$$\mathbf{n} = \mathrm{sgn}\{u_2^{''}(u_1^{'}+1)\} \left(-u_2^{'}\mathbf{e}_1 + \sqrt{1-(u_2^{'})^2}\,\mathbf{e}_2\right), \tag{16}$$

or equivalently

$$\mathbf{n} = \mathrm{sgn}(\theta^{'})\ (-\sin\theta\mathbf{e}_1 + \cos\theta\mathbf{e}_2)\,. \tag{17}$$

In conclusion, the *signed curvature* χ reads

$$\chi = \mathrm{sgn}(u_1^{'}+1)\,\frac{u_2^{''}}{\sqrt{1-(u_2^{'})^2}}, \quad \text{or} \quad \chi = \theta^{'}. \tag{18}$$

2.2 Constitutive equation, total potential energy and the elastica

The constitutive equation used for the inextensible planar elastica comes from Jacob Bernoulli's celebrated assumption, which, neglecting the effects of normal and shearing forces, defines a linear relation between the bending moment $M(s)$ and the curvature $\theta^{'}(s)$ as

$$M(s) = B\theta^{'}(s), \tag{19}$$

where B is the bending stiffness (considered constant along the rod), defined as the product of the Young's modulus with the principal moment of inertia of the cross section of the rod about the axis normal to the inflection plane.

With reference to the elastic systems reported in Fig. 2, where the rod is loaded at its right end by a longitudinal force P, the total potential energy $\mathcal{V}(\theta(s))$ can be written as

$$\mathcal{V}(\theta(s)) = \int_0^l B\frac{(\theta^{'}(s))^2}{2}\mathrm{d}s - P\left(l - \int_0^l \cos\theta(s)\mathrm{d}s\right) - R\int_0^l \sin\theta(s)\,\mathrm{d}s, \tag{20}$$

where the first integral is the bending strain energy, the second term corresponds to the work done by the external force P, and R is a Lagrange multiplier (representing –as will be shown below– the vertical reaction at the supports) enforcing a global kinematic compatibility condition that corresponds to the vanishing of the relative, vertical displacement of the rod

In *CISM Lecture Notes No. 562*
"Extremely Deformable Structures" D. Bigoni
Ed. Springer, Wien–New York, 2015
ISBN 978-3-7091-1876-4 doi 10.1007/978-3-7091-1877-1

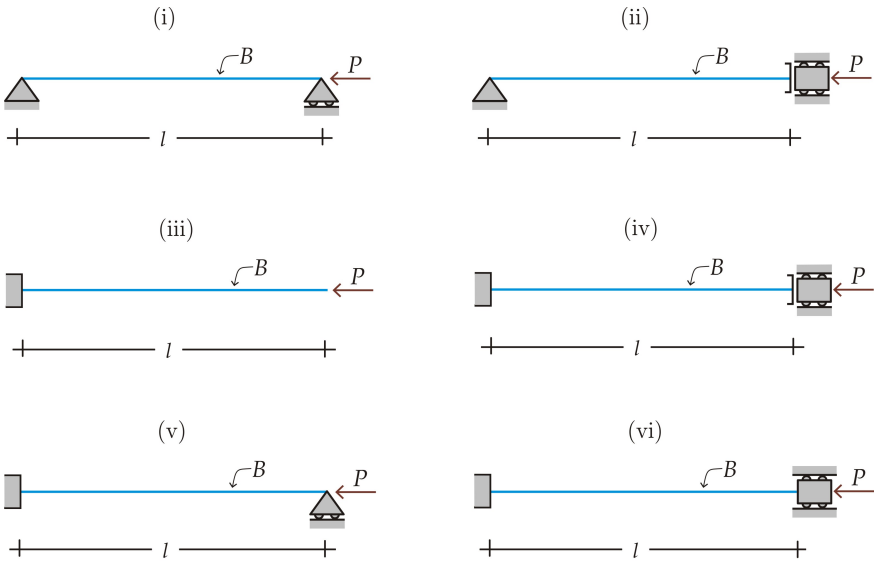

Figure 2. An elastic, inextensible rod loaded by an axial thrust P (positive when compressive) and subject to different constraints at its ends.

extremities. This condition will be enforced while considering the systems (v.) and (vi.) of Fig. 2, as well as in a particular case of system (i.). In contrast, the multiplier R will be set to zero for the elastic structures (ii.)-(iv.).

The functional (20) is defined over the set of kinematically admissible rotation fields, meaning every differentiable rotation field $\theta(s)$ satisfying the boundary conditions introduced by the constraints at the ends of the systems (i.)-(vi.) reported in Fig. 2, namely

$$\begin{aligned}
&\text{i)} \quad \int_0^l \sin\theta(s)\mathrm{d}s = 0,\\
&\text{ii)} \quad \theta(l) = 0,\\
&\text{iii)} \quad \theta(0) = 0,\\
&\text{iv)} \quad \theta(0) = \theta(l) = 0,\\
&\text{v)} \quad \theta(0) = 0 \quad \text{and} \quad \int_0^l \sin\theta(s)\mathrm{d}s = 0,\\
&\text{vi)} \quad \theta(0) = \theta(l) = 0 \quad \text{and} \quad \int_0^l \sin\theta(s)\mathrm{d}s = 0.
\end{aligned} \tag{21}$$

In *CISM Lecture Notes No. 562*
"Extremely Deformable Structures" D. Bigoni
Ed. Springer, Wien–New York, 2015
ISBN 978-3-7091-1876-4 doi 10.1007/978-3-7091-1877-1

Let us consider now variations $\tilde{\theta}(s)$ of the rotation field $\theta(s)$, satisfying the boundary conditions relevant to each system, namely

$$\begin{aligned}
&\text{i)} \quad \textstyle\int_0^l \sin\tilde{\theta}(s)\mathrm{d}s = 0,\\
&\text{ii)} \quad \tilde{\theta}(l) = 0,\\
&\text{iii)} \quad \tilde{\theta}(0) = 0,\\
&\text{iv)} \quad \tilde{\theta}(0) = \tilde{\theta}(l) = 0,\\
&\text{v)} \quad \tilde{\theta}(0) = 0 \quad \text{and} \quad \textstyle\int_0^l \sin\tilde{\theta}(s)\mathrm{d}s = 0,\\
&\text{vi)} \quad \tilde{\theta}(0) = \tilde{\theta}(l) = 0 \quad \text{and} \quad \textstyle\int_0^l \sin\tilde{\theta}(s)\mathrm{d}s = 0.
\end{aligned} \tag{22}$$

Keeping into account integration by parts

$$\int_0^l \theta'(s)\tilde{\theta}'(s)\,\mathrm{d}s = -\int_0^l \theta''(s)\tilde{\theta}(s)\,\mathrm{d}s + \theta'(l)\tilde{\theta}(l) - \theta'(0)\tilde{\theta}(0),$$

the first variation $\delta\mathcal{V}$ of functional $\mathcal{V}$ is obtained as

$$\delta\mathcal{V} = \int_0^l \left[\theta''(s) + \frac{P}{B}\sin\theta(s) + \frac{R}{B}\cos\theta(s)\right]\tilde{\theta}(s)\,\mathrm{d}s - \theta'(l)\tilde{\theta}(l) + \theta'(0)\tilde{\theta}(0), \tag{23}$$

holding for all kinematically admissible variation $\tilde{\theta}(s)$.

Imposing the vanishing of the first variation (23) for every admissible variation $\tilde{\theta}(s)$ yields the nonlinear differential equation for the elastica

$$\theta''(s) + \frac{P}{B}\sin\theta(s) + \frac{R}{B}\cos\theta(s) = 0, \tag{24}$$

and the following natural boundary conditions for the cases (i.)-(iii.) and (v.)

$$\begin{aligned}
&\text{i)} \quad \theta'(0) = \theta'(l) = 0,\\
&\text{ii)} \quad \theta'(0) = 0,\\
&\text{iii)} \quad \theta'(l) = 0,\\
&\text{v)} \quad \theta'(l) = 0.
\end{aligned} \tag{25}$$

In *CISM Lecture Notes No. 562*
"Extremely Deformable Structures" D. Bigoni
Ed. Springer, Wien–New York, 2015
ISBN 978-3-7091-1876-4 doi 10.1007/978-3-7091-1877-1

Notice that in the equilibrium equation (24) it is apparent that the Lagrange multiplier R corresponds to the vertical reaction at the supports, which are always null except in the following cases:

- ◇ for the structure (i.), in the special situation when the two supports coincide;
- ◇ for the structure (v.);
- ◇ for the structure (vi.), when antisymmetric buckling modes are considered.

Simply supported elastica Let us start by considering the doubly pinned rod (i.), so that, defining $\lambda^2 = P/B$, the equations governing the equilibrium of the elastica are

$$\begin{aligned}
&\theta''(s) + \lambda^2 \sin\theta(s) = 0 \quad \forall\, s \in [0, l], && \text{governing diff. equation}\\
&\theta'(0) = \theta'(l) = 0, && \text{b.c.: null moment at both supports}\\
&u_1(0) = 0, && \text{b.c.: null horiz. displ. at left support}\\
&u_2(0) = u_2(l) = 0, && \text{b.c.: null vert. displ. at both supports}\\
&u_1'(s) = \cos\theta(s) - 1 \quad \forall\, s \in [0, l], && \text{diff. equation for the horizontal displ.}\\
&u_2'(s) = \sin\theta(s) \quad \forall\, s \in [0, l]. && \text{diff. equation for the vertical displ.}
\end{aligned} \tag{26}$$

Equations (26) define a *nonlinear eigenvalue problem*, for which the *trivial solution* $\theta(s) = u_1(s) = u_2(s) = 0$ is always possible, so that the question arises whether nontrival solutions exist or not. Bifurcation corresponds to the situation in which the trivial solution (or possibly a bifurcated solution) of (26) splits into two or more, as λ passes through a critical value λ_{cr}, called 'bifurcation point'.

Before embarking in the solution of the non-linear problem (26), let us consider its linearization about the trivial solution $\theta(s) = 0$, such that the horizontal displacement is null, i.e. $u_1(s) = 0$, and the remaining equations

In *CISM Lecture Notes No. 562*
"Extremely Deformable Structures" D. Bigoni
Ed. Springer, Wien–New York, 2015
ISBN 978-3-7091-1876-4 doi 10.1007/978-3-7091-1877-1

read

$$\begin{aligned}
&\theta''(s) + \lambda^2\theta(s) = 0 \quad \forall\, s \in [0,l], && \text{governing diff. equation}\\
&\theta'(0) = \theta'(l) = 0, && \text{boundary conditions}\\
&u_2(0) = u_2(l) = 0, && \text{boundary conditions}\\
&u_2'(s) = \theta(s) \quad \forall\, s \in [0,l]. && \text{diff. equation for the vertical displ.}
\end{aligned} \tag{27}$$

Equations (27) define a *linear eigenvalue problem*, also called 'Sturm-Liouville problem' (Broman, 1970). It admits the infinite solutions

$$\theta(s) = A_n \cos\frac{n\pi s}{l}, \quad n = 0, 1, 2, ... \tag{28}$$

and

$$\underbrace{u_2 = A_0 = 0, \quad n = 0}_{\text{trivial solution}}, \qquad \underbrace{u_2 = \frac{lA_n}{n\pi}\sin\frac{n\pi s}{l}, \quad n = 1, 2, ...}_{\text{nontrivial solutions}} \tag{29}$$

where the trivial solution holds for every thrust P, while the nontrivial solutions hold if and only if

$$\lambda = \lambda_n = \frac{n\pi}{l}, \quad \Leftrightarrow \quad P = P_n^{cr} = \frac{n^2\pi^2 B}{l^2}, \quad n = 1, 2, ... \tag{30}$$

which defines the Euler's critical loads. As a consequence of the linearization, the amplitudes A_n $(n = 1, 2, ...)$ of the bifurcation modes remain undetermined, nevertheless the critical loads correctly identify the bifurcation points on the trivial path, λ_n, as will be proven below.

Let us now solve the nonlinear problem (26). First of all, we note that if

$$\theta(s), \quad u_1(s), \quad u_2(s),$$

represent a solution corresponding to λ^2, the fields

$$\pm\theta(s) + 2n\pi, \quad u_1(s), \quad \pm u_2(s), \qquad n = ..., -2, -1, 0, 1, 2, ...$$

also represent solutions (symmetrical with respect to the x_1–axis) and the fields

$$\pm\theta(s) + (2n+1)\pi, \quad -u_1(s) - 2s, \quad u_2(s), \qquad n = ..., -2, -1, 0, 1, 2, ...$$

are valid for $-\lambda^2$. These are symmetric solutions with respect to the x_1– or the x_2–axis and, without loss of generality, will be ignored in the following.

In *CISM Lecture Notes No. 562*
"Extremely Deformable Structures" D. Bigoni
Ed. Springer, Wien–New York, 2015
ISBN 978-3-7091-1876-4 doi 10.1007/978-3-7091-1877-1

Therefore, defining $\hat{\theta} = \theta(\hat{s})$, where $\hat{s}$ is the curvilinear coordinate at which the bending moment is null, for the case under consideration

$$\hat{\theta} = \theta(0), \tag{31}$$

and we only address solutions such that $0 \leq \hat{\theta} \leq \pi$. A multiplication of equation $(26)_1$ by $\theta^{'}(s)$ yields

$$\frac{\mathrm{d}}{\mathrm{d}s}\left[\frac{1}{2}(\theta^{'}(s))^2 - \lambda^2 \cos\theta(s)\right] = 0, \tag{32}$$

so that its integration, considering the boundary conditions $(26)_2$ and equation (31), leads to

$$\theta^{'}(s) = \lambda\sqrt{2(\cos\theta(s) - \cos\hat{\theta})}, \tag{33}$$

where we have selected the positive root, since the two solutions merely differ in sign.

An equation formally identical to equation (33) is usually obtained in the analysis of the oscillation of a simple pendulum (Temme, 1996), so that it is a standard expedient to operate the following change of variables

$$\kappa = \sin\frac{\hat{\theta}}{2}, \quad \kappa\sin\phi(s) = \sin\frac{\theta(s)}{2}, \tag{34}$$

leading through trigonometric formulae to the differential problem

$$\frac{\mathrm{d}\,\phi(s)}{\mathrm{d}s} = \lambda\sqrt{1 - \kappa^2\sin^2\phi(s)}. \tag{35}$$

The boundary conditions imply that $\sin\phi(0) = 1$ and $\sin^2\phi(l) = 1$, so that

$$\phi(0) = \frac{4h+1}{2}\pi, \quad \phi(l) = \frac{2j+1}{2}\pi, \quad h, j = 0, \pm1, \pm2, ... \tag{36}$$

and therefore integration of equation (35) by separation of the variables yields

$$s\lambda = \int_{\frac{4h+1}{2}\pi}^{\phi(s)} \frac{\mathrm{d}\phi}{\sqrt{1 - \kappa^2\sin^2\phi}}, \quad h = 0, \pm1, \pm2, ... \tag{37}$$

which, for $s = l$, becomes

$$l\lambda = \int_{\frac{4h+1}{2}\pi}^{\frac{2j+1}{2}\pi} \frac{\mathrm{d}\phi}{\sqrt{1 - \kappa^2\sin^2\phi}}, \quad h, j = 0, \pm1, \pm2, ... \tag{38}$$

In *CISM Lecture Notes No. 562*
"Extremely Deformable Structures" D. Bigoni
Ed. Springer, Wien–New York, 2015
ISBN 978-3-7091-1876-4 doi 10.1007/978-3-7091-1877-1

Taken over one period, the integral (38) is equal to $2\mathcal{K}(\kappa)$, where

$$\mathcal{K}(\kappa) = \int_0^{\frac{\pi}{2}} \frac{\mathrm{d}\phi}{\sqrt{1-\kappa^2 \sin^2 \phi}}, \tag{39}$$

is the complete elliptic integral of the first kind or the so-called 'real quarter period of the elliptic function' (Byrd and Friedman, 1954; Temme, 1996).

The integral in equation (38) can be rewritten as a function of an integer m as

$$l\lambda = 2m\mathcal{K}(\kappa), \quad \Leftrightarrow \quad P = \frac{B}{l^2} 4m^2 \left[\mathcal{K}\left(\sin\frac{\hat{\theta}}{2}\right)\right]^2, \tag{40}$$

an equation providing the relation between the applied load P and the rotation of the left rod's extremity associated to the m–th bifurcation mode (Reiss, 1969).

For small $\hat{\theta}$, a Taylor series expansion of equation (40) provides exactly equation (30), thus proving that the critical Euler loads (30), calculated from the linearized theory, correctly determine the bifurcation points emanating from the trivial path. Note that this results has a conceptual relevance, since it validates the calculations usually done on the linearized eigenvalue problem.

Let us go back now to equation (37) and note that the integral on the right-hand side can always be written as

$$\int_{\frac{4m+1}{2}\pi}^{\phi(s)} (\cdots)\,\mathrm{d}s = -\int_0^{\frac{4m+1}{2}\pi} (\cdots)\,\mathrm{d}s + \int_0^{\phi(s)} (\cdots)\,\mathrm{d}s, \tag{41}$$

so that, since (Byrd and Friedman, 1954)

$$\int_0^{\frac{4m+1}{2}\pi} \frac{\mathrm{d}\phi}{\sqrt{1-\kappa^2 \sin^2 \phi}} = (4m+1)\mathcal{K}(\kappa), \quad m = 0, \pm 1, \pm 2, ... \tag{42}$$

we obtain

$$s\lambda + (4m+1)\mathcal{K}(\kappa) = \int_0^{\phi(s)} \frac{\mathrm{d}\phi}{\sqrt{1-\kappa^2 \sin^2 \phi}}, \quad m = 0, \pm 1, \pm 2, ... \tag{43}$$

which provides

$$\phi(s) = \mathrm{am}\,(s\lambda + (4m+1)\mathcal{K}(\kappa), \kappa), \quad m = 0, \pm 1, \pm 2, ... \tag{44}$$

In *CISM Lecture Notes No. 562*
"Extremely Deformable Structures" D. Bigoni
Ed. Springer, Wien–New York, 2015
ISBN 978-3-7091-1876-4 doi 10.1007/978-3-7091-1877-1

where 'am' denotes the Jacobi amplitude function of modulus κ. Employing the property (Byrd and Friedman, 1954)

$$\mathrm{am}\left(x \pm 2n\mathcal{K}(\kappa), \kappa\right) = \mathrm{am}\left(x, \kappa\right) \pm n\pi, \quad n = 0, \pm 1, \pm 2, ...$$

equation (44) can be simplified to

$$\phi(s) = \mathrm{am}\left(s\lambda + \mathcal{K}(\kappa), \kappa\right) + 2m\pi, \quad m = 0, \pm 1, \pm 2, ... \tag{45}$$

so that the definition of $\phi(s)$, equation $(34)_2$, yields

$$\sin\frac{\theta(s)}{2} = \kappa\,\mathrm{sn}\left(s\lambda + \mathcal{K}(\kappa), \kappa\right), \tag{46}$$

where 'sn' is the Jacobi sine amplitude function, defined as

$$\mathrm{sn}\left(x, \kappa\right) = \sin\left(\mathrm{am}\left(x, \kappa\right)\right). \tag{47}$$

A substitution of equation (46) into equation (33), where the identity $\cos\theta = 1 - 2\sin^2(\theta/2)$ is employed, yields

$$\theta^{'}(s) = 2\lambda\kappa\,\mathrm{cn}\left(s\lambda + \mathcal{K}(\kappa), \kappa\right), \tag{48}$$

where 'cn' is the Jacobi cosine amplitude function, defined as

$$\mathrm{cn}\left(x, \kappa\right) = \cos\left(\mathrm{am}\left(x, \kappa\right)\right).$$

Note that, due to the properties

$$\mathrm{cn}\left(\mathcal{K}(\kappa), \kappa\right) = \mathrm{cn}\left(3\mathcal{K}(\kappa), \kappa\right) = \mathrm{cn}\left[(2m+1)\mathcal{K}(\kappa), \kappa\right] = 0, \quad m = 0, \pm 1, \pm 2, \pm 3$$

the boundary conditions $(26)_2$, namely $\theta^{'}(0) = \theta^{'}(l) = 0$, are satisfied[1].

According to equations (11) and $(26)_{(5,6)}$, the differential equations determining the points $\mathbf{x}$ of the deformed elastica are

$$x_1^{'}(s) = \cos\theta(s), \quad x_2^{'}(s) = \sin\theta(s), \tag{49}$$

which, since $\cos\theta = 1 - 2\sin^2(\theta/2)$ and $\sin\theta = 2\sin(\theta/2)\sqrt{1 - \sin^2(\theta/2)}$, and using equation (46), provide the two differential equations

$$\begin{aligned} x_1^{'}(s) &= 1 - 2\kappa^2\,\mathrm{sn}^2(s\lambda + \mathcal{K}(\kappa), \kappa), \\ x_2^{'}(s) &= 2\kappa\,\mathrm{sn}\left(s\lambda + \mathcal{K}(\kappa), \kappa\right)\mathrm{dn}\left(s\lambda + \mathcal{K}(\kappa), \kappa\right), \end{aligned} \tag{50}$$

[1] Equation (40) has been used in the boundary condition at $\theta^{'}(l)$.

In *CISM Lecture Notes No. 562*
"Extremely Deformable Structures" D. Bigoni
Ed. Springer, Wien–New York, 2015
ISBN 978-3-7091-1876-4 doi 10.1007/978-3-7091-1877-1

where 'dn' is the Jacobi elliptic function, defined as

$$\mathrm{dn}\left(s\lambda+\mathcal{K}(\kappa),\kappa\right)=\sqrt{1-\kappa^2\,\mathrm{sn}^2(s\lambda+\mathcal{K}(\kappa),\kappa)}. \tag{51}$$

Since the following differentiation rules are known (Byrd and Friedman, 1954)

$$\begin{aligned}
&\frac{\partial}{\partial x}E(x,\kappa)=\sqrt{1-\kappa^2\sin^2 x},\\
&\frac{\partial}{\partial x}\,\mathrm{am}\,(x,\kappa)=\,\mathrm{dn}\,(x,\kappa),\\
&\frac{\partial}{\partial x}\,\mathrm{cn}\,(x,\kappa)=-\,\mathrm{sn}\,(x,\kappa)\,\mathrm{dn}\,(x,\kappa),
\end{aligned} \tag{52}$$

where $E(x,\kappa)$ is the incomplete elliptic integral of the second kind of modulus κ,

$$E(x,\kappa)=\int_0^x\sqrt{1-\kappa\sin^2 t}\,\mathrm{d}t,$$

taking into account the boundary conditions $(26)_{3,4}$, we integrate equations (50), thus arriving at the equations describing the deformed shape of the elastica[2]

$$\begin{aligned}
x_1(s)&=-s+\frac{2}{\lambda}\left\{E\left[\mathrm{am}\left(s\lambda+\mathcal{K}(\kappa),\kappa\right),\kappa\right]-\,E\left[\mathrm{am}\left(\mathcal{K}(\kappa),\kappa\right),\kappa\right]\right\},\\
x_2(s)&=-\frac{2\kappa}{\lambda}\,\mathrm{cn}(s\lambda+\mathcal{K}(\kappa)),
\end{aligned} \tag{53}$$

which are identical with those provided by Love (1927). For compressive loads ($P>0$) the displacement $u_1(l)$ is negative and, since $|u_1(l)|=l-x_1(l)$, its absolute value can be immediately obtained from equations $(53)_1$ in the form

$$|u_1(l)|=2l-\frac{2}{\lambda}\left\{E\left[\mathrm{am}\left(l\lambda+\mathcal{K}(\kappa),\kappa\right),\kappa\right]-\,E\left[\mathrm{am}\left(\mathcal{K}(\kappa),\kappa\right),\kappa\right]\right\}, \tag{54}$$

so that using now equation (40) we obtain

$$\frac{|u_1(l)|}{l}=2-\frac{E\left[\mathrm{am}\left((2m+1)\mathcal{K}(\kappa),\kappa\right),\kappa\right]-\,E\left[\mathrm{am}\left(\mathcal{K}(\kappa),\kappa\right),\kappa\right]}{m\mathcal{K}(\kappa)},\quad m=1,2,... \tag{55}$$

[2]These relations are also valid for the hinged-clamped case (ii), where the value of λ as a function of the rotation at the inflexion point, $\hat{\theta}=\theta(0)$, is obtained through the relation $l\lambda=(2m-1)\mathcal{K}\left(\sin\dfrac{\hat{\theta}}{2}\right)$.

In *CISM Lecture Notes No. 562*
"Extremely Deformable Structures" D. Bigoni
Ed. Springer, Wien–New York, 2015
ISBN 978-3-7091-1876-4 doi 10.1007/978-3-7091-1877-1

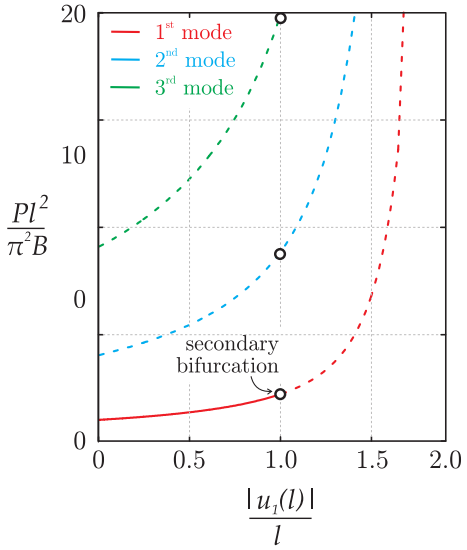

Figure 3. Dimensionless load $Pl^2/(\pi^2 B)$ of a doubly supported rod versus dimensionless displacement $u_1(l)/l$. The first three primary bifurcation points and branches are reported together with the first three secondary bifurcation points. All equilibrium configurations on the second and third branch are unstable (dashed curves). The first branch becomes unstable after the secondary bifurcation point.

which eventually can be simplified to (Reiss, 1969)[3]

$$\frac{|u_1(l)|}{l} = 2 - \frac{2\,E\,(\kappa)}{\mathcal{K}(\kappa)}, \tag{56}$$

where $E(\pi/2, \kappa) = E(\kappa)$ represents the complete elliptic integral of the second kind. Note that equation (56) is independent of the bifurcation mode m, so that the displacement of the right pin of the rod depends only on $\hat{\theta}$ (through κ).

The mid-span deflection of the rod, null for even values of the mode m, can be evaluated for odd m as

$$\frac{|u_2(l/2)|}{l} = \frac{\kappa}{m\,\mathcal{K}(\kappa)}, \quad m = 1, 3, 5, ... \tag{57}$$

[3]The following identities turn out to be useful (Byrd and Friedman, 1954):

$$\mathrm{am}\,[\mathcal{K}(\kappa), \kappa] = \pi/2, \quad \mathrm{am}[(2m+1)\mathcal{K}(\kappa), \kappa] = (2m+1)\pi/2, \quad E(n\pi/2, \kappa) = n\,E(\kappa).$$

In *CISM Lecture Notes No. 562*
"Extremely Deformable Structures" D. Bigoni
Ed. Springer, Wien–New York, 2015
ISBN 978-3-7091-1876-4 doi 10.1007/978-3-7091-1877-1

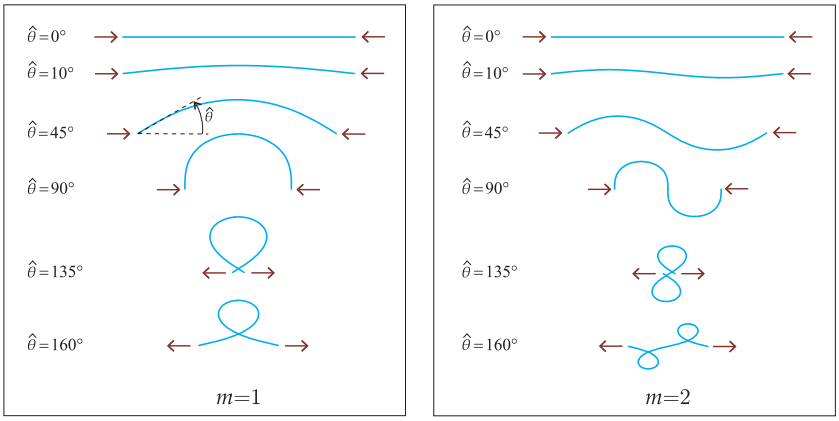

Figure 4. Deformed shapes for the first two modes $m = 1, 2$ of a doubly supported rod at different values of parameters setting the deformation: the initial inflexion angle $\hat{\theta} = \{0, 10°, 45°, 90°, 135°, 160°\}$ and corresponding dimensionless displacement of the end of the rod $u_1(l)/l = \{0, 0.008, 0.149, 0.543, 1.049, 1.340\}$ for both the modes. The deformed shapes of the elastica represent the post-critical behaviour of the structure.

In summary, for a given $\hat{\theta}$ and for a given mode m we can calculate the corresponding λ (using equation (40)) and $u_1(l)$ (using equation (56)) and plot the elastica (using equations (53)). The bifurcation diagram showing the load P (made dimensionless through multiplication by $l^2/(\pi^2 B)$) as a function of the displacement of the right pin of the rod (divided by l) is shown in Fig. 3. In the figure, the first three critical loads and the corresponding three branches are reported. We may note that the branches do not cross each other and the load is continuously increasing during the post-critical behaviour.

The deformed elastic lines have been evaluated and plotted in Fig. 4 for the first two branches at fixed values of $\hat{\theta}$, namely, {10°,45°,90°,135°, 160°}. These values of rotation correspond to rod end displacements, respectively equal to {0.008, 0.149, 0.543, 1.049, 1.340} l. Note that in Fig. 4 also the undeformed configuration, corresponding to $\hat{\theta} = 0°$, is reported in order to provide the scale bar for the displacement.

It should be noticed that the line of thrust (joining the two forces in Fig. 4) intersects the elastica at points of inflexion (where $\theta' = 0$), separating different so-called 'bays' in the Love's terminology.

In *CISM Lecture Notes No. 562*
"Extremely Deformable Structures" D. Bigoni
Ed. Springer, Wien–New York, 2015
ISBN 978-3-7091-1876-4 doi 10.1007/978-3-7091-1877-1

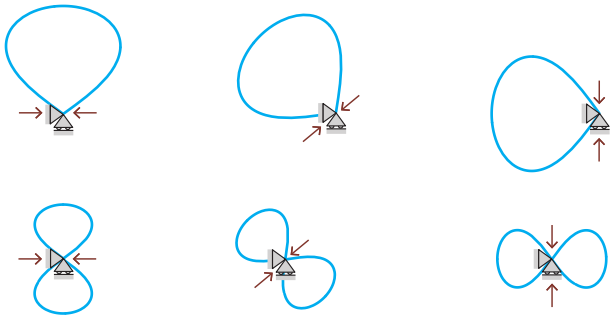

Figure 5. Sketches of the in-plane secondary bifurcation modes of the simply supported elastica, referred to the first (upper part) and second (lower part) mode. When the two supports coincide the structure can suffer a rigid-body rotation. During this rotation, the horizontal load drops to zero (value reached when the elastica is rotated by 90°), so that the force is maintained by the vertical reaction of the support. For rotation angles greater than 90° (not reported) the force changes sign. For an horizontal dead load, the structure becomes unstable when the two supports coincide and snaps to the configuration $u_1 = -2l$, where it is in equilibrium with a tensile load.

In-plane secondary bifurcations of the simply-supported elastica
Let us go back to Fig. 3 and note that on each bifurcated branch there is a secondary bifurcation point (marked with a circle). This condition occurs when the two supports of the rod coincide, namely, when $u_1(l) = -l$, corresponding to $\hat{\theta} = 130.7099°$ and different load values: $Pl^2/(\pi B) = 2.1833$ for the first mode, $Pl^2/(\pi B) = 8.7335$ for the second mode, $Pl^2/(\pi B) = 19.6504$ for the third mode, and so on.

These secondary bifurcation modes, which passed unnoticed until Maddocks (1984) (see also Kuznetsov and Levyakov, 2002), have a simple explanation. In fact, *when the two supports of the rod momentarily coincide during deformation along the bifurcation path, the structure can rigidly rotate about the pin*. During the rigid-body rotation, vertical reactions are generated at the two supports, so that the horizontal load P drops and is reduced to zero when the structure is rotated by 90°. Similarly, further rotations imply a negative horizontal force. This situation is sketched in Fig. 5, with reference to the first two modes.

For the case of imposed horizontal load, the situation in which the two supports coincide marks an instability point in the sense that: (i.) at this point the structure rigidly rotates and snaps to the configuration $u_1 = -2l$, where it is subject to a tensile load; (ii.) equilibrium configurations belonging to the post-critical path $m = 1$ and $\hat{\theta} > 130.7099°$ are unstable.

In *CISM Lecture Notes No. 562*
"Extremely Deformable Structures" D. Bigoni
Ed. Springer, Wien–New York, 2015
ISBN 978-3-7091-1876-4 doi 10.1007/978-3-7091-1877-1

Doubly clamped elastica The equations governing the equilibrium configurations of a doubly clamped elastica are

$$\begin{aligned}
&\theta''(s) + \frac{P}{B}\sin\theta(s) + \frac{R}{B}\cos\theta(s) = 0 \quad \forall\, s \in [0,l], && \text{governing diff. equation}\\
&\theta(0) = \theta(l) = 0, && \text{b.c.: null rotation}\\
&u_1(0) = 0, && \text{b.c.: null horizontal displ.}\\
&u_2(0) = u_2(l) = 0, && \text{b.c.: null vertical displ.}\\
&u_1'(s) = \cos\theta(s) - 1 \quad \forall\, s \in [0,l], && \text{diff. eq. for horiz. displ.}\\
&u_2'(s) = \sin\theta(s) \quad \forall\, s \in [0,l]. && \text{diff. eq. for vert. displ.}
\end{aligned} \tag{58}$$

Similarly to the case of a simply supported rod, equations (58) define a *nonlinear eigenvalue problem*, for which the *trivial solution* $\theta(s) = 0$ is always possible, so that we look for non-trivial solutions.

When symmetric deformed configurations are considered, such that $2m$ inflection points are present, vertical equilibrium requires that $R = 0$ and so the differential equation $(58)_1$ reduces to that governing the previous case of a simply supported rod.

A different solution arises when antisymmetric configurations are sought. In this case, $2m + 1$ inflection points are present and a non-zero vertical reaction R acts at the constraints. A linearization of the problem (58) about the solution $\theta(s) = 0$ leads to

$$\begin{aligned}
&\theta''(s) + \frac{P}{B}\theta(s) = -\frac{R}{B} \quad \forall\, s \in [0,l], && \text{governing diff. equation}\\
&\theta(0) = \theta(l) = 0, \quad \int_0^l \theta(s)\mathrm{d}s = 0. && \text{boundary conditions}
\end{aligned} \tag{59}$$

Equations (59) define a *linear eigenvalue problem* that admits the trivial solution $\theta(s) = 0$ for every thrust P, whereas infinite, non trivial (symmetric and antisymmetric) solutions are only possible when the following characteristic equation is satisfied

$$2\left(1 - \cos\sqrt{\frac{Pl^2}{B}}\right) = \sqrt{\frac{Pl^2}{B}}\sin\sqrt{\frac{Pl^2}{B}}, \tag{60}$$

In *CISM Lecture Notes No. 562*
"Extremely Deformable Structures" D. Bigoni
Ed. Springer, Wien–New York, 2015
ISBN 978-3-7091-1876-4 doi 10.1007/978-3-7091-1877-1

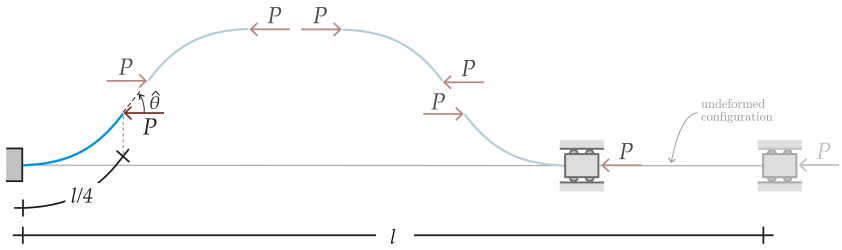

Figure 6. Deformed (and undeformed) configuration for the first (symmetric) mode of the doubly clamped rod. Note that, thanks to symmetry, the problem is reduced to the analysis of a cantilever rod of length $l/4$ loaded with an end thrust P.

defining the Euler's bifurcation loads for the doubly clamped rod as

$$P_1^{cr} = \frac{4\pi^2 B}{l^2}, \quad P_2^{cr} = \frac{8.1830\pi^2 B}{l^2}, \quad P_3^{cr} = \frac{16\pi^2 B}{l^2}, \quad P_4^{cr} = \frac{24.1872\pi^2 B}{l^2}, \ldots \tag{61}$$

where an odd (even) subscript in the definition of the critical loads corresponds to symmetric (antisymmetric) bifurcation paths.

Symmetric buckling modes With reference to the symmetric buckling modes with $2m$ inflection points ($R = 0$), the rotation field $\theta(s)$ is solution of the following differential problem

$$\begin{aligned} &\theta''(s) + \lambda^2 \sin\theta(s) = 0 \quad \forall\, s \in [0, l], \\ &\theta(0) = \theta(l) = 0, \end{aligned} \tag{62}$$

so that, a multiplication of equation $(62)_1$ by $\theta'(s)$ and its integration leads to

$$\theta'(s) = \pm\lambda\sqrt{2(\cos\theta(s) - \cos\hat{\theta})}, \tag{63}$$

where, in this case, $\hat{\theta}$ represents the angle of rotation at the inflection point at the coordinate $s = l/4$.

In order to facilitate the analytical description, the symmetry properties can be exploited, so that four simply clamped rods, of equal length $l/4$, can be identified in the structure, as sketched in Fig. 6.

Therefore, limiting the attention only to one quarter of the rod, $s \in [0, l/4]$, and considering the positive root (representing the curvature) of equation (63) for $s \in [0, l/4]$, the change of variables (34) leads to the

In *CISM Lecture Notes No. 562*
"Extremely Deformable Structures" D. Bigoni
Ed. Springer, Wien–New York, 2015
ISBN 978-3-7091-1876-4 doi 10.1007/978-3-7091-1877-1

differential problem

$$\frac{\mathrm{d}\phi(s)}{\mathrm{d}s} = \lambda\sqrt{1-\kappa^2\sin^2\phi}. \tag{64}$$

The boundary conditions for the considered problem imply that $\sin\phi(0) = 0$ and $\sin\phi(l/4) = 1$, so that

$$\phi(0) = h\pi, \quad \phi(l/4) = \frac{2j+1}{2}\pi, \quad h, j = 0, \pm1, \pm2, ... \tag{65}$$

and therefore integration of equation (64) by separation of the variables yields

$$s\lambda = \int_{h\pi}^{\phi(s)} \frac{\mathrm{d}\phi}{\sqrt{1-k^2\sin^2\phi}}, \quad h = 0, \pm1, \pm2, ... \tag{66}$$

which, for $s = l/4$, becomes

$$\frac{l}{4}\lambda = \int_{h\pi}^{\frac{2j+1}{2}\pi} \frac{\mathrm{d}\phi}{\sqrt{1-k^2\sin^2\phi}}, \quad h, j = 0, \pm1, \pm2, ... \tag{67}$$

and can be rewritten as a function of an odd integer m as

$$l\lambda = 2(m+1)\mathcal{K}(\kappa), \quad \Leftrightarrow \quad P = \frac{B}{l^2}4(m+1)^2\left[\mathcal{K}\left(\sin\frac{\hat{\theta}}{2}\right)\right]^2, \quad m = 1, 3, 5, ... \tag{68}$$

This equation provides the relation between the applied load P and the rotation $\hat{\theta}$ at the inflection point ($s = l/4$) associated with the odd (symmetric) m–th buckling mode.

For small $\hat{\theta}$, a Taylor series expansion of equation (68) provides exactly the odd critical Euler's loads calculated through linearization of the governing equations and reported in equation (61).

Going back to equation (66) and employing the definition of $\phi(s)$, equation (34), in addition to the odd nature of Jacobi amplitude function, namely,

$$\mathrm{am}\,(x, \kappa) = -\mathrm{am}\,(-x, \kappa),$$

we can write the rotation field along the rod as[4]

$$\theta(s) = 2\arcsin\left(\kappa\,\mathrm{sn}\,(s\lambda, \kappa)\right) \quad \forall\, s \in [0, l]. \tag{69}$$

[4]We may note that the equations describing the rotational field, equation (69), and the shape of the elastica, equation (70), remain the same also for structure (iii). The only difference lies in the relation between the load P and the angle of the free end $\hat{\theta} = \theta(l)$, associated to the m-th bifurcation mode, which is $l\lambda = (2m-1)\mathcal{K}\left(\sin\frac{\hat{\theta}}{2}\right)$.

In *CISM Lecture Notes No. 562*
"Extremely Deformable Structures" D. Bigoni
Ed. Springer, Wien–New York, 2015
ISBN 978-3-7091-1876-4 doi 10.1007/978-3-7091-1877-1

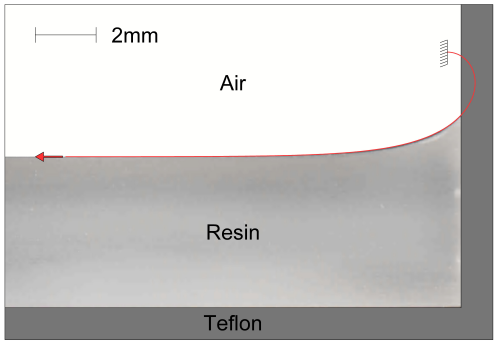

Figure 7. The solution of the elastica superimposed to a photo of fluid (an epoxy resin) forming a meniscus near the boundary of a teflon mould shows that the shape of an elastic cantilever (marked in red) subjected to large displacements (induced by a dead force applied at its free end) is identical to the shape of a fluid meniscus in a capillary channel.

According to equations (11) and (69), and taking into account the boundary conditions $(21)_6$, the analytical formulae describing the shape of the elastica for the entire rod, with $s \in [0, l]$, can be written as[5]

$$\begin{aligned} x_1(s) &= -s + \frac{2}{\lambda}\left\{E\left[\mathrm{am}\left(s\lambda, \kappa\right), \kappa\right]\right\}, \\ x_2(s) &= \frac{2\kappa}{\lambda}\left[1 - \mathrm{cn}(s\lambda)\right]. \end{aligned} \tag{70}$$

It might be interesting to notice that a formal analogy exists between the two differential equations governing the equilibrium configurations of an elastic rod and the free surface of a fluid meniscus, see Lamb (1928). Specifically, the term P/B of the elastica is replaced in the case of a fluid meniscus by the ratio between the unit weight and the surface tension of the fluid. This fact is depicted in Fig. 7, where the deformed shape of a clamped elastic rod has been superimposed to a photo of a meniscus formed by an epoxy resin at a boundary of a teflon mould.

Proceeding with our treatment, since $|u_1(l)| = l - x_1(l)$, the displacement of the point of application of the force can be immediately obtained from

[5] Equations (70) describe also the deformed configuration of system (iv), together with the relation (40), providing a connection between the thrust P and the angle $\hat{\theta} = \theta(l/2)$ for different m buckling modes.

In *CISM Lecture Notes No. 562*
"Extremely Deformable Structures" D. Bigoni
Ed. Springer, Wien–New York, 2015
ISBN 978-3-7091-1876-4 doi 10.1007/978-3-7091-1877-1

equation $(70)_1$ in the form

$$\frac{|u_1(l)|}{l} = -2\left(\frac{E(\kappa)}{\mathcal{K}(\kappa)} - 1\right), \tag{71}$$

which is independent of the bifurcation mode m, so that the displacement of the right end of the rod depends only on $\hat{\theta}$ (through κ). The bifurcation diagram showing the load P (made dimensionless through multiplication by $l^2/(\pi^2 B)$) as a function of the displacement of the right-hand movable end of the rod (divided by l) is shown in Fig. 9 together with the bifurcation diagram valid for antisymmetric buckling modes. In the figure, the first three critical loads and the corresponding three branches (two symmetric and one antisymmetric) are reported. The deformed elastic lines have been evaluated and plotted in Fig. 10 for the first symmetric branch (first buckling mode) at fixed values of $|u_1(l)|/l = \{0, 0.2, 0.6, 1.0, 1.4\}$, together with the first anti-symmetric branch (second buckling mode), described by equations (86), (89), and (95). Note that in Fig. 10 also the undeformed configuration is reported, providing the scale bar for the displacements.

Antisymmetric buckling modes Let us now go back to equations (58) and solve them in the case of antisymmetric (even) buckling modes characterized by $2m+1$ inflection points ($R \neq 0$). Antisymmetry properties allow us to conclude that one inflection point is located at $s = l/2$, so that we may observe that the structure can be regarded as composed of two equal clamped-hinged rods subject to an end thrust P, see Fig. 8. Therefore, we consider only one half of the rod, such that its equilibrium is governed by the following differential problem[6]

$$\begin{aligned}
&\theta''(s) + \frac{P}{B}\sin\theta(s) + \frac{R}{B}\cos\theta(s) = 0 \quad \forall s \in [0, l/2]\,,\\
&\theta(0) = \theta'(l/2) = 0,\\
&\int_0^{l/2} \sin\theta(s)\mathrm{d}s = 0.
\end{aligned} \tag{72}$$

We write $\gamma^2 = \sqrt{P^2 + R^2}/B$ and we introduce the angle $\psi(s) = \theta(s) + \beta$, where β defines the inclination of the resultant of P and R with respect to

[6] We note that the equations for the structure (v.) correspond to those governing the antisymmetric equilibrium configuration of the structure (vi.).

In *CISM Lecture Notes No. 562*
"Extremely Deformable Structures" D. Bigoni
Ed. Springer, Wien–New York, 2015
ISBN 978-3-7091-1876-4 doi 10.1007/978-3-7091-1877-1

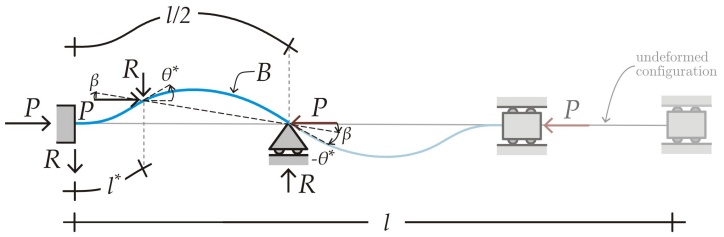

Figure 8. Deformed configuration for the second (antisymmetric) mode of the doubly clamped rod. Note that, thanks to the antisymmetry, one inflection point is located at the mid-span, so that the problem can be reduced to a clamped-guided rod of length $l/2$.

the horizontal axis, so that

$$\cos\beta = \frac{P}{\sqrt{P^2+R^2}}, \qquad \sin\beta = \frac{R}{\sqrt{P^2+R^2}}, \tag{73}$$

and the differential problem (72) can be rewritten as

$$\begin{aligned} &\psi''(s) + \gamma^2 \sin\psi(s) = 0 \quad \forall\, s \in [0, l/2] \\ &\psi(0) = \beta, \quad \psi'(l/2) = 0, \\ &\int_0^{l/2} \sin\left(\psi(s) - \beta\right) \mathrm{d}s = 0. \end{aligned} \tag{74}$$

Before proceeding with the derivation of the non-trivial solutions of the differential problem (74), let us define $\theta(l/2) = -\theta^*$, such that $\psi(l/2) = -\psi^* = -\theta^* + \beta$ and an inflection point exists at $s = l^*$, where the angle of rotation is defined as $\theta(l^*) = \theta^*$, with $\theta'(l^*) = 0$ (note that $\psi(l^*) = \psi^*$ and $\psi'(l^*) = 0$), see Fig. 8. Multiplication of equation $(74)_1$ by $\psi'(s)$ and integration in the variable s yields

$$\frac{\mathrm{d}}{\mathrm{d}s}\left[\frac{1}{2}(\psi'(s))^2 - \gamma^2 \cos\psi(s)\right] = 0, \tag{75}$$

so that imposition of the boundary conditions at the inflection point $s = l^*$ leads to

$$\psi'(s) = \pm\lambda\sqrt{2(\cos\psi(s) - \cos\psi^*)}, \tag{76}$$

In *CISM Lecture Notes No. 562*
"Extremely Deformable Structures" D. Bigoni
Ed. Springer, Wien–New York, 2015
ISBN 978-3-7091-1876-4 doi 10.1007/978-3-7091-1877-1

where the + (−) sign corresponds to a positive (negative) curvature. Keeping in mind the sketch of Fig. 8, equation (76) provides the following conditions

$$\begin{aligned} \psi'(s) &= +\lambda\sqrt{2\left(\cos\psi(s)-\cos\psi^*\right)} \quad \forall\, s\in(0,l^*)\,, \\ \psi'(s) &= -\lambda\sqrt{2\left(\cos\psi(s)-\cos\psi^*\right)} \quad \forall\, s\in(l^*,l/2)\,. \end{aligned} \tag{77}$$

It is a standard expedient to operate the following change of variables

$$\eta=\sin\frac{\psi^*}{2}, \qquad \eta\sin\omega(s)=\sin\frac{\psi(s)}{2}, \tag{78}$$

leading to the following differential equation

$$\frac{\mathrm{d}\,\omega(s)}{\mathrm{d}s}=\pm\gamma\sqrt{1-\eta^2\sin^2\omega(s)}. \tag{79}$$

Furthermore, the boundary conditions imply that

$$\omega(0)=\omega_\beta, \quad \omega(l^*)=\frac{\pi}{2}, \quad \omega\left(l/2\right)=-\frac{\pi}{2}, \tag{80}$$

where $\omega_\beta=\arcsin\left(\dfrac{1}{\eta}\sin\left(\dfrac{\beta}{2}\right)\right)$.

Therefore, separation of the variables and integration of the positive root of equation (79) between 0 and l^* yields

$$\int_0^{l^*}\gamma\mathrm{d}s=\int_{\omega_\beta}^{\frac{\pi}{2}}\frac{\mathrm{d}\omega}{\sqrt{1-\eta^2\sin^2\omega}}, \tag{81}$$

which expresses the non-trivial solution for l^*, related to η, γ and β as

$$l^*\gamma=\mathcal{K}(\eta)-\mathcal{K}\left(\omega_\beta,\eta\right), \tag{82}$$

where

$$\mathcal{K}(x,\eta)=\int_0^{x}\frac{\mathrm{d}\omega}{\sqrt{1-\eta^2\sin^2\omega}}, \tag{83}$$

is the incomplete elliptic integral of the first kind. Now, let us integrate the negative root of equation (79) between l^* and $l/2$. By using the Riemann theorem and the following property for the integral of even functions

$$-\int_{\frac{\pi}{2}}^{-\frac{\pi}{2}}\frac{\mathrm{d}\omega}{\sqrt{1-\eta^2\sin^2\omega}}=2\int_0^{\frac{\pi}{2}}\frac{\mathrm{d}\omega}{\sqrt{1-\eta^2\sin^2\omega}} \tag{84}$$

In *CISM Lecture Notes No. 562*
"Extremely Deformable Structures" D. Bigoni
Ed. Springer, Wien–New York, 2015
ISBN 978-3-7091-1876-4 doi 10.1007/978-3-7091-1877-1

we obtain

$$\gamma\left(\frac{l}{2}-l^*\right)=2\mathcal{K}(\eta), \tag{85}$$

so that, considering the periodicity of the boundary conditions (80) and using equations (82) and (85), we arrive at

$$\gamma l=2\left[(m+1)\mathcal{K}(\eta)-\mathcal{K}\left(\omega_\beta,\eta\right)\right] \qquad m=2,4,6,... \tag{86}$$

Note that equation (86) provides the relation between the external load P and the angles θ^* (through η and ψ^*) and β associated with the even, antisymmetric m–th buckled mode. The relation above provides one of the two equations to be solved for the problem under consideration. The other relation that allows for the solution of the problem can be obtained from equation $(72)_3$, which can be rewritten as

$$\int_0^{l^*}\sin\left(\psi(s)-\beta\right)\mathrm{d}s+\int_{l^*}^{l/2}\sin\left(\psi(s)-\beta\right)\mathrm{d}s=0, \tag{87}$$

so that, considering equations (78), we obtain

$$\begin{aligned}&\int_\beta^{\psi^*}\frac{\sin\psi\cos\beta}{\gamma\sqrt{2(\cos\psi-\cos\psi^*)}}\mathrm{d}\psi-\int_\beta^{\psi^*}\frac{\sin\beta\cos\psi}{\gamma\sqrt{2(\cos\psi-\cos\psi^*)}}\mathrm{d}\psi+\\&-\int_{\psi^*}^{-\psi^*}\frac{\sin\psi\cos\beta}{\gamma\sqrt{2(\cos\psi-\cos\psi^*)}}\mathrm{d}\psi+\int_{\psi^*}^{-\psi^*}\frac{\sin\beta\cos\psi}{\gamma\sqrt{2(\cos\psi-\cos\psi^*)}}\mathrm{d}\psi=0.\end{aligned} \tag{88}$$

The third integral in equation (88) is null (in fact the integrand is an odd function of ψ), whereas the other terms can be rewritten, by using equation (78) and by exploiting the following relations

$$\cos\psi=1-2\sin^2(\psi/2), \qquad \sin\psi=2\sin(\psi/2)\sqrt{1-\sin^2(\psi/2)},$$

in the final form (Mikata, 2007)

$$\begin{aligned}&-2\eta\cos\omega_\beta\left(1-2\eta^2\sin^2\omega_\beta\right)+2\eta\sin\omega_\beta\sqrt{1-\eta^2\sin^2\omega_\beta}\Big\{(m+1)\big[2E(\eta)+\\&-\mathcal{K}(\eta)\big]-\left[2E(\omega_\beta,\eta)-\mathcal{K}(\omega_\beta,\eta)\right]\Big\}=0, \qquad m=2,4,6,...\end{aligned} \tag{89}$$

Equations (86) and (89) are highly non-linear and allow for the determination of the nontrivial, antisymmetric equilibrium solution. The relation

In *CISM Lecture Notes No. 562*
"Extremely Deformable Structures" D. Bigoni
Ed. Springer, Wien–New York, 2015
ISBN 978-3-7091-1876-4 doi 10.1007/978-3-7091-1877-1

between β and θ^* (the former contained in ω_β and the latter in η) can be numerically obtained from equation (89) and used into equation (86) to obtain the relation $P - \theta^*$.

Our aim is now to compute the deformed shape of the buckled rod. To this purpose, we first integrate equation (79) from $s = 0$ to a generic point on the left of the inflection $s = l^*$

$$\int_0^s \gamma \mathrm{d}s = \int_{\omega_\beta}^{\omega(s)} \frac{\mathrm{d}\omega}{\sqrt{1 - \eta^2 \sin^2 \omega}}. \tag{90}$$

We then consider the decomposition (41), equation $(78)_2$, and the following properties of the elliptic function 'sn' (Byrd and Friedman, 1954)

$$\mathrm{sn}(-x + 2\mathcal{K}(\eta), \eta) = -\mathrm{sn}(-x, \eta) = \mathrm{sn}(x, \eta), \tag{91}$$

such that we obtain

$$\sin\left(\frac{\omega}{2}\right) = \eta \,\mathrm{sn}\left[\gamma s + \mathcal{K}(\omega_\beta, \eta), \eta\right] \quad \forall s \in [0, l]. \tag{92}$$

Finally, integration of the kinematic fields (11) provides the analytical expressions for the deformed shape of the rod, holding for $s \in (0, l)$, as[7]

[7] Equation (95) holds also for the structure (v.), together with

$$\gamma l = (2m + 1)\mathcal{K}(\eta) - \mathcal{K}\left(\omega_\beta, \eta\right), \qquad m = 1, 2, 3, ... \tag{93}$$

and

$$-2\eta \cos\omega_\beta \left(1 - 2\eta^2 \sin^2 \omega_\beta\right)$$
$$+2\eta \sin\omega_\beta \sqrt{1 - \eta^2 \sin^2 \omega_\beta} \left\{(2m + 1)\left[2E(\eta) - K(\eta)\right] - \left[2E(\omega_\beta, \eta) - K(\omega_\beta, \eta)\right]\right\} = 0, \tag{94}$$

defining the relation between P, β and θ^* associated with the m–th bifurcation mode.

In *CISM Lecture Notes No. 562*
"Extremely Deformable Structures" D. Bigoni
Ed. Springer, Wien–New York, 2015
ISBN 978-3-7091-1876-4 doi 10.1007/978-3-7091-1877-1

$$
\begin{aligned}
x_1(s) = &+\sin\beta\left[-\frac{2\eta}{\gamma}\mathrm{cn}\big(\gamma s+\mathcal{K}(\omega_\beta,\eta),\eta\big)+\frac{2\eta}{\gamma}\mathrm{cn}\big(\mathcal{K}(\omega_\beta,\eta),\eta\big)\right]\\
&+\cos\beta\Bigg\{-s+\frac{2}{\gamma}\Big[E\left[\mathrm{am}\left(\gamma s+\mathcal{K}(\omega_\beta,\eta),\eta\right),\eta\right]\\
&-E\left[\mathrm{am}\left(\mathcal{K}(\omega_\beta,\eta),\eta\right),\eta\right]\Big]\Bigg\},\\
x_2(s) = &\cos\beta\left[-\frac{2\eta}{\gamma}\mathrm{cn}\big(\gamma s+\mathcal{K}(\omega_\beta,\eta),\eta\big)+\frac{2\eta}{\gamma}\mathrm{cn}\big(\mathcal{K}(\omega_\beta,\eta),\eta\big)\right]\\
&-\sin\beta\Bigg\{-s+\frac{2}{\gamma}\Big[E\left[\mathrm{am}\left(\gamma s+\mathcal{K}(\omega_\beta,\eta),\eta\right),\eta\right]\\
&-E\left[\mathrm{am}\left(\mathcal{K}(\omega_\beta,\eta),\eta\right),\eta\right]\Big]\Bigg\}.
\end{aligned}
\tag{95}
$$

The displacement of the movable, clamped end, where the thrust is applied, can be obtained from equation (95), since $|u_1(l)| = l - x_1(l)$. For a given θ^* and a given even mode m, we can obtain β (through equation (89)), P (using equations (86) and (73)) and $|u_1(l)|$ (through equation $(95)_1$). The bifurcation diagram showing the load P (made dimensionless through multiplication by $l^2/(\pi^2 B)$) as a function of the displacement of the right movable end of the rod (divided by l) is shown in Fig. 9, together with the bifurcation diagram valid for the first and third symmetric buckling mode, see equation (71).

In-plane secondary bifurcation of the doubly clamped elastica It can be noticed from Fig. 9 that the doubly clamped elastica, i.e. the structure (vi.), exhibits a secondary bifurcation (marked with a circle) occurring when the two ends of the rod coincide, namely, when $\hat{\theta} = 130.7099°$ [8]. Under this condition, an '8-shaped' unstable equilibrium configuration is realized by the rod (see the sketches in Fig. 10) and vertical reactions are generated at its ends. By further increasing the external thrust P, the rod snaps onto the stable, 'S-shaped' configuration corresponding to the antisymmetric second mode (Domokos, 1994), see also Fig. 12. The stability of the equilibrium configurations will be addressed in the next section.

[8] The angle $\hat{\theta} = 130.7099°$ corresponds to the value $\kappa = 0.9089$, which is the root of the equation $2E(\kappa) - \mathcal{K}(\kappa) = 0$.

In *CISM Lecture Notes No. 562*
"Extremely Deformable Structures" D. Bigoni
Ed. Springer, Wien–New York, 2015
ISBN 978-3-7091-1876-4 doi 10.1007/978-3-7091-1877-1

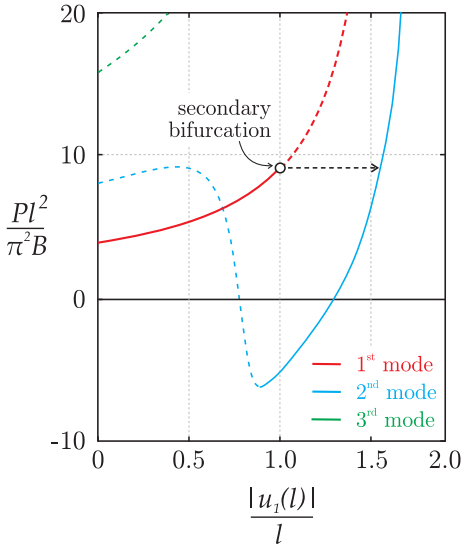

Figure 9. Dimensionless load $Pl^2/(\pi^2 B)$ for a doubly clamped rod versus the dimensionless displacement $|u_1(l)|/l$. The first three bifurcation points and branches are reported together with the secondary bifurcation point. The solid lines represent stable equilibrium configurations, while dashed curves correspond to unstable configurations. Note that the first branch becomes unstable after the secondary bifurcation point.

2.3 Stability of the elastica

The stability of the elastica equilibrium configurations can be judged by analyzing the sign of the second variation of the total potential energy $\mathcal{V}$ with respect to variations $\tilde{\theta}(s)$ compatible with the boundary conditions reported in equation (22), plus the supplementary condition

$$\int_0^l \tilde{\theta}(s)\cos\theta(s)\,\mathrm{d}s = 0, \tag{96}$$

following from the vanishing of the integral constraint in equations $(22)_1$, $(22)_5$, and $(22)_6$ and holding for the systems (i.), (v.) and (vi.), in which both the ends of the rod are constrained to null vertical displacements.

In *CISM Lecture Notes No. 562*
"Extremely Deformable Structures" D. Bigoni
Ed. Springer, Wien–New York, 2015
ISBN 978-3-7091-1876-4 doi 10.1007/978-3-7091-1877-1

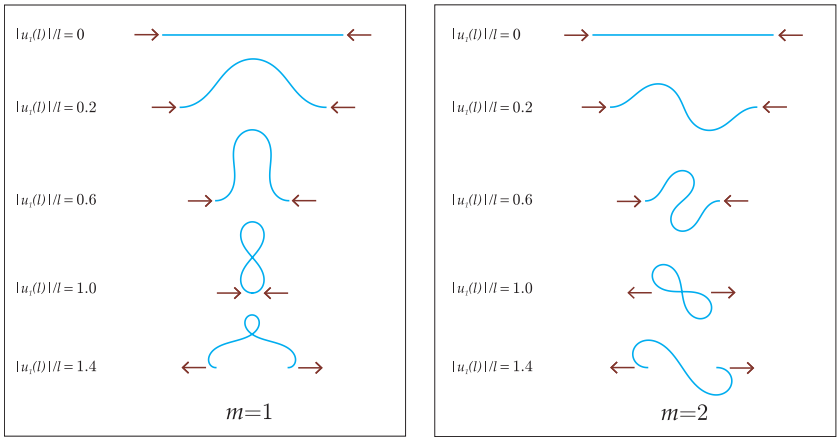

Figure 10. Deformed elastic lines for the first two modes $m = 1, 2$ (symmetric and antisymmetric) at different values of dimensionless displacements $|u_1(l)|/l = \{0, 0.2, 0.6, 1.0, 1.4\}$. The deformed shapes of the elastica represent the post-critical behaviour of the structure.

The second variation of the functional $\mathcal{V}$ can be computed as

$$\delta^2\mathcal{V} = \int_0^l \left[\left(\tilde{\theta}'(s)\right)^2 - \frac{P}{B}\tilde{\theta}^2(s)\cos\theta(s) + \frac{R}{B}\tilde{\theta}^2(s)\sin\theta(s) \right] \mathrm{d}s, \tag{97}$$

an equation that, using integration by parts

$$\int_0^l \left(\tilde{\theta}'(s)\right)^2 \mathrm{d}s = -\int_0^l \tilde{\theta}''(s)\tilde{\theta}(s)\,\mathrm{d}s,$$

yields

$$\delta^2\mathcal{V} = -\int_0^l \left[\tilde{\theta}''(s) + \frac{P}{B}\tilde{\theta}(s)\cos\theta(s) - \frac{R}{B}\tilde{\theta}(s)\sin\theta(s) \right] \tilde{\theta}(s)\,\mathrm{d}s, \tag{98}$$

for all kinematically admissible rotation fields $\tilde{\theta}(s)$, so that the *stability criterion* reads

$$\delta^2\mathcal{V} \begin{cases} > 0 & \text{stability}, \\ < 0 & \text{instability}. \end{cases} \tag{99}$$

In *CISM Lecture Notes No. 562*
"Extremely Deformable Structures" D. Bigoni
Ed. Springer, Wien–New York, 2015
ISBN 978-3-7091-1876-4 doi 10.1007/978-3-7091-1877-1

In order to treat condition (98), let us denote with $\phi_n(s)$ (where $s \in [0, l]$) the non-trivial solutions of the following Sturm-Liouville problem[9]

$$\phi_n^{''}(s) + \delta_n \left(\frac{P}{B} \cos\theta(s) - \frac{R}{B} \sin\theta(s) \right) \phi_n(s) = C_{Rn} \cos\theta(s), \tag{101}$$

subject to the following constraints representing the boundary conditions (21)

$$\begin{aligned}
&\text{i)} \quad \phi_n^{'}(0) = \phi_n^{'}(l) = 0 \quad \text{and} \quad \int_0^l \cos\theta(s)\phi_n(s)\mathrm{d}s = 0,\\
&\text{ii)} \quad \phi_n^{'}(0) = \phi_n(l) = 0,\\
&\text{iii)} \quad \phi_n(0) = \phi_n^{'}(l) = 0,\\
&\text{iv)} \quad \phi_n(0) = \phi_n(l) = 0,\\
&\text{v)} \quad \phi_n(0) = \phi_n^{'}(l) = 0 \quad \text{and} \quad \int_0^l \cos\theta(s)\phi_n(s)\mathrm{d}s = 0,\\
&\text{vi)} \quad \phi_n(0) = \phi_n(l) = 0 \quad \text{and} \quad \int_0^l \cos\theta(s)\phi_n(s)\mathrm{d}s = 0.
\end{aligned} \tag{102}$$

In the equations above, $\phi_n(s)$ are the eigenfunctions associated to the eigenvalues δ_n with weight function

$$\frac{P}{B} \cos\theta(s) - \frac{R}{B} \sin\theta(s), \tag{103}$$

and C_{Rn} is a constant that represents the isoperimetric constraint (96) and is 'linked' to R, so that for the unconstrained systems (for the systems (ii.), (iii.), (iv.), and (i.), but the last except when the two supports coincide) $C_{Rn} = 0$.

It is known (Broman, 1970) that: (i.) problem (101) admits a countably infinite set of eigenvalues δ_n and these can be arranged in an increasing sequence ($\delta_n < \delta_{n+1}$ for each integer n)[10], (ii.) $\delta_n \longrightarrow \infty$ when $n \longrightarrow \infty$,

[9] When isoperimetric constraints are not present, namely condition (96) is absent, stability can also be addressed by evaluating the eigenvalues δ_n of the following Sturm-Liouville problem

$$-\phi_n^{''}(s) - \left(\frac{P}{B} \cos\theta(s) - \frac{R}{B} \sin\theta(s) \right) \phi_n(s) = \delta_n \phi_n(s). \tag{100}$$

When at least one eigenvalue is negative, the associated equilibrium configuration is *unstable*, while, if all eigenvalues are positive, the equilibrium is *stable*, see Manning et al. (1998) and Hoffman et al. (2002).

[10] Note in addition that $\delta_n \geq 0$, see Broman (1970), pag. 41 – 44.

In *CISM Lecture Notes No. 562*
"Extremely Deformable Structures" D. Bigoni
Ed. Springer, Wien–New York, 2015
ISBN 978-3-7091-1876-4 doi 10.1007/978-3-7091-1877-1

(iii.) the system $\phi_n(s)$ is an orthogonal system with the weight function (103). Multiplication of the differential equation (101) by ϕ_n and integration between 0 and l yields (keeping into account the boundary conditions (102) and using integration by parts)

$$\delta_n \int_0^l \left(\frac{P}{B} \cos\theta(s) - \frac{R}{B} \sin\theta(s) \right) \phi_n^2(s)\, \mathrm{d}s = \int_0^l (\phi_n^{'}(s))^2\, \mathrm{d}s, \tag{104}$$

while writing equation (101) for the eigenfunction ϕ_m, that is

$$\phi_m^{''}(s) + \delta_m \left(\frac{P}{B} \cos\theta(s) - \frac{R}{B} \sin\theta(s) \right) \phi_m(s) = C_{Rm} \cos\theta(s), \tag{105}$$

and combining equations (101) and (105) multiplied by ϕ_m and ϕ_n, respectively, integration between 0 and l (taking into account the boundary conditions) provides the following orthogonality condition

$$\int_0^l \phi_n(s)\phi_m(s) \left(\frac{P}{B} \cos\theta(s) - \frac{R}{B} \sin\theta(s) \right) \mathrm{d}s = 0, \quad n \neq m. \tag{106}$$

Condition (104) defines a norm and equation (106) a weighted orthogonality condition for the functions $\phi_n(s)$ with weight function (103).

Therefore, the system $\phi_n(s)$ with weight function (103) can be used to provide a Fourier series representation (converging in the mean) to the square-integrable function $\tilde{\theta}(s)$,

$$\tilde{\theta}(s) = \sum_{n=1}^{\infty} c_n \phi_n(s), \tag{107}$$

where c_n are the Fourier coefficients.

We do not need to specify the coefficients c_n, rather we can simply substitute the Fourier representation (107) into condition (98) and keep into consideration equation (101) to obtain

$$\begin{aligned} \delta^2 \mathcal{V} = \int_0^l & \left[\sum_{n=1}^{\infty} (\delta_n - 1) c_n \phi_n(s) \left(\frac{P}{B} \cos\theta(s) - \frac{R}{B} \sin\theta(s) \right) \right] \\ & \times \left[\sum_{m=1}^{\infty} c_m \phi_m(s) \right] \mathrm{d}s, \end{aligned} \tag{108}$$

In *CISM Lecture Notes No. 562*
"Extremely Deformable Structures" D. Bigoni
Ed. Springer, Wien–New York, 2015
ISBN 978-3-7091-1876-4 doi 10.1007/978-3-7091-1877-1

which, employing conditions (104) and (106) finally becomes

$$\delta^2\mathcal{V} = \sum_{n=1}^{\infty}(1-\frac{1}{\delta_n})c_n^2\int_0^l(\phi_n^{'}(s))^2\,\mathrm{d}s \quad \begin{cases} >0 & \text{stability,} \\ \\ <0 & \text{instability,} \end{cases} \tag{109}$$

so that we arrive at the following stability requirement

$$\begin{cases} \delta_n \notin [0,1] & \text{stability,} \\ \\ \delta_n \in [0,1] & \text{instability,} \end{cases} \tag{110}$$

where δ_n are solutions of the Sturm-Liouville problem (101). The values $\delta_n = 0$ or $\delta_n = 1$ represent 'transition' points and thus are called 'critical'.

Stability of the simply supported elastica Let us consider first the stability of the straight configuration of a simply supported rod, such that $\cos\theta(s) = 1$. In this case, $R = C_{Rn} = 0$ and the Sturm-Liouville problem, equation (101), becomes

$$\phi_n^{''}(s) + \delta_n\frac{P}{B}\phi_n(s) = 0, \quad \phi_n^{'}(0) = \phi_n^{'}(l) = 0, \tag{111}$$

which has the nontrivial solutions

$$\phi_n(s) = \cos\frac{n\pi s}{l}, \quad \delta_n = \frac{P_n^{cr}}{P}, \tag{112}$$

where P_n^{cr} is the Euler's critical load corresponding to the n-th buckling mode, so that when $\delta_1 < 0$ or $\delta_1 > 1$ ($0 < \delta_1 < 1$) the straight configuration is stable (unstable) and $P < P_1^{cr}$ ($P > P_1^{cr}$)[11].

To judge the stability of the deformed configurations, we can substitute equation (40) into equation (50) to obtain

$$\cos\theta(s) = 1 - 2\kappa^2\,\mathrm{sn}^2\left[\left(\frac{s}{l}2m+1\right)\mathcal{K}(\kappa),\kappa\right], \tag{113}$$

[11] This statement hold also true for other structures when $R = 0$, namely systems (ii.), (iii.) and (iv.), whose nontrivial solutions are

ii) $\phi_n(s) = \cos\dfrac{\pi+2n\pi}{2}\dfrac{s}{l}$,

iii) $\phi_n(s) = \sin\dfrac{\pi+2n\pi}{2}\dfrac{s}{l}$,

iv) $\phi_n(s) = \sin\dfrac{n\pi s}{l}$,

with $\delta_n = \dfrac{P_n^{cr}}{P}$.

In *CISM Lecture Notes No. 562*
"Extremely Deformable Structures" D. Bigoni
Ed. Springer, Wien–New York, 2015
ISBN 978-3-7091-1876-4 doi 10.1007/978-3-7091-1877-1

and rewrite the Sturm-Liouville problem (101) using the dimensionless variable $\tilde{s} = s/l \in [0,1]$, so that, for a given mode m and rotation of the rod end $\kappa = \sin(\hat{\theta}/2)$, the *smallest eigenvalue* δ_m has to be determined as solution of

$$\phi_m^{''}(\tilde{s}) + \delta_m \, 4m^2 \mathcal{K}^2(\kappa) \left\{1 - 2\kappa^2 \, \mathrm{sn}^2 \left[(2m\,\tilde{s} + 1)\,\mathcal{K}(\kappa), \kappa\right]\right\} \phi_m(\tilde{s}) = 0, \quad (114)$$

(where now a prime denotes differentiation with respect to $\tilde{s}$) subject to the boundary conditions $(101)_2$, namely, $\phi_m^{'}(0) = \phi_m^{'}(1) = 0$.

The solutions of equation (114) can be easily computed by means of a numerical routine. As noticed by Kuznetsov and Levyakov (2002), a numerical procedure can be easily set, solving the differential equation (114) with the boundary conditions

$$\phi_m(0) = 1, \quad \phi_m^{'}(0) = 0, \quad (115)$$

so that the trivial solution is always eliminated and iterations on δ_m can be performed to match the condition $\phi_m^{'}(1) = 0$[12]. A numerical integration and iterations performed on the basis of a bisection method yield the graphs reported in Fig. 11.

The smallest eigenvalues δ_m for the first three modes $m = 1, 2, 3$ are reported versus the inclination $\hat{\theta}$ (in degrees) of the ends of the deformed rod. It is clear that the first mode, $m = 1$, is stable (the eigenvalues range between 1 and 10) until the two supports coincide for $\hat{\theta} = 130.7099°$, at which point the eigenvalues become discontinuous and fall to values within $[0,1]$ (in particular, $\delta_1 = 9.9228$ at $\hat{\theta} = 130.7°$ and $\delta_1 = 0.0059$ at $\hat{\theta} = 130.8°$). All modes higher than the first ($m = 2, 3$) are unstable with eigenvalues belonging to $[0,1]$. Note that for the considered modes, all the eigenvalues coincide when $\hat{\theta} \geq 130.7099°$.

With respect to the unstable configuration that occurs at $\hat{\theta} > 130.7099°$ for $m = 1$ (Maddocks, 1984), the instability mode and the corresponding 'self-intersecting' elastica is illustrated through an experiment in Bigoni (2012).

[12] The nontrivial solution of the Sturm-Liouville problem (101) for the systems (ii.), (iii.) and (iv.) can be numerically found using the following boundary conditions

ii) $\phi_m^{'}(0) = 0, \quad \phi_m(l) = 0, \quad \phi_m(0) = 1,$

iii) $\phi_m(0) = 0, \quad \phi_m^{'}(l) = 0, \quad \phi_m(l) = 1,$

iv) $\phi_m(0) = 0, \quad \phi_m(l) = 0, \quad \phi_m^{'}(0) = 1.$

In all these cases, the first mode, $m = 1$, is stable (all eigenvalues are external to $[0,1]$), while the higher modes $m = 2, 3$ are both unstable with at least one eigenvalue belonging to the interval [0,1].

In *CISM Lecture Notes No. 562*
"Extremely Deformable Structures" D. Bigoni
Ed. Springer, Wien–New York, 2015
ISBN 978-3-7091-1876-4 doi 10.1007/978-3-7091-1877-1

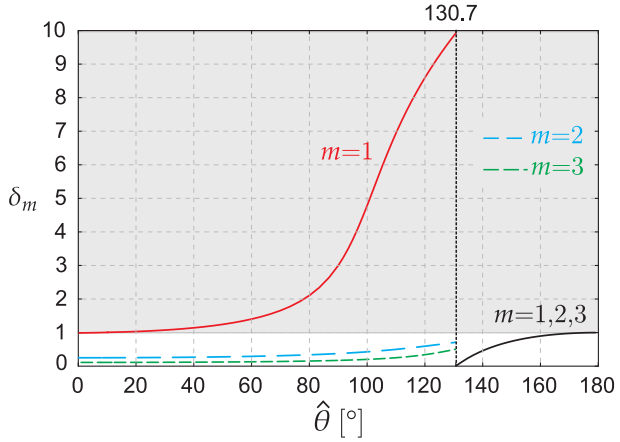

Figure 11. The smallest eigenvalues δ_m of the Sturm-Liouville problem (114) as functions of the rotation $\hat{\theta}$ of the ends of the simply supported rod. These determine the stability of the different modes of the elastica ($m = 1, 2, 3$ are investigated). The light gray region corresponds to stability, so that only the first mode $m = 1$ is stable and only until the two supports of the rod coincide, a situation corresponding to $\hat{\theta} = 130.7099°$.

We finally note that, with the proposed procedure to check stability, it is not directly possible to conclude that *all* the modes with $m > 1$ are unstable, though physical intuition suggests that this might be the case. In fact, our stability study for the modes $m = 2, 3$ substantiates the Love's (Love, 1927) statement according to which 'the instability of forms of the elastica with more than the smallest possible number of inflexions between the ends is well known as an experimental fact'.

Stability of the doubly clamped elastica We move now to the analysis of a doubly clamped rod: system (vi.) in Fig. 2. Stability of the straight configuration can be analyzed by noting that $\sin\theta(s) = 0$ and $\cos\theta(s) = 1$, so that the Sturm-Liouville problem (101) becomes

$$\phi_n''(s) + \delta_n \frac{P}{B}\phi_n(s) = C_{Rn}, \quad \phi_n(0) = \phi_n(l) = 0, \quad \int_0^l \phi_n(s)\mathrm{d}s = 0, \quad (116)$$

and admits solutions in the following form

$$\phi_n(s) = A_1 \cos\left(\sqrt{\frac{\delta_n P}{B}}\, s\right) + A_2 \sin\left(\sqrt{\frac{\delta_n P}{B}}\, s\right) + \frac{A_3 B}{\delta_n P}, \quad (117)$$

In *CISM Lecture Notes No. 562*
"Extremely Deformable Structures" D. Bigoni
Ed. Springer, Wien–New York, 2015
ISBN 978-3-7091-1876-4 doi 10.1007/978-3-7091-1877-1

where A_1, A_2, and A_3 are constants. By substitution of equation (117) into the boundary conditions of the Sturm-Liouville problem (116), we arrive at a system of homogeneous equations for A_1, A_2 and A_3 which can be written in the following matrix form

$$\begin{bmatrix} \dfrac{\delta_n P}{B} & 0 & 1 \\ \cos\left(\sqrt{\dfrac{\delta_n P}{B}}\, l\right) & \sin\left(\sqrt{\dfrac{\delta_n P}{B}}\, l\right) & \dfrac{B}{\delta_n P} \\ \dfrac{\delta_n P}{B}\sin\left(\sqrt{\dfrac{\delta_n P}{B}}\, l\right) & \dfrac{\delta_n P}{B}\cos\left(\sqrt{\dfrac{\delta_n P}{B}}\, l\right) & l \end{bmatrix} \begin{bmatrix} A_1 \\ A_2 \\ A_3 \end{bmatrix} = \begin{bmatrix} 0 \\ 0 \\ 0 \end{bmatrix}. \tag{118}$$

Therefore, nontrivial solutions of the system (117) can be obtained by imposing the vanishing of the determinant of its coefficient matrix. This leads to the following characteristic equation

$$2\left[\cos\left(\sqrt{\frac{\delta_n P}{B}}\, l\right) - 1\right] + \sqrt{\frac{\delta_n P}{B}}\, l \sin\left(\sqrt{\frac{\delta_n P}{B}}\, l\right) = 0, \tag{119}$$

which can be numerically solved for δ_n to show that the straight, natural configuration is stable only for $P < P_1^{cr}$. In fact, when $P > P_1^{cr}$ at least one eigenvalue δ_n belongs to the interval $[0, 1]$, and therefore the trivial configuration becomes unstable.

We explore in what follows the stability of the nontrivial equilibrium configurations and, to that purpose, we make use of the numerical procedure proposed by Levyakov and Kuznetsov (2010) while retaining as much as possible the notation employed by those authors[13]. We introduce the dimensionless arc-length $\tilde{s} = s/l \in [0, 1]$, such that the Sturm-Liouville problem (101) for a given mode m can be rewritten as

$$\phi_m''(\tilde{s}) + \delta_m\, L(\tilde{s})\, \phi_m(\tilde{s}) = C_{Rm}\, N(\tilde{s}), \tag{120}$$

where

$$L(\tilde{s}) = \begin{cases} \dfrac{P}{B}\cos\theta(\tilde{s}), & \text{for odd modes} \\ \dfrac{P}{B}\cos\theta(\tilde{s}) - \dfrac{R}{B}\sin\theta(\tilde{s}), & \text{for even modes} \end{cases} \tag{121}$$

[13] The analysis of stability with isoperimetric constraints can be also performed following Manning et al. (1998), Hoffman et al. (2002) and Manning (2009, 2014) through the conjugate point theory.

In *CISM Lecture Notes No. 562*
"Extremely Deformable Structures" D. Bigoni
Ed. Springer, Wien–New York, 2015
ISBN 978-3-7091-1876-4 doi 10.1007/978-3-7091-1877-1

and $N(\tilde{s}) = \cos\theta(\tilde{s})$. Notice that, for the odd buckling modes with $2m$ inflections, equation $(68)_1$ can be substituted into the definition of $\cos\theta(s)$ to obtain

$$\cos\theta(\tilde{s}) = 1 - 2\kappa^2 \,\mathrm{sn}^2\left[(2(m+1)\tilde{s})\,\mathcal{K}(\kappa), \kappa\right], \qquad m = 1, 3, 5, \tag{122}$$

which is a function of the rotation $\hat{\theta}$ of the rod at the inflection point.

For the even buckling modes with $2m+1$ inflections, we can write

$$\begin{aligned} \cos\theta(\tilde{s}) &= \sin\beta\left[2\eta\,\mathrm{sn}\left[\gamma\tilde{s} + \mathcal{K}(\omega_\beta, \eta), \eta\right]\mathrm{dn}\left[\gamma\tilde{s} + \mathcal{K}(\omega_\beta, \eta), \eta\right]\right] \\ &\quad + \cos\beta\left[1 - 2\eta^2\,\mathrm{sn}^2\left[\gamma\tilde{s} + \mathcal{K}(\omega_\beta, \eta), \eta\right]\right], \\ \sin\theta(\tilde{s}) &= \cos\beta\left[2\eta\,\mathrm{sn}\left[\gamma\tilde{s} + \mathcal{K}(\omega_\beta, \eta), \eta\right]\mathrm{dn}\left[\gamma\tilde{s} + \mathcal{K}(\omega_\beta, \eta), \eta\right]\right] \\ &\quad - \sin\beta\left[1 - 2\eta^2\,\mathrm{sn}^2\left[\gamma\tilde{s} + \mathcal{K}(\omega_\beta, \eta), \eta\right]\right], \end{aligned} \tag{123}$$

where β, γ, P and R can be computed through equations (89), (86) and (73) as functions of the rotation θ^* of the rod at inflection point. Notice also that equations (120) are subjected to the boundary conditions $\phi_m(0) = 0$, $\phi_m(1) = 0$[14] and to the additional constraint

$$\int_0^1 \phi_m(\tilde{s}) N(\tilde{s}) \mathrm{d}\tilde{s} = 0. \tag{124}$$

The numerical procedure to compute the eigenvalues δ_m consists in partitioning the interval $0 \le \tilde{s} \le 1$ into n segments of equal length $h = n^{-1}$, such that the coordinates of the starting points of the segments can be denoted by $s_{i-1} = h(i-1)$, with $i = 1, ..., n$. For the i-th segment, the functions $L(\tilde{s})$ and $N(\tilde{s})$ are approximated by their average values L_i and N_i as computed at the midpoint of the segment, so that equation (120) becomes

$$\phi_m''(\tilde{s}) + \delta_m\, L_i\, \phi_m(\tilde{s}) = C_{Rm}\, N_i, \tag{125}$$

an ordinary differential equation with constant coefficients, which solution is

$$\phi_m(\tilde{s}) = A_{1i} F_{1i}(\tilde{s} - \tilde{s}_{i-1}) + A_{2i} F_{2i}(\tilde{s} - \tilde{s}_{i-1}) + C_{Rm} \frac{N_i}{\delta_n\, L_i}. \tag{126}$$

In equation (126), A_{1i} and A_{2i} are constants, whereas the coefficients F_{1i} and F_{2i} are defined for $\delta_m L_i > 0$ as

$$F_{1i}(\tilde{s} - \tilde{s}_{i-1}) = \cos\, a_i(\tilde{s} - \tilde{s}_{i-1}), \quad F_{2i}(\tilde{s} - \tilde{s}_{i-1}) = \sin\, a_i(\tilde{s} - \tilde{s}_{i-1}), \tag{127}$$

[14] For the system (v.) the boundary conditions are $\phi_m(0) = \phi_m'(1) = 0$.

In *CISM Lecture Notes No. 562*
"Extremely Deformable Structures" D. Bigoni
Ed. Springer, Wien–New York, 2015
ISBN 978-3-7091-1876-4 doi 10.1007/978-3-7091-1877-1

while for $\delta_m L_i < 0$ they are

$$F_{1i}(\tilde{s}-\tilde{s}_{i-1}) = \cosh\, a_i(\tilde{s}-\tilde{s}_{i-1}), \quad F_{2i}(\tilde{s}-\tilde{s}_{i-1}) = \sinh\, a_i(\tilde{s}-\tilde{s}_{i-1}), \tag{128}$$

with $a_i = \sqrt{|\delta_m\, L_i|}$. Furthermore, the constants A_{1i} and A_{2i} can be expressed by means of $\phi_m(\tilde{s}_{i-1}) = \phi_{m,i-1}$ and by means of $\phi_m^{'}(\tilde{s}_{i-1}) = \phi_{m,i-1}^{'}$ as

$$A_{1i} = \phi_{m,i-1} - C_{Rm}\frac{N_i}{\delta_m\, L_i}, \qquad A_{2i} = \frac{\phi_{m,i-1}^{'}}{a_i}, \tag{129}$$

so that the quantity $\phi_m(\tilde{s}_i) = \phi_{m,i}$ at the right end of the segment is computed as

$$\phi_{m,i} = \phi_{m,i-1}\, F_{1i}(h) + \phi_{m,i-1}^{'}\, \frac{F_{2i}(h)}{a_i} + C_{Rm} N_i \frac{1-F_{1i}(h)}{\delta_m\, L_i}, \tag{130}$$

and its derivative reads

$$\phi_{m,i}^{'} = \phi_{m,i-1}\, F_{1i}^{'}(h) + \phi_{m,i-1}^{'}\, \frac{F_{2i}^{'}(h)}{a_i} - C_{Rm} N_i \frac{F_{1i}^{'}(h)}{\delta_m\, L_i}. \tag{131}$$

The general solution of equation (125) can now be constructed by using equations (130)-(131) and the condition of continuity of ϕ_m and $\phi_m^{'}$ at the extremities of every integration segment. Since equation (125) is linear, its general solution can be written as a combination of three particular solutions, that is

$$\phi_m(\tilde{s}) = c_1\varphi_1(\tilde{s}) + c_2\varphi_2(\tilde{s}) + C_{Rm}\varphi_3(\tilde{s}), \tag{132}$$

where c_1 and c_2 are constants. Using the following initial data

$$\begin{aligned} &\varphi_1(0) = 1, \qquad &&\varphi_1^{'}(0) = 0, \qquad &&C_{Rm} = 0, \\ &\varphi_2(0) = 0, \qquad &&\varphi_2^{'}(0) = 1, \qquad &&C_{Rm} = 0, \\ &\varphi_3(0) = 0, \qquad &&\varphi_3^{'}(0) = 0, \qquad &&C_{Rm} = 1, \end{aligned} \tag{133}$$

the functions $\varphi_i(\tilde{s})$ $(i = 1, 2, 3)$ can be constructed separately using the recurrence relations (130) and (131). Note that the particular solutions $\varphi_i(\tilde{s})$ can also be obtained by numerically solving the differential equation (120) –where $\phi_m(\tilde{s})$ is replaced by $\varphi_i(\tilde{s})$– through the function NDSolve of Mathematica© and imposing the boundary conditions (133).

By substituting the general solution (132) into the relation (124), the constraint can be rewritten as

$$\int_0^1 \left[c_1\varphi_1(\tilde{s}) + c_2\varphi_2(\tilde{s}) + C_{Rm}\varphi_3(\tilde{s})\right] N(\tilde{s})\mathrm{d}\tilde{s} = 0, \tag{134}$$

In *CISM Lecture Notes No. 562*
"Extremely Deformable Structures" D. Bigoni
Ed. Springer, Wien–New York, 2015
ISBN 978-3-7091-1876-4 doi 10.1007/978-3-7091-1877-1

while the boundary conditions $\phi_m(0) = 0$ and $\phi_m(1) = 0$ provide the following relations

$$\begin{aligned} &c_1 = 0, \\ &c_1\varphi_1(1) + c_2\varphi_2(1) + C_{Rm}\varphi_3(1) = 0. \end{aligned} \tag{135}$$

Equations (134) and $(135)_2$ represent an homogeneous system of algebraic equations for c_2 and C_{Rm}, which can be rewritten in matrix form as

$$\begin{bmatrix} \varphi_2(1) & \varphi_3(1) \\ \displaystyle\int_0^1 \varphi_2(\tilde{s})N(\tilde{s})\mathrm{d}\tilde{s} & \displaystyle\int_0^1 \varphi_3(\tilde{s})N(\tilde{s})\mathrm{d}\tilde{s} \end{bmatrix} \begin{bmatrix} c_2 \\ C_{Rm} \end{bmatrix} = \begin{bmatrix} 0 \\ 0 \end{bmatrix}. \tag{136}$$

Nontrivial solutions of the system (136) can be obtained by imposing the vanishing of the coefficient matrix's determinant Δ, so that, by varying the eigenvalue δ_m from 0 to 1, we can study the behaviour of Δ. When at least one value of $\delta_m \in [0, 1]$ exists such that the determinant vanishes, the non trivial solution of (132) satisfies the boundary conditions, so that the corresponding equilibrium configuration is *unstable*. Therefore, the stability of the equilibrium configurations of the doubly clamped elastica can be judged by analyzing the determinant Δ, which becomes[15]

$$\Delta = \varphi_2(1)\int_0^1 \varphi_3(\tilde{s})N(\tilde{s})\mathrm{d}\tilde{s} - \varphi_3(1)\int_0^1 \varphi_2(\tilde{s})N(\tilde{s})\mathrm{d}\tilde{s}, \tag{137}$$

where the integrals have to be numerically computed. The above mentioned numerical procedure arrives at the results reported in Fig. 9, where a stable (unstable) equilibrium path is depicted by a solid (dashed) curve. Note the secondary bifurcation point that is highlighted in the figure by a circle along the red path: once the critical configuration is attained such that the two ends of the rod touch, the elastic system snaps from the fist into the second mode.

In order to better understand the instability mode that takes place for $m = 1$ and $\hat{\theta} > 130.7099°$, a qualitative experiment was performed with a beam model made up of a PMMA strip of overall dimensions 490 mm ×

[15] For the elastic system (v.), the determinant of the coefficient matrix is $\Delta = \varphi_2'(1)\displaystyle\int_0^1 \varphi_3(\tilde{s})N(\tilde{s})\mathrm{d}\tilde{s} - \varphi_3'(1)\int_0^1 \varphi_2(\tilde{s})N(\tilde{s})\mathrm{d}\tilde{s}$.

In *CISM Lecture Notes No. 562*
"Extremely Deformable Structures" D. Bigoni
Ed. Springer, Wien–New York, 2015
ISBN 978-3-7091-1876-4 doi 10.1007/978-3-7091-1877-1

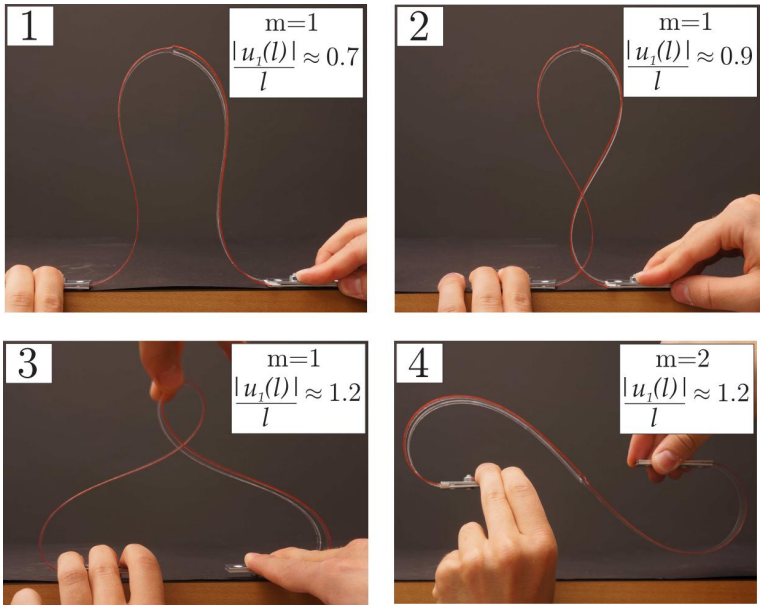

Figure 12. An experiment documenting the stability predictions obtained for the doubly clamped elastica. Configurations (1) and (2) of the first mode are stable for $|u_1(l)|/l < 1$; the photo (3) shows an unstable self-intersecting configuration of the first symmetric mode beyond the secondary bifurcation point (note that this configuration is held in position by hand, otherwise the structure would snap to configuration (4)). The configuration realized in (4) for the second 'S-shaped' antisymmetric mode is stable when $|u_1(l)|/l > 1$.

25 mm × 1.5 mm. The realization of the corresponding 'self-intersecting' configurations of the elastica was made possible by providing the model with a longitudinal 13 mm wide cut, dividing the strip into two parts (one 12 mm wide and the other '∩-shaped' with each of the two legs 6 mm wide). Four configurations of the model are reported in Fig. 12, fully confirming the theoretical expectations.

In *CISM Lecture Notes No. 562*
"Extremely Deformable Structures" D. Bigoni
Ed. Springer, Wien–New York, 2015
ISBN 978-3-7091-1876-4 doi 10.1007/978-3-7091-1877-1

3 Buckling under tensile dead loading

Buckling of elastic structures is known from the ancient times[16] and is typically associated to compressive forces[17]. Examples have been provided of elastic systems exhibiting buckling under a tensile load, such as those proposed by Ziegler (1977), though instability of these structures is clearly linked to the presence of compressed elements, which are responsible for buckling[18]. Another example of tensile buckling is that reported by Gajewski and Palej (1974), but in that case the applied load is not dead, rather it is provided by a container partially filled with a liquid, i.e., an example of live load.

The first example of an elastic system exhibiting buckling under tensile dead loading has been provided by Zaccaria et al. (2011) and is reported in Fig. 13. The one-degree-of-freedom structure comprises two rigid bars, hinged at their extremities and internally connected through a 'slider', a mechanical, frictionless device that keeps the two bars parallel, leaving the possibility of relative transversal sliding. Notice that the two bars composing the elastic system are subject to tension.

The buckling load and the equilibrium paths of the structure sketched in Fig. 13 can be easily computed with reference to its deformed shape, that is defined by the rotation ϕ. The elongation of the system reads

$$\Delta = 2l\left(\frac{1}{\cos\phi} - 1\right), \tag{138}$$

so that the total potential energy is

$$\mathcal{V}(\phi) = \frac{1}{2}k\phi^2 - 2Fl\left(\frac{1}{\cos\phi} - 1\right), \tag{139}$$

and the solutions of the equilibrium problem are

$$F = \frac{k}{2l}\frac{\phi\,\cos^2\phi}{\sin\phi}, \tag{140}$$

[16] In fact, it has been experimentally investigated by Pieter van Musschenbrok (1692-1761) and mathematically solved by Leonhard Euler (1707-1783).

[17] We refer here only to manifestations of structural instability and not of material instability such as necking of cylindrical bars, wrinkling of membranes and shear bands formation.

[18] For instance, one of these examples can be exemplified as a system of three rigid bars of equal length and connected by elastic hinges, whose natural configuration is the flat, folded configuration AB-BA-AB (like after flattening the Z letter). When the endpoints A and B are pulled apart, this system of 3 bars unfolds by an instability, but buckling here is clearly due to the element subject to compression.

In *CISM Lecture Notes No. 562*
"Extremely Deformable Structures" D. Bigoni
Ed. Springer, Wien–New York, 2015
ISBN 978-3-7091-1876-4 doi 10.1007/978-3-7091-1877-1

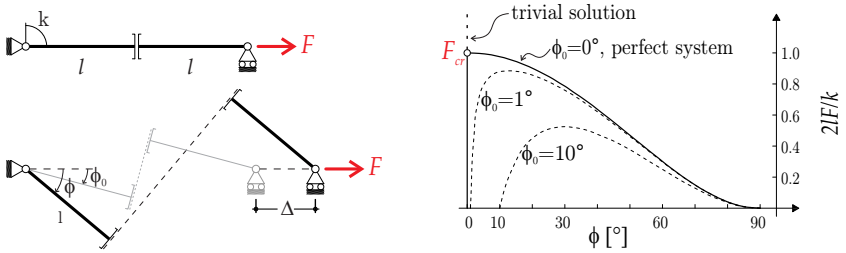

Figure 13. Bifurcation of an elastic one-degree-of-freedom system under *tensile dead loading*. The system comprises two rigid bars of length l that are internally jointed by a slider, whereas a rotational spring of stiffness k provides the elasticity to the structure. An imperfect system is also shown on the left, and its imperfection is given by the initial inclination ϕ_0 of the bars. Note that bifurcation is 'purely geometrical' and is induced by the internal constraint which transmits rotation, but not shear. The bifurcation diagram is reported on the right for $\phi_0 = \{0°, 1°, 10°\}$ and shows that the structure suffers softening once the critical load is attained.

plus the trivial solution $\phi = 0$, $\forall F$. The stability of the equilibrium solutions can be judged by studying the sign of the higher order derivatives of the total potential energy $\mathcal{V}(\phi)$. For the system being considered, we find that the trivial solution is stable up to the critical load

$$F_{cr} = \frac{k}{2l}, \tag{141}$$

while the nontrivial path, *evidencing softening*, is always unstable. The imperfect system, characterized by an initial rotation ϕ_0, can be analyzed in a similar manner. In fact, its elongation reads now as

$$\Delta = 2l\left(\frac{1}{\cos\phi} - \frac{1}{\cos\phi_0}\right), \tag{142}$$

and hence the total potential energy becomes a function of both the rotation ϕ and of the imperfection ϕ_0, that is

$$\mathcal{V}(\phi, \phi_0) = \frac{1}{2}k\left(\phi - \phi_0\right)^2 - 2Fl\left(\frac{1}{\cos\phi} - \frac{1}{\cos\phi_0}\right), \tag{143}$$

so that the equilibrium configurations are obtained as

$$F = \frac{k}{2l}\frac{\left(\phi - \phi_0\right)\cos^2\phi}{\sin\phi}. \tag{144}$$

In *CISM Lecture Notes No. 562*
"Extremely Deformable Structures" D. Bigoni
Ed. Springer, Wien–New York, 2015
ISBN 978-3-7091-1876-4 doi 10.1007/978-3-7091-1877-1

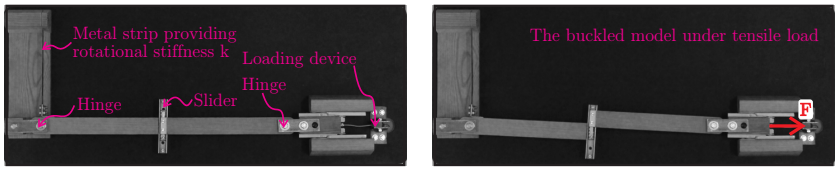

Figure 14. The practical realization of the one-degree-of-freedom system sketched in Fig. 13 (left). Two wooden rods have been employed and joined by means of a linear bearing, whereas elasticity has been provided to the system by clamping a thin metal strip to the hinge at the left end of the structure. The buckled configuration, as obtained by pulling with a dead load at the right end of the structure, is reported on the right.

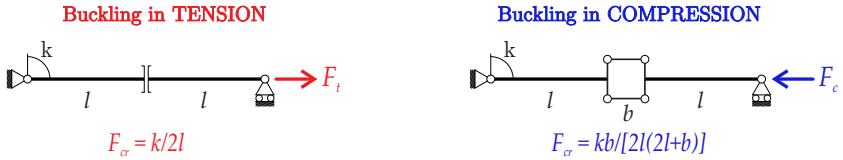

Figure 15. Two one-degree-of-freedom elastic systems composed by two rigid bars internally joined either with a slider (left) or with a parallelogram linkage (right). Although the linearized behaviour of the two examples is the same, it turns out that buckling under tensile loading is only feasible when the internal constraint is realized with a slider.

In order to provide experimental evidence of buckling under tensile dead loading, a physical model was built that resembles the structure sketched in Fig. 13. Specifically, two wooden rods were joined by means of two linear bearings (type Easy Rail SN22-80-500-610 from Rollon®), whereas elasticity was provided to the system by clamping a thin metal strip to its left end. The prototype is shown in Fig. 14, together with its buckled configuration as obtained by hanging a dead load at its right end.

Notice that bifurcation of the system in Fig. 13 is 'purely geometrical' and due to the presence of the internal constraint that connects the rigid bars. The central role of the slider in promoting tensile buckling can be further emphasized by comparing the two structural systems sketched in Fig. 15. Although the linearized behaviour of the two examples is the same, it turns out that by replacing the slider (left) with a parallelogram linkage (right) tensile buckling is suppressed and the structure can only buckle for a compressive force.

Once we have understood the crucial role played by the slider in favoring tensile buckling, we can exploit the concept to invent other structures with

In *CISM Lecture Notes No. 562*
"Extremely Deformable Structures" D. Bigoni
Ed. Springer, Wien–New York, 2015
ISBN 978-3-7091-1876-4 doi 10.1007/978-3-7091-1877-1

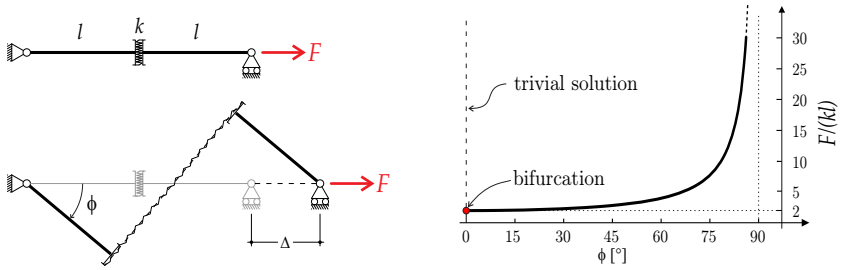

Figure 16. A one-degree-of-freedom elastic system (left) subject to a tensile dead load and having a linear elastic spring of stiffness k acting within the slider. Buckling of this structure still occurs by tensile loading, but now the post-critical behavior (right) exhibits hardening and hence is stable.

specific elastic responses.

A first example is that of Fig. 16, where the rotational spring has been replaced by a linear spring of stiffness k acting within the slider. It is worth noting that buckling still occurs for a tensile dead load, but now the post-critical behavior shows hardening instead of softening and consequently is stable.

Another example of structures buckling under tensile loading is shown in Fig. 17. A 'T-shaped' frame comprises three sliders and is simultaneously loaded by a horizontal force F and a vertical force αF, whereas elasticity is again provided by a rotational spring of stiffness k. Buckling and post-critical behaviour of this system are highly sensitive to the ratio α between the vertical and the horizontal force as shown on the right-hand side of Fig. 17.

A further generalization of the concepts presented above to elastic structures is possible by replacing the rigid bars of the system of Fig. 13 by two flexible elastic rods of equal length l and bending stiffness B, clamped at their outer extremities and internally connected by a slider, see Fig. 18. This elastic structure was first proposed and analyzed in detail by Zaccaria et al. (2011).

With reference to the sketch of Fig. 18, the determination of the critical loads of the system under consideration requires integration of the linearized equation of the elastica,

$$\frac{d^4v(z)}{dz^4} - \alpha^2 \operatorname{sgn}(F) \frac{d^2v(z)}{dz^2} = 0, \tag{145}$$

where F is assumed positive when tensile and $\alpha^2 = |F|/B$. Equation (145)

In *CISM Lecture Notes No. 562*
"Extremely Deformable Structures" D. Bigoni
Ed. Springer, Wien–New York, 2015
ISBN 978-3-7091-1876-4 doi 10.1007/978-3-7091-1877-1

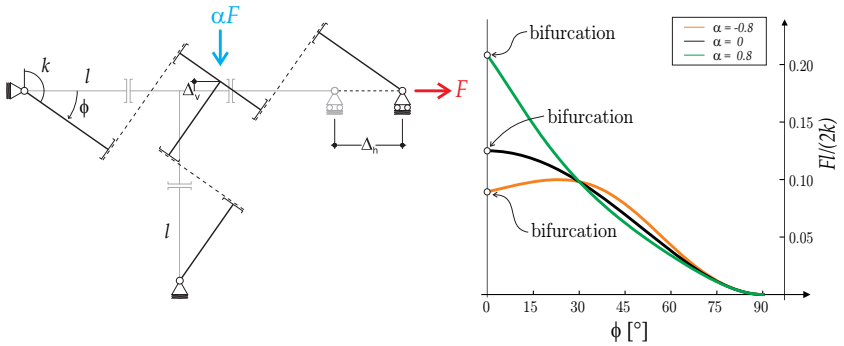

Figure 17. A 'T-shaped' frame exhibiting tensile buckling. The structure (left) comprises three sliders and is simultaneously subject to a horizontal force F and a vertical force αF; elasticity is provided by a rotational spring of stiffness k. Note that both buckling and post-critical behaviour (right) are significantly influenced by the ratio α between the two applied forces.

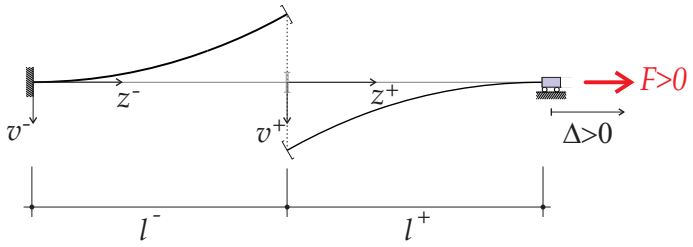

Figure 18. An elastic structure exhibiting buckling both under tensile ($F > 0$) and compressive ($F < 0$) loading. The structure has been designed by replacing the rigid bars of the one-degree-of-freedom system with elastic, flexible rods of length l and bending stiffness B.

In *CISM Lecture Notes No. 562*
"Extremely Deformable Structures" D. Bigoni
Ed. Springer, Wien–New York, 2015
ISBN 978-3-7091-1876-4 doi 10.1007/978-3-7091-1877-1

holds for both the left and right rod, denoted in the following by '$-$' and '$+$', respectively, and its integration requires the following boundary conditions to be imposed (a prime denotes differentiation with respect to z),

$$\begin{aligned}
&v_-(0) = v_-'(0) = v_+(l) = v_+'(l) = 0, && \text{zero displ. and rot. at clamps}\\
&v_-'(l) = v_+'(0), && \text{continuity of rot. at the slider}\\
&v_-'''(l) = v_+'''(0) = 0, && \text{zero shear force at the slider}\\
&v_-''(l) - v_+''(0) = \alpha^2\,\mathrm{sgn}(F)[v_-(l) - v_+(0)]. && \text{equilibrium of the slider}
\end{aligned} \tag{146}$$

For the case of elastic rods of equal length[19], we obtain the following characteristic equations for the critical loads

$$\begin{cases}
\sinh(\alpha\, l)\,[1 - \alpha\, l\, \tanh(\alpha\, l)] = 0, & \text{for } F > 0,\\
\sin(\alpha\, l)\,[1 + \alpha\, l\, \tan(\alpha\, l)] = 0, & \text{for } F < 0.
\end{cases} \tag{147}$$

showing that there is only one bifurcation load in tension, whereas there are infinite bifurcation loads in compression. Specifically, buckling of the elastic structure depicted in Fig. 18 occurs when

$$\frac{F_{cr}(2l)^2}{\pi^2 B} = \quad +0.58, \quad -3.17, \quad -4, \quad -15.19, \quad -16, \quad \ldots \tag{148}$$

A more detailed analysis of the structure, including the determination of its post-critical behaviour, can be developed through integration of the nonlinear equation of the elastica. To attack this problem we start by employing the local reference systems shown in Fig. 19, and then we impose one global kinematic compatibility condition and three equilibrium conditions. These are listed in the following.

- ◇ Kinematic compatibility condition: the jump in displacement across the slider (measured orthogonally to the line of the elastica), i.e. Δ_s, can be related to the angle of rotation of the slider Φ_s as

$$\left[x_1^-(l^-) + x_1^+(l^+)\right]\tan\Phi_s + x_2^-(l^-) + x_2^+(l^+) + \Delta_s = 0, \tag{149}$$

  where $x_1^\pm(l^\pm)$ and $x_2^\pm(l^\pm)$ are the coordinates of the elastica evaluated at $s = l^\pm$. Note that Φ_s is assumed positive when anticlockwise and Δ_s is not restricted in sign (negative in the case of Fig. 19).

[19] The treatment of the more general case of two rods of different length is reported in Zaccaria et al. (2011).

In *CISM Lecture Notes No. 562*
"Extremely Deformable Structures" D. Bigoni
Ed. Springer, Wien–New York, 2015
ISBN 978-3-7091-1876-4 doi 10.1007/978-3-7091-1877-1

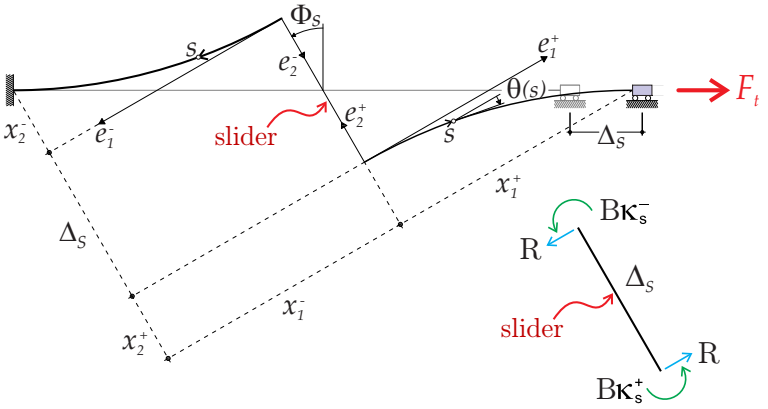

Figure 19. A sketch of the planar problem of the elastica at large displacements under tensile axial loading. Note the local reference systems employed to carry out the analysis.

◇ Global equilibrium of the structure: since the slider can only transmit a moment and a force R orthogonal to it, equilibrium of the structure requires that (see the inset of Fig. 19)

$$R = \frac{F}{\cos \Phi_s}, \tag{150}$$

where F is the external, axial force applied to the system, assumed positive (negative) when tensile (compressive). Since $\Phi_s \in [-\pi/2, \pi/2]$, R is positive (negative) for tensile (compressive) loading. Notice also that with the above definitions we have

$$\theta^+(0) = \theta^-(0) = 0, \quad \theta^+(l^+) = \theta^-(l^-) = -\Phi_s. \tag{151}$$

◇ Rotational equilibrium of the slider:

$$\kappa_s^- + \kappa_s^+ = \frac{R}{B}\Delta_s, \tag{152}$$

where B is the bending stiffness of the rods and $\kappa_s^\pm$ denotes their curvature evaluated at $s = l^\pm$. Note that B is positive by definition, but R, $\kappa_s^\pm$ and Δ_s can take any sign.

◇ Equation of the elastica for both the rods:

$$\theta''(s) - \frac{R}{B}\sin\theta(s) = 0, \tag{153}$$

In *CISM Lecture Notes No. 562*
"Extremely Deformable Structures" D. Bigoni
Ed. Springer, Wien–New York, 2015
ISBN 978-3-7091-1876-4 doi 10.1007/978-3-7091-1877-1

where $\theta(s)$ is the rotation of the normal to the elastica at each point s, assumed positive when anticlockwise.

Equation (153) is usually[20] written with a sign '+' replacing the sign '−', meaning that R is assumed positive when compressive.

Integration of the elastica (details can be found in Zaccaria et al., 2011) leads to the coordinates x_1 and x_2 of the deformed elastic rod expressed in terms of the co-ordinate $u = s/\xi\sqrt{|R|/B}$, that is

$$\begin{cases} x_1 = \dfrac{1}{\xi\,\tilde{\alpha}}\left[\left(2-\xi^2\right)u - 2\,\mathrm{E}\left[\mathrm{am}\left[u,\xi\right],\xi\right] + 2\xi^2 \mathrm{sn}\left[u,\xi\right]\mathrm{cn}\left[u,\xi\right]\right], \\ x_2 = \dfrac{2}{\xi\,\tilde{\alpha}}\sqrt{1-\xi^2}\left(\dfrac{1-\mathrm{dn}\left[u,\xi\right]}{\mathrm{dn}\left[u,\xi\right]}\right), \end{cases} \tag{154}$$

for a tensile ($R > 0$) axial load, whereas for a compressive ($R < 0$) axial load

$$\begin{cases} x_1 = \dfrac{1}{\xi\,\tilde{\alpha}}\left[\left(\xi^2-2\right)u + 2\,\mathrm{E}\left[\mathrm{am}\left[u,\xi\right],\xi\right]\right], \\ x_2 = \dfrac{2}{\xi\,\tilde{\alpha}}\left(1-\mathrm{dn}\left[u,\xi\right]\right). \end{cases} \tag{155}$$

To derive equations (154)-(155), the constants of integration have been chosen such that x_1 and x_2 vanish at $s = 0$, whereas $\tilde{\alpha} = \sqrt{|R|/B}$. Moreover, am, dn, sn, cn and E are elliptic functions (Byrd and Friedman, 1971) of modulus $\xi = 2\tilde{\alpha}/\sqrt{\kappa_s^2 + 4\tilde{\alpha}^2 H(R)}$, in which H denotes the Heaviside step function.

With reference to Fig. 19, we may also note that the horizontal displacement Δ_c of the right clamp can be written in the form

$$\Delta_c = \frac{x_1^-(l^-) + x_1^+(l^+)}{\cos\Phi_s} - \left(l^+ + l^-\right). \tag{156}$$

Finding the axial load F as a function of the slider rotation Φ_s, or similarly as a function of the end displacement Δ_c, is not particularly difficult, although the procedure involves the numerical solution of the nonlinear equation that arises from the global kinematic compatibility condition (149), see Zaccaria et al. (2011) for details. For reference, computed deformed elastica in tension and compression (the first mode in tension and the first mode in compression) are reported in Fig. 20.

[20] See equation (24), where R has be taken null and P plays the role of R in equation (153).

In *CISM Lecture Notes No. 562*
"Extremely Deformable Structures" D. Bigoni
Ed. Springer, Wien–New York, 2015
ISBN 978-3-7091-1876-4 doi 10.1007/978-3-7091-1877-1

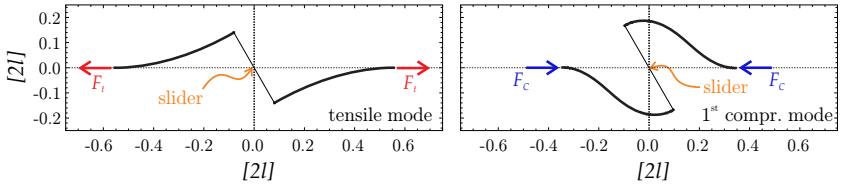

Figure 20. Deformed shapes in tension (left) and in compression (right) of the structure shown in Fig. 19 (with rods of equal length) at a slider rotation of 30°. Note that the scale of the axes is $2l$.

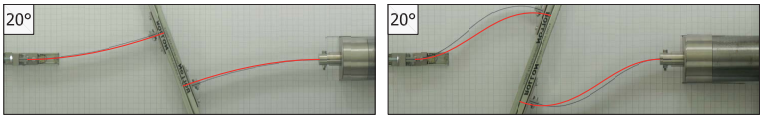

Figure 21. Computed deformed shapes (red lines) superimposed on photos taken during experimentation. Note the remarkable agreement between theory and experiments both in the case of a test under tensile (left) and compressive (right) loading.

The theoretical predictions have been compared with experimental results obtained by means of the structural model shown in the inset of Fig. 22. A first comparison is reported in Fig. 21, where computed deformed shapes (red, solid curves) have been superimposed on photos taken during experimentation. Note the remarkable agreement between theory and experiments both in the case of a test under tensile and compressive loading. An additional comparison between experiments and theory is reported in Fig. 22 in terms of buckling load and post-critical response of the elastic structure shown in the inset.

As a final remark, we emphasize the analogy between the deformed shape of an elastic rod buckled in tension and the shape of a water meniscus in a capillary channel (already pointed out, see Fig. 7). This can be appreciated from the comparison reported in Fig. 23 and is a consequence of the fact that both the physical phenomena are governed by the same differential equation.

4 Influence of constraint's curvature on buckling

The influence of the constraints upon the stability of elastic, structural systems has been pointed out by Zaccaria et al. (2011), showing that a

In *CISM Lecture Notes No. 562*
"Extremely Deformable Structures" D. Bigoni
Ed. Springer, Wien–New York, 2015
ISBN 978-3-7091-1876-4 doi 10.1007/978-3-7091-1877-1

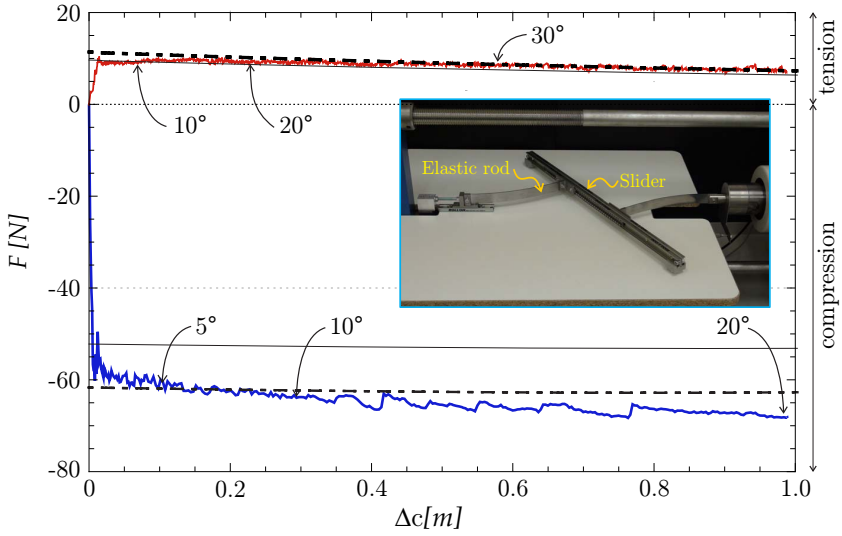

Figure 22. Buckling and post-critical response of the elastic system: theoretical prediction (black dashed line) versus experiments reported in red (tension) and blue (compression) lines. Numbers in degrees refer to slider rotations.

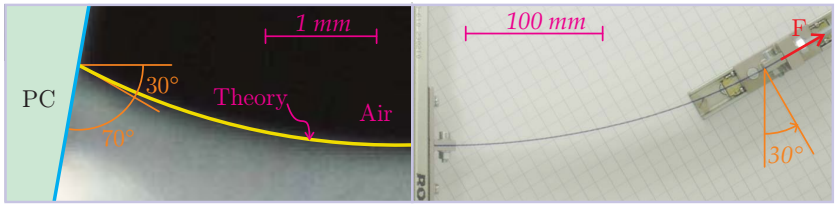

Water meniscus in air Elastic rod in tension

Figure 23. The shape of a water meniscus in a capillary channel (left: photo near a water-air-Polycarbonate contact superimposed to the solution of the elastica, highlighted with a yellow line) versus the elastic line of a rod buckled under tensile loading (right: photo taken during an experiment).

In *CISM Lecture Notes No. 562*
"Extremely Deformable Structures" D. Bigoni
Ed. Springer, Wien–New York, 2015
ISBN 978-3-7091-1876-4 doi 10.1007/978-3-7091-1877-1

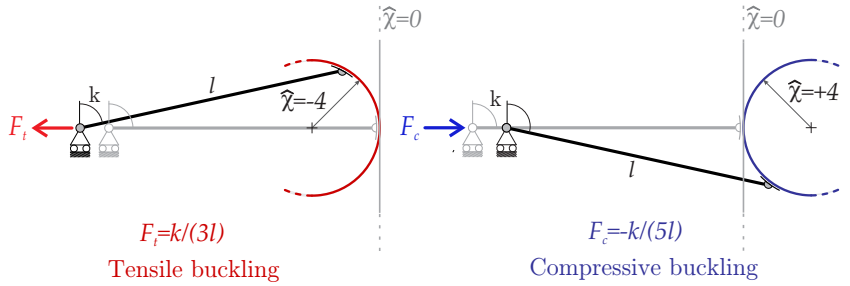

Figure 24. A one-degree-of-freedom structure (with a rotational elastic spring at its left end) evidencing compressive (right) or tensile (left) buckling as a function of the curvature of the constraint (a circular profile with constant curvature, $\widehat{\chi} = \pm 4$) along which the pin on the right of the structure has to slide.

slider can induce tensile buckling of elastic structures, and by Bigoni et al. (2012, 2014a), demonstrating the deep influence of the constraint curvature on buckling and post-critical behaviour.

In fact, the curvature of a constraint plays a fundamental role in a bifurcation problem, as highlighted by the one-degree-of-freedom structure shown in Fig. 24, where a rigid bar is connected to a rotational spring on its left end and to a roller on its right end, which is constrained to move along a circle of radius R_c centered on the bar's axis. The structure is subject to a horizontal force F, so that when this load is compressive and the circle degenerates to a line (null curvature), the structure buckles at the compressive force $F = -k/l$. But the curvature of the circle strongly affects the critical load, which results to be *tensile* in the case of negative curvature ($F_t = k/(3l)$, for $\widehat{\chi} = l/R_c = -4$, see Fig. 24 on the left) and compressive in the case of positive curvature ($F_c = -k/(5l)$, for $\widehat{\chi} = l/R_c = 4$, see Fig. 24 on the right).

To extend this analysis to systems with diffuse elasticity, the rigid bar can be replaced by an elastic rod, as shown in Fig. 25, and the fully nonlinear problem can be solved through integration of the elastica, see Bigoni et al. (2012) for the treatment. The analytical solution to this problem is reported in Fig. 26 and is compared with results of experiments shown as orange lines. A remarkable feature of the system is the force reversal found along the post-critical behaviour both in tension and in compression (points '2' and '5' in the figure).

Since the constraint's curvature deeply influences both buckling and post-critical behaviour, one may think to exploit this feature in an alter-

In *CISM Lecture Notes No. 562*
"Extremely Deformable Structures" D. Bigoni
Ed. Springer, Wien–New York, 2015
ISBN 978-3-7091-1876-4 doi 10.1007/978-3-7091-1877-1

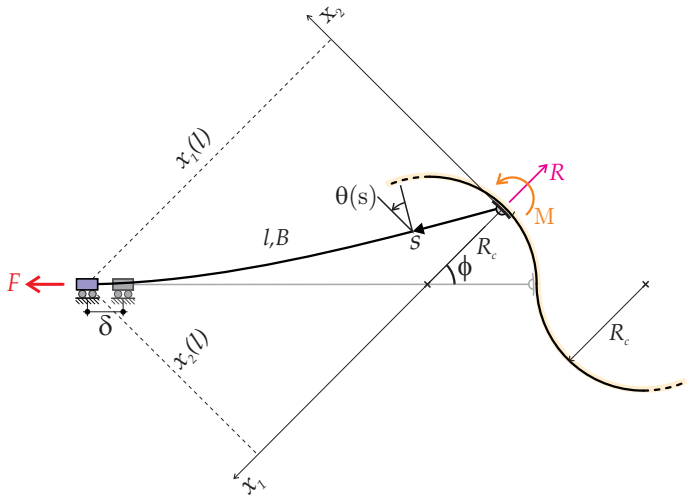

Figure 25. The elastica problem of a rod clamped at the left end and constrained to slide with a roller along a circle at its right end. Note the reference system employed in the analysis.

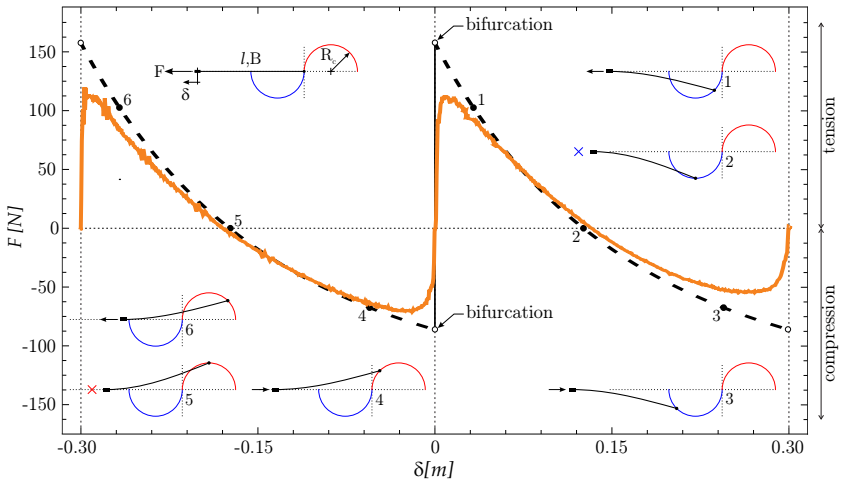

Figure 26. Load/displacement experimental results (orange, solid line) versus theoretical prediction (black, dashed line) for an elastic rod constrained to slide along a 'S-shaped', bi-circular profile. Deformed shapes are also reported in the insets.

In *CISM Lecture Notes No. 562*
"Extremely Deformable Structures" D. Bigoni
Ed. Springer, Wien–New York, 2015
ISBN 978-3-7091-1876-4 doi 10.1007/978-3-7091-1877-1

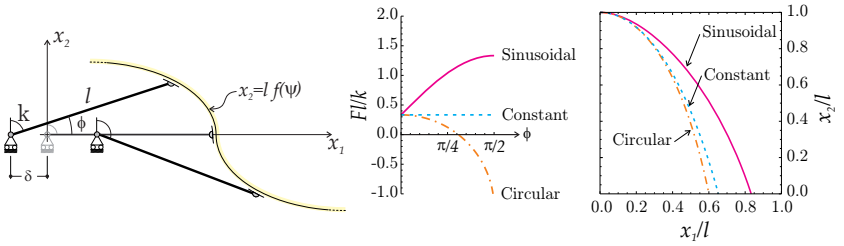

Figure 27. A one-degree-of-freedom structure (left) with one end constrained to slide along a generic, curved profile. Three distinct post-critical behaviours are shown (centre) together with the shape of the constraint (right) that was designed to realize them. Specifically, the three force-versus-rotation relations correspond to a sinusoidal, a circular and a constant (or 'neutral') elastic behaviour.

native way. In other words, one could think to design the shape of the constraint's profile (on which one end of the elastic system is prescribed to move) to obtain a 'desired post-critical behaviour' (for details see Bigoni et al., 2012). Fig. 27 reports on three examples of elastic structures with curved profiles designed to obtain a sinusoidal, a circular, and a constant post-critical response in terms of force F versus rotation ϕ. Furthermore, experiments have been performed to confirm the relation between the geometry of the constraint's profile and post-critical response of elastic systems. As an example, Fig. 28 shows the setup that was used to carry out experiments on the one-degree-of freedom structure exhibiting a 'neutral' post-critical behaviour shown in Fig. 27 (for further details see Bigoni et al., 2012, 2014a).

5 Eshelby-like forces in elastic structures with variable length

Eshelby (1956) introduced the concept of configurational force, acting on inhomogeneities or defects in solids to move them until the total potential energy is minimized. In other words, considering a defect in an elastic body characterized by a configurational parameter ν, so that the total potential energy of the body is $\mathcal{V}(\nu)$, the configurational force is defined as

$$-\frac{\partial \mathcal{V}(\nu)}{\partial \nu}.$$

The Peach-Koehler force acting on a dislocation, the crack-extension force of fracture mechanics, and the material force developing on a phase boundary

In *CISM Lecture Notes No. 562*
"Extremely Deformable Structures" D. Bigoni
Ed. Springer, Wien–New York, 2015
ISBN 978-3-7091-1876-4 doi 10.1007/978-3-7091-1877-1

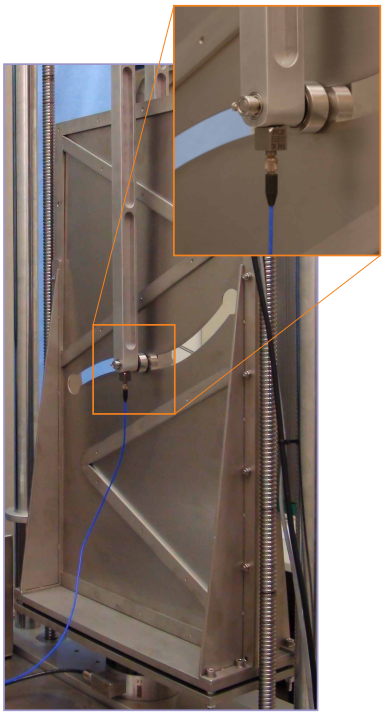

Figure 28. The experimental setup employed to test the one-degree-of-freedom system prescribed to move along a profile that was designed to provide a constant post-critical response.

in a solid under loading are all known examples of Eshelby forces, so that they are considered nowadays the cornerstone of a well-developed theory (see for instance Gurtin, 2000; Kienzler and Herrmann, 2000; Maugin, 1993, 2011; Dascalu et al., 2010; Bigoni and Deseri, 2011). The purpose of this section is to show that Eshelby-like forces can develop in elastic structures when the configuration of the structure changes. The simplest example of evidence of a configurational force is shown in Fig. 29, where an elastic inextensible rod of total length $\bar{l}$, bending stiffness B, and straight in its undeformed configuration is constrained with a sliding sleeve on the left end and loaded with a transversal dead load P at the other end. The sliding sleeve fully constrains rotation and vertical displacement for the part of the rod currently contained in it, but leaves the possibility of free

In *CISM Lecture Notes No. 562*
"Extremely Deformable Structures" D. Bigoni
Ed. Springer, Wien–New York, 2015
ISBN 978-3-7091-1876-4 doi 10.1007/978-3-7091-1877-1

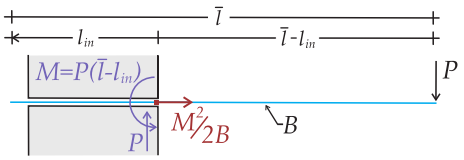

Figure 29. An elastic rod of total length $\bar{l}$, constrained with a sliding sleeve on its left, is subject to a transversal load P on its right end. Equilibrium of this configuration is impossible, because a horizontal Eshelby-like force is generated in the sliding sleeve. The Eshelby-like force equals the square of the bending moment at the end of the sliding sleeve, $P^2(\bar{l}-l_{in})^2$, divided by twice the flexural bending stiffness of the rod, $2B$.

horizontal sliding (without friction). Therefore, the elastic system has a variable length $\bar{l}-l_{in}$ and the total potential energy $\mathcal{V}(l_{in})$ can be evaluated as a function of the free configurational parameter l_{in}, defining the amount of the rod constrained by the sliding sleeve. Restricting for the moment attention to small displacements of the rod, the linear elastic solution for this structure yields a transverse displacement at the point of application of the force equal to $P(\bar{l}-l_{in})^3/(3B)$, so that the total potential energy is

$$\mathcal{V}(l_{in}) = \frac{P^2(\bar{l}-l_{in})^3}{6B}. \tag{157}$$

In analogy with the Eshelby concept of configurational force, the derivative of the potential energy (157) with respect to the configurational parameter l_{in} yields the following non-null horizontal Eshelby-like force

$$-\frac{\partial \mathcal{V}(l_{in})}{\partial l_{in}} = \frac{P^2(\bar{l}-l_{in})^2}{2B} = \frac{M^2}{2B}. \tag{158}$$

Note that the equilibrium for the elastic system (Fig. 29) is impossible since the Eshelby-like force (158) is not null except in the trivial cases of $P=0$ or $l_{in}=\bar{l}$. The Eshelby-like force can also be expressed in terms of the transverse displacement at the loaded end of the structure $v_{\bar{l}} = P(\bar{l}-l_{in})^3/(3B)$ as

$$-\frac{\partial \mathcal{V}(l_{in})}{\partial l_{in}} = \frac{9B}{2(\bar{l}-l_{in})^2}\left(\frac{v_{\bar{l}}}{\bar{l}-l_{in}}\right)^2, \tag{159}$$

showing that for small deflections the force is small, but, as we will see later, this force grows and becomes dominant when displacements are large.

Following Bigoni et al. (2015), an inextensible elastic rod (straight in its unloaded configuration, with bending stiffness B and total length $\bar{l}$) is considered now in a more general setting. In particular, the rod is constrained

In *CISM Lecture Notes No. 562*
"Extremely Deformable Structures" D. Bigoni
Ed. Springer, Wien–New York, 2015
ISBN 978-3-7091-1876-4 doi 10.1007/978-3-7091-1877-1

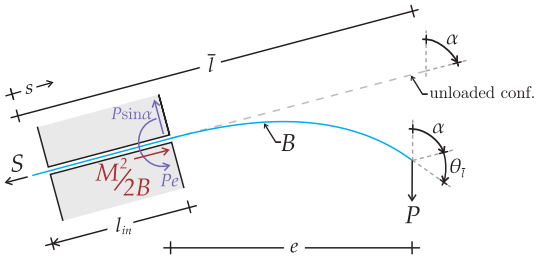

Figure 30. Structural scheme of the elastic system used to demonstrate an Eshelby-like force. The elastic rod of total length $\bar{l}$ is subject to a dead vertical load P on its right end, is constrained with a sliding sleeve inclined at an angle α (with respect to the vertical) and has a axial dead force S applied at its left end. The presence of the Eshelby-like force $M^2/(2B)$ influences the force S at equilibrium, which results different from $P\cos\alpha$. The other reactions at the end of the sliding sleeve are the force $P\sin\alpha$ perpendicular to the axis of the sleeve and the counterclockwise reaction moment Pe.

with a sliding sleeve as in Fig. 29, but is now inclined with respect to the horizontal direction and is subject at one end to an axial (dead) force S, while the other end is subject to a dead load P (inclined at an angle α), see Fig. 30.

Introducing the curvilinear coordinate $s \in [0, \bar{l}]$, the length l_{in} of the segment of the rod inside the sliding sleeve, and the rotation $\theta(s)$ of the rod's axis, the constraint imposes the condition

$$\theta(s) = 0 \text{ for } s \in [0, l_{in}].$$

Denoting by a prime the derivative with respect to s, the bending moment along the elastic rod is $M(s) = B\theta'(s)$, so that at the loaded end of the rod, the zero-moment boundary condition $\theta'(\bar{l}) = 0$ has to hold.

The total potential energy of the system is

$$\begin{aligned}\mathcal{V}(\theta(s), l_{in}) = B\int_{l_{in}}^{\bar{l}} \frac{\left[\theta'(s)\right]^2}{2}\mathrm{d}s - P\Bigg[\bar{l}\cos\alpha - \cos\alpha\int_{l_{in}}^{\bar{l}}\cos\theta(s)\mathrm{d}s \\ + \sin\alpha\int_{l_{in}}^{\bar{l}}\sin\theta(s)\mathrm{d}s\Bigg] - S\,l_{in},\end{aligned} \tag{160}$$

In *CISM Lecture Notes No. 562*
"Extremely Deformable Structures" D. Bigoni
Ed. Springer, Wien–New York, 2015
ISBN 978-3-7091-1876-4 doi 10.1007/978-3-7091-1877-1

which at equilibrium becomes

$$\mathcal{V}(\theta_{eq}(s,l_{eq}),l_{eq}) = B\int_{l_{eq}}^{\bar{l}} \frac{\left[\theta'_{eq}(s,l_{eq})\right]^2}{2}\mathrm{d}s - S\,l_{eq} - P\Bigg[\bar{l}\cos\alpha - \cos\alpha\int_{l_{eq}}^{\bar{l}}\cos\theta_{eq}(s,l_{eq})\mathrm{d}s + \sin\alpha\int_{l_{eq}}^{\bar{l}}\sin\theta_{eq}(s,l_{eq})\mathrm{d}s\Bigg], \tag{161}$$

where l_{eq} is the length of the amount of the elastic rod inside the sliding sleeve and θ_{eq} is the rotation of the rod's axis at the equilibrium.

The Eshelbian force related to the presence of the sliding sleeve can be calculated by differentiating with respect to l_{eq} the total potential energy at equilibrium, equation (161), which, considering the Leibniz's rule[21], becomes

$$\frac{\partial\mathcal{V}(l_{eq})}{\partial l_{eq}} = B\int_{l_{eq}}^{\bar{l}}\theta'_{eq}(s)\frac{\partial\theta'_{eq}(s)}{\partial l_{eq}}\mathrm{d}s + P\Bigg[\cos\alpha\int_{l_{eq}}^{\bar{l}}\sin\theta_{eq}(s)\frac{\partial\theta_{eq}(s)}{\partial l_{eq}}\mathrm{d}s - \sin\alpha\int_{l_{eq}}^{\bar{l}}\cos\theta_{eq}(s)\frac{\partial\theta_{eq}(s)}{\partial l_{eq}}\mathrm{d}s\Bigg] - P\cos\alpha - B\frac{[\theta'_{eq}(l_{eq})]^2}{2} - S. \tag{163}$$

From equation (163), keeping into account integration by parts

$$\theta'_{eq}\frac{\partial\theta'_{eq}}{\partial l_{eq}} = \left(\theta'_{eq}\frac{\partial\theta_{eq}}{\partial l_{eq}}\right)' - \theta''_{eq}\frac{\partial\theta_{eq}}{\partial l_{eq}}, \tag{164}$$

the elastica

$$B\theta''_{eq}(s) + P\left[\cos\alpha\sin\theta_{eq}(s) + \sin\alpha\cos\theta_{eq}(s)\right] = 0, \qquad s\in[l_{eq},\bar{l}] \tag{165}$$

[21] The Leibniz rule of differentiation is

$$\frac{\mathrm{d}}{\mathrm{d}\zeta}\int_{\alpha(\zeta)}^{\beta(\zeta)} f(x,\zeta)\mathrm{d}x = f(\beta,\zeta)\frac{\mathrm{d}\beta}{\mathrm{d}\zeta} - f(\alpha,\zeta)\frac{\mathrm{d}\alpha}{\mathrm{d}\zeta} + \int_{\alpha(\zeta)}^{\beta(\zeta)}\frac{\partial f(x,\zeta)}{\partial\zeta}\,\mathrm{d}x. \tag{162}$$

In *CISM Lecture Notes No. 562*
"Extremely Deformable Structures" D. Bigoni
Ed. Springer, Wien–New York, 2015
ISBN 978-3-7091-1876-4 doi 10.1007/978-3-7091-1877-1

and the boundary condition $\theta'_{eq}(\bar{l}) = 0$, the following expression for the Eshelby-like force is obtained

$$-\frac{\partial \mathcal{V}(l_{eq})}{\partial l_{eq}} = B\frac{[\theta'_{eq}(l_{eq})]^2}{2} + B\theta'_{eq}(l_{eq})\left.\frac{\partial \theta_{eq}}{\partial l_{eq}}\right|_{s=l_{eq}} + P\cos\alpha + S. \tag{166}$$

Considering that θ_{eq} is a function of $s - l_{eq}$ and of the angle of rotation of the rod at the loaded end $\theta_{\bar{l}}$ (function itself of l_{eq}) one arrives at the following condition

$$\left.\frac{\partial \theta_{eq}}{\partial l_{eq}}\right|_{s=l_{eq}} = -\left.\frac{\partial \theta_{eq}}{\partial s}\right|_{s=l_{eq}} + \left.\frac{\partial \theta_{eq}}{\partial \theta_{\bar{l}}}\frac{\partial \theta_{\bar{l}}}{\partial l_{eq}}\right|_{s=l_{eq}}. \tag{167}$$

Since θ_{eq} is always zero at $s = l_{eq}$ for all $\theta_{\bar{l}}$, the second term in the right-hand side of equation (167) is null, so that equation (167) becomes

$$\left.\frac{\partial \theta_{eq}}{\partial l_{eq}}\right|_{s=l_{eq}} = -\theta'_{eq}(l_{eq}). \tag{168}$$

Therefore, the vanishing of the Eshelby-like force, namely, of the derivative of the total potential energy $\mathcal{V}(l_{eq})$ with respect to l_{eq}, eqn (166), represents the global axial equilibrium for the structure shown in Fig. 30

$$\underbrace{\frac{M^2}{2B}}_{\text{Eshelby-like force}} = S + P\cos\alpha, \tag{169}$$

where $M = B\theta'_{eq}(l_{eq})$ is the reaction moment, equal to Pe, where e is the load eccentricity (to the sliding sleeve).

The term $M^2/(2B)$ is a 'counterintuitive term' which depends on the configurational parameter l_{eq} (and would be absent if the elastic rod were constrained with a movable clamp instead than a sliding sleeve) and is for this reason indicated as the 'Eshelby-like force'. This term has wrongly been neglected by a number of authors who have considered sliding sleeve constraints. On the other hand, a term $M^2/(2B)$ was previously correctly considered in a context different from that addressed here, namely, adhesion mechanics, in which the term is equated to an 'adhesion energy' (Majidi, 2007; Majidi et al., 2012) .

In the following the existence of the Eshelby-like force (169) will be theoretically demonstrated via two independent approaches, namely an asymptotic method and a variational technique.

In *CISM Lecture Notes No. 562*
"Extremely Deformable Structures" D. Bigoni
Ed. Springer, Wien–New York, 2015
ISBN 978-3-7091-1876-4 doi 10.1007/978-3-7091-1877-1

5.1 Asymptotic technique

The Eshelby-like force (169) can be obtained via an asymptotic approach (inspired by the work by Balabukh et al. (1970)) where an imperfect sliding sleeve having a small gap Δ (the distance between the two rigid, frictionless and parallel surfaces making the sliding device) is considered, Fig. 31. Within this gap, the elastic rod is deflected, so that $\vartheta(\Delta)$ denotes the angle at its right contact point, where the forces H, V, M are applied. The length of the rod detached from the two surfaces representing the imperfect sliding sleeve is denoted with $a(\Delta)$. The frictionless contact generates the reaction forces R and Q, in equilibrium with the axial dead force S at the other end. For small Δ, the equilibrium is given by

$$Q = \frac{M}{a(\Delta)}, \qquad R = V + \frac{M}{a(\Delta)}, \qquad S = \left(V + \frac{M}{a(\Delta)}\right)\vartheta(\Delta) - H. \quad (170)$$

On application of the virtual work for a linear elastic inextensible rod yields the geometric quantities $a(\Delta)$ and $\vartheta(\Delta)$

$$a(\Delta) = \sqrt{\frac{6B\Delta}{M}}, \qquad \vartheta(\Delta) = \frac{1}{2}\sqrt{\frac{6M\Delta}{B}}, \quad (171)$$

so that forces Q, R and S can be rewritten as

$$Q = M\sqrt{\frac{M}{6B\Delta}}, \qquad R = V + M\sqrt{\frac{M}{6B\Delta}}, \qquad S = \frac{M^2}{2B} + \frac{V}{2}\sqrt{\frac{6M\Delta}{B}} - H. \quad (172)$$

In the limit of perfect (zero-thickness) sliding sleeve, $\Delta \to 0$, the horizontal component of the reaction R *does not vanish*, but becomes the Eshelby-like force (169)

$$\lim_{\Delta\to 0} R(\Delta)\vartheta(\Delta) = \frac{M^2}{2B}. \quad (173)$$

5.2 Variational technique

The total potential energy (160) has a movable boundary l_{in}, so that it is expedient (Courant and Hilbert, 1962; Majidi et al., 2012) to introduce a small parameter ϵ and take variations (subscript 'var') of an equilibrium configuration (subscript 'eq') in the form

$$\theta(s,\epsilon) = \theta_{eq}(s) + \epsilon\theta_{var}(s), \qquad l_{in}(\epsilon) = l_{eq} + \epsilon l_{var}\ , \quad (174)$$

with the boundary conditions

$$\theta_{eq}(l_{eq}) = 0, \quad \theta(l_{eq} + \epsilon l_{var}) = 0, \quad \theta'_{eq}(\bar{l}) = 0. \quad (175)$$

In *CISM Lecture Notes No. 562*
"Extremely Deformable Structures" D. Bigoni
Ed. Springer, Wien–New York, 2015
ISBN 978-3-7091-1876-4 doi 10.1007/978-3-7091-1877-1

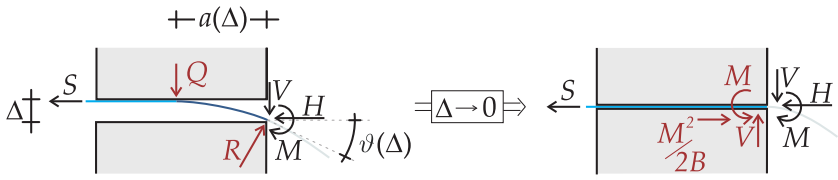

Figure 31. Deformed configuration of an elastic rod within an imperfect sliding sleeve made up of two smooth, rigid and frictionless planes placed at a distance Δ. Applied and reaction forces (left) and values obtained in the limit $\Delta \to 0$, revealing the Eshelbian force (right).

A Taylor series expansion of $\theta(l_{in})$ for small ϵ yields

$$\begin{aligned}\theta(l_{eq}+\epsilon l_{var},\epsilon) = \theta_{eq}(l_{eq}) + \epsilon\left(\theta_{var}(l_{eq}) + \theta'_{eq}(l_{eq})l_{var}\right) \\ + \frac{\epsilon^2}{2} l_{var}\left(2\theta'_{var}(l_{eq}) + \theta''_{eq}(l_{eq})l_{var}\right) + \mathcal{O}\left(\epsilon^3\right),\end{aligned} \tag{176}$$

so that the boundary conditions (175) lead to the following compatibility equations

$$\theta_{var}(l_{eq}) + \theta'_{eq}(l_{eq})l_{var} = 0, \quad 2\theta'_{var}(l_{eq}) + \theta''_{eq}(l_{eq})l_{var} = 0. \tag{177}$$

Taking into account the Leibniz rule of differentiation (162) and the boundary (175) and compatibility (177) conditions, through integration by parts, the first variation of the functional $\mathcal{V}$ is obtained in the following form

$$\begin{aligned}\delta_\epsilon \mathcal{V} &= -\int_{l_{eq}}^{\bar{l}} \left[B\theta''_{eq}(s) + P\left(\cos\alpha \sin\theta_{eq}(s) + \sin\alpha\cos\theta_{eq}(s)\right)\right]\theta_{var}(s)\mathrm{d}s \\ &+ \left[B\frac{\theta'_{eq}(l_{eq})^2}{2} - P\cos\alpha - S\right] l_{var},\end{aligned} \tag{178}$$

so that the equilibrium equations (165) and (169) are derived, the latter of which, representing the so-called 'transversality condition' of Courant and Hilbert (1962), provides the Eshelby-like force.

5.3 Analytical expression of the Eshelby-like force

The equilibrium configuration of the elastic rod satisfies the elastica equation (165) (see Love, 1927; Bigoni, 2012), that introducing the auxiliary angle $\varphi(s) = \theta_{eq}(s) + \alpha$ and the dimensionless load $\lambda^2 = P/B$ writes

In *CISM Lecture Notes No. 562*
"Extremely Deformable Structures" D. Bigoni
Ed. Springer, Wien–New York, 2015
ISBN 978-3-7091-1876-4 doi 10.1007/978-3-7091-1877-1

as

$$\varphi^{''}(s) + \lambda^2 \sin\varphi(s) = 0, \qquad s \in [l_{eq}, \bar{l}] \tag{179}$$

subject to the boundary conditions $\varphi(l_{eq}) = \alpha$ and $\varphi^{'}(\bar{l}) = 0$. Integration of equation (179) yields

$$\varphi^{'}(s) = \pm\lambda\sqrt{2\left[\cos\varphi(s) - \cos(\theta_{\bar{l}} + \alpha)\right]}, \tag{180}$$

taken in the following with the '+' sign, so that introducing the change of variable

$$\eta = \sin\frac{\theta_{\bar{l}} + \alpha}{2}, \qquad \eta\sin\phi(s) = \sin\frac{\varphi(s)}{2}, \tag{181}$$

where $\theta_{\bar{l}} = \theta_{eq}(\bar{l})$ represents the rotation measured at the free end of the rod, we end up with the following differential problem

$$\phi^{'}(s) = \lambda\sqrt{1 - \eta^2\sin^2\phi(s)}, \tag{182}$$

subject to $\phi(l_{eq}) = m = \arcsin\left[\sin(\alpha/2)/\,\eta\right]$ and $\phi(\bar{l}) = \pi/2$.

Restricting the attention to the first (stable) mode of deformation, the integration of equation (182) leads to the relation between the rotation measured at the free end of the rod $\theta_{\bar{l}}$ and the applied vertical load

$$P = \frac{B}{(\bar{l} - l_{eq})^2}\left[\mathcal{K}(\eta) - \mathcal{K}(m, \eta)\right]^2, \tag{183}$$

where $\mathcal{K}(\eta)$ is the complete elliptic integral of the first kind (39), whereas $\mathcal{K}(m, \eta)$ is the incomplete elliptic integral of the first kind (83). Moreover, through the integration of equation (182) and the implemented change of variable, the rotation field (for the first mode) can be obtained as

$$\theta_{eq}(s) = 2\arcsin\left[\eta\,\mathrm{sn}\left((s - l_{eq})\sqrt{\frac{P}{B}} + \mathcal{K}(m, \eta), \eta\right)\right] - \alpha, \tag{184}$$

where sn is the Jacobi sine amplitude function (47).

The Eshelby-like force (169) can be expressed, taking into account equation (180), as

$$\frac{M^2}{2B} = 2P\left(\eta^2 - \sin^2\frac{\alpha}{2}\right), \tag{185}$$

so that the axial force S at the end of the sliding sleeve (which has been experimentally measured through a load cell by Bigoni et al. (2015)) is given by

$$S = -P\cos(\alpha + \theta_{\bar{l}}) = -P\cos\alpha + \underbrace{2P\left(\sin^2\frac{\theta_{\bar{l}} + \alpha}{2} - \sin^2\frac{\alpha}{2}\right)}_{\text{Eshelby-like force}}. \tag{186}$$

In *CISM Lecture Notes No. 562*
"Extremely Deformable Structures" D. Bigoni
Ed. Springer, Wien–New York, 2015
ISBN 978-3-7091-1876-4 doi 10.1007/978-3-7091-1877-1

From equation (186) it can be noted that the load S is (in modulus) bounded by P and that it tends to P only in the 'membrane limit', when B tends to zero and $\theta_{\bar{l}} + \alpha$ to π.

The following three different cases may arise, explaining the experiments shown in Fig. 33:

(i.) the elastic rod within the sliding sleeve is in compression, or 'pushed in', if $\theta_{\bar{l}} + \alpha < \pi/2$;

(ii.) the elastic rod within the sliding sleeve is unloaded if $\theta_{\bar{l}} + \alpha = \pi/2$;

(iii.) the elastic rod within the sliding sleeve is in tension, or 'pulled out', if $\theta_{\bar{l}} + \alpha > \pi/2$.

The case of null axial force, $S = 0$, occurs when $M^2/(2B)$ equals the axial component of the dead load, $P\cos\alpha$, and corresponds to deformed configurations having the tangent at the free end orthogonal to the direction of the load P, as in Fig. 33 (center).

Finally, it can be noted that the Eshelby-like force $M^2/(2B)$ is greater than the applied load P when

$$\cos\alpha - 2\cos^2\left(\frac{\theta_{\bar{l}} + \alpha}{2}\right) > 0. \tag{187}$$

Regions in the $\theta_{\bar{l}} - \alpha$ plane where the axial force S is positive/negative and where $M^2/(2B) > P$ are shown in Fig. 32. From the figure it can be concluded that $M^2/(2B) > P$ is possible only for positive axial load, $S > 0$, and high deflections of the rod (for rotations at the free end $\theta_{\bar{l}}$ greater than $\pi/3$).

5.4 Experimental evidence of configurational force

Fig. 33 gives a qualitative (but indisputable) proof of the existence of the Eshelby-like force in the structure shown in Fig. 30, in fact for this system equilibrium is only possible when equation (169) is satisfied, so that the presence of the Eshelby-like force (parallel to the direction of sliding) explains the reason why the configuration shown in the central photo in Fig. 33 is in equilibrium and why the rod is 'expelled' from the sliding sleeve in the lower photo.

'Expulsion' of the elastic rod is consequent to a value of the Eshelby-like force exceeding the axial component of P, namely, $P\cos\alpha$. Quantitative experiments are reported in Bigoni et al. (2015), whereas movies of the experiments can be found at http://ssmg.unitn.it/eshelbylikeforce.html. The purpose is now to analyze the effects of Eshelby-like force on bifurcation and instability of structures.

In *CISM Lecture Notes No. 562*
"Extremely Deformable Structures" D. Bigoni
Ed. Springer, Wien–New York, 2015
ISBN 978-3-7091-1876-4 doi 10.1007/978-3-7091-1877-1

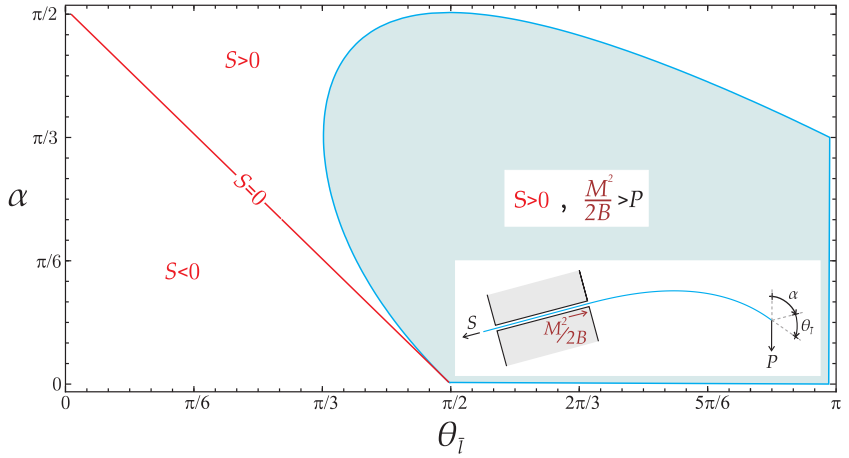

Figure 32. Regions in the plane $\theta_{\bar{l}} - \alpha$ where $S > 0$, $S < 0$ and $M^2/(2B) > P$.

6 Configurational forces and buckling

To highlight the effects of configurational forces on elastic structures, we consider the problem in which a blade (an elastic planar rod) is forced to penetrate into an elastic compliant sliding sleeve clamp (a frictionless sliding sleeve with a final linear spring of stiffness k) through the application of a dead compressive load P at the other end.

A structural system with a free end loaded with an axial dead force was shown to exhibit several surprising and counterintuitive mechanical behaviours by Bigoni et al. (2014b) and will not be repeated here. In the following, the governing equations will be obtained for the structures shown in Fig. 34, differing only in the boundary conditions at the right end. These structures are similar to those analyzed in Section 2, except for the presence of the Eshelby-like force, arising from the sliding sleeve and which strongly affects the post-critical behaviour and its stability (see Bigoni et al., 2014b).

6.1 Finite number of critical loads

The Euler formula for an inextensible elastic planar rod (of length l) provides the n-th critical load (associated to the n-th instability mode) as

$$P_{cr,n} = \frac{\pi^2 B}{(\rho_n l)^2}, \qquad n \in \mathbb{N}^+, \tag{188}$$

In *CISM Lecture Notes No. 562*
"Extremely Deformable Structures" D. Bigoni
Ed. Springer, Wien–New York, 2015
ISBN 978-3-7091-1876-4 doi 10.1007/978-3-7091-1877-1

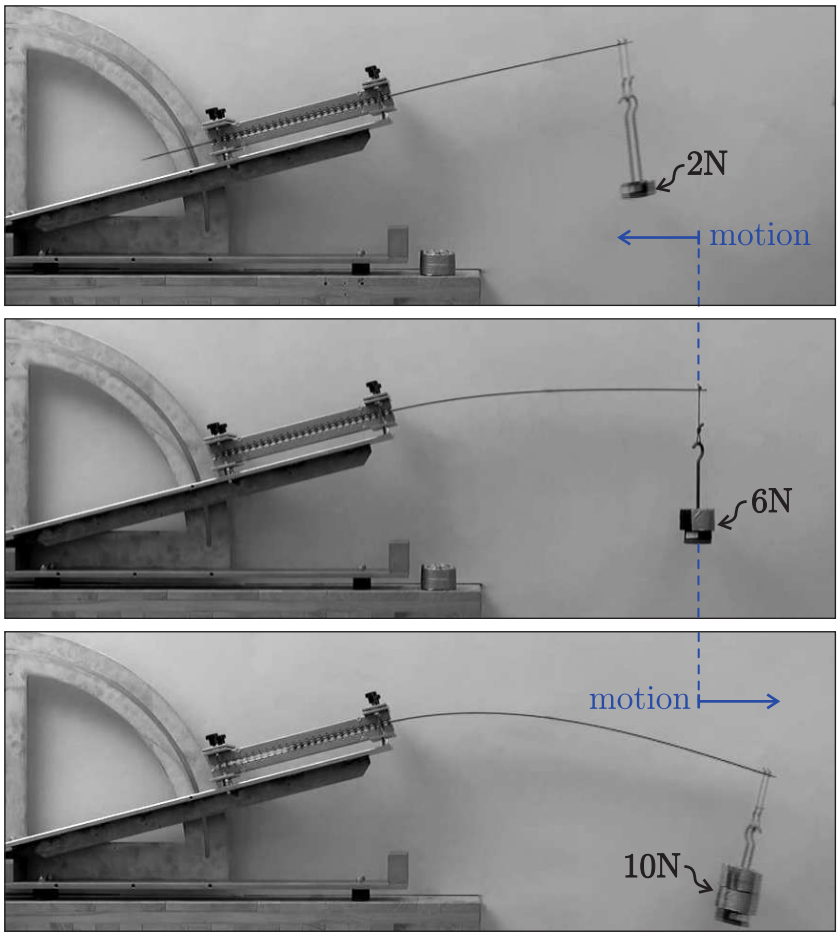

Figure 33. The practical realization of the elastic structure shown in Fig. 30 reveals an axial Eshelby-like force, so that, while at low vertical force (2 N) the elastic rod tends, as expected, to slip inside the sliding sleeve (upper photo), at 6 N the equilibrium is surprisingly possible (note that the tangent at the loaded end of the elastic rod is horizontal, see the photo in the centre) and at 10 N the elastic rod is expelled from the sliding sleeve (lower photo), even if the system is inclined at 15° with respect to the horizontal direction ($\alpha = 75°$).

In *CISM Lecture Notes No. 562*
"Extremely Deformable Structures" D. Bigoni
Ed. Springer, Wien–New York, 2015
ISBN 978-3-7091-1876-4 doi 10.1007/978-3-7091-1877-1

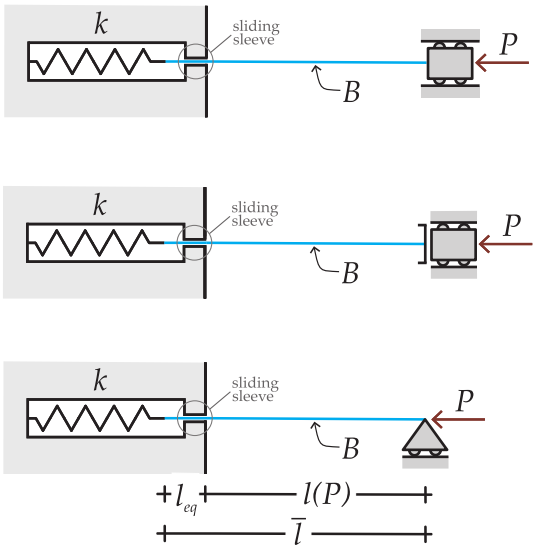

Figure 34. The penetrating blade is an elastic planar rod whose free length l is a function of the amount of the applied axial dead load P. The blade slides into a frictionless sleeve and is restrained by an axial linear spring, while at the other loaded end three types of constraints are considered: clamped (upper), constrained rotation (center) and simply supported (lower).

where ρ_n is a slenderness factor (depending on the constraints applied to the elastic system[22]). Equation (188) shows that the n-th critical load P_{cr} is unique whenever the rod length l is fixed, but this uniqueness may be lost when the length becomes a function of the applied axial load, $l = l(P)$.

If an axial spring is introduced (as shown in Fig. 34), the elastic rod (or 'blade') can penetrate the constraint (a sliding sleeve) by a length l_{eq}, so

[22] With reference to a structure with the left end constrained by a sliding sleeve, the factor ρ_n is

- $\rho_n = 1/(n+1)$ for $n = 1, 3, 5, ...$, $\rho_2 \approx 0.350$, $\rho_4 \approx 0.203$, and $\rho_n \approx 1/(n+1)$ for $n = 6, 8, 10, ...$ for the structure with the clamped right end, Fig. 34 (upper part);
- $\rho_n = 1/n$, for the structure with constrained rotation at the right end, Fig. 34 (central part);
- $\rho_1 = 0.699$, $\rho_2 = 0.407$ $\rho_n \approx \dfrac{2}{2n+1}$ for $n \geq 3$, for the structure with simply supported right end, Fig. 34 (lower part).

In *CISM Lecture Notes No. 562*
"Extremely Deformable Structures" D. Bigoni
Ed. Springer, Wien–New York, 2015
ISBN 978-3-7091-1876-4 doi 10.1007/978-3-7091-1877-1

that

$$l(P) = \bar{l} - l_{eq}(P), \tag{189}$$

where $\bar{l}$ is the outer length of the blade at null axial load P, $l(P=0) = \bar{l}$. In the particular case of a linear spring with stiffness k and considering the blade in the straight configuration[23] the equilibrium equation in the axial direction is given by

$$P = k l_{eq}, \tag{190}$$

so that the length of the outer part of the blade is $l(P) = \bar{l} - P/k$ and the Euler formula (188) becomes

$$P_{cr,n} = \frac{\pi^2 B}{\rho_n^2 \left(\bar{l} - \dfrac{P_{cr,n}}{k}\right)^2}, \qquad n \in \mathbb{N}^+. \tag{191}$$

The determination of the critical load $P_{cr,n}$ defined by equation (191) leads to the following cubic equation,

$$p_{cr,n}^3 - 2p_{cr,n}^2 + p_{cr,n} - \frac{4}{27 q_n} = 0, \qquad n \in \mathbb{N}^+, \tag{192}$$

where $p_{cr,n}$ and q_n are respectively the dimensionless n-th critical load and dimensionless relative stiffness (spring stiffness multiplied by the rod's length and divided by a critical load) of the elastic system given as,

$$p = \frac{P}{k\bar{l}}, \qquad q_n = \frac{4\rho_n^2 k \bar{l}^3}{27\pi^2 B}, \qquad n \in \mathbb{N}^+. \tag{193}$$

Note that the dimensionless stiffness parameter is positive, $q_n > 0$, and that the dimensionless critical load has to satisfy the following inequality,[24]

$$p_{cr,n} \leq 1, \qquad n \in \mathbb{N}^+, \tag{194}$$

to avoid the the full penetration of the blade, occurring when $l(P) < 0$.

From the cubic equation (192) it can be concluded that:

[23] If the rod is in a deformed configuration, an Eshelby-like force affects the axial equilibrium, see section 5.

[24] This restriction holds only for the calculation of the critical loads. Indeed, equilibrium configurations with $p \geq 1$ are possible for non-trivial deformation paths (see Bigoni et al., 2014b).

In *CISM Lecture Notes No. 562*
"Extremely Deformable Structures" D. Bigoni
Ed. Springer, Wien–New York, 2015
ISBN 978-3-7091-1876-4 doi 10.1007/978-3-7091-1877-1

i) since all the coefficients of the cubic equation (192) are real, the following infinite sequence always exists of real roots

$$p^{\mathcal{C}}_{cr,n} = \frac{1}{3}\left[2 + \sqrt[3]{\frac{q_n}{2-q_n+2\sqrt{1-q_n}}} + \sqrt[3]{\frac{2-q_n+2\sqrt{1-q_n}}{q_n}}\right] > 1, \quad n \in \mathbb{N}^+, \tag{195}$$

all violating the constraint (194) and thus representing mathematical solutions which are meaningless from mechanical point of view;

ii) in the case when for a given $m \in \mathbb{N}^+$ the inequality

$$q_{m+1} < 1 < q_m, \qquad \text{or equivalently} \qquad \left(\frac{\rho_1}{\rho_m}\right)^2 < q_1 < \left(\frac{\rho_1}{\rho_{m+1}}\right)^2, \tag{196}$$

is satisfied, in addition to the sequence of real roots (195) other $2m$ real roots exist for the cubic equation (192),

$$\left.\begin{matrix} p^{\mathcal{A}}_{cr,n} \\ p^{\mathcal{B}}_{cr,n} \end{matrix}\right\} = \frac{1}{3}\left[2 - \frac{1 \pm i\sqrt{3}}{2}\sqrt[3]{\frac{q_n}{2-q_n+2\sqrt{1-q_n}}} - \frac{1 \mp i\sqrt{3}}{2}\sqrt[3]{\frac{2-q_n+2\sqrt{1-q_n}}{q_n}}\right], \qquad n \in \mathbb{N}^+ \tag{197}$$

satisfying

$$0 < p^{\mathcal{A}}_{cr,n} \le p^{\mathcal{A}}_{cr,m} \le p^{\mathcal{B}}_{cr,m} \le p^{\mathcal{B}}_{cr,n} < 1, \qquad n \le m \qquad n, m \in \mathbb{N}^+ \tag{198}$$

so that $2m$ critical loads are obtained, corresponding to two critical loads referred to the same n-th instability mode;

iii) in the particular case when $q_m = 1$ (or equivalently $q_1 = \rho_1^2/\rho_m^2$), two real roots associated to the m-th mode (197) are coincident,

$$p^{\mathcal{A}}_{cr,m} = p^{\mathcal{B}}_{cr,m} = \frac{1}{3}, \qquad m \in \mathbb{N}^+, \tag{199}$$

therefore $2m-1$ critical loads are obtained in this case.

In Bigoni et al. (2014b) it is shown that $p^{\mathcal{A}}_{cr}$ corresponds to a critical *buckling* load, while $p^{\mathcal{B}}_{cr}$ to a critical *restabilization* load for which the trivial path returns to be stable. In a similar vein, it can be concluded for the structures now under consideration that:

In *CISM Lecture Notes No. 562*
"Extremely Deformable Structures" D. Bigoni
Ed. Springer, Wien–New York, 2015
ISBN 978-3-7091-1876-4 doi 10.1007/978-3-7091-1877-1

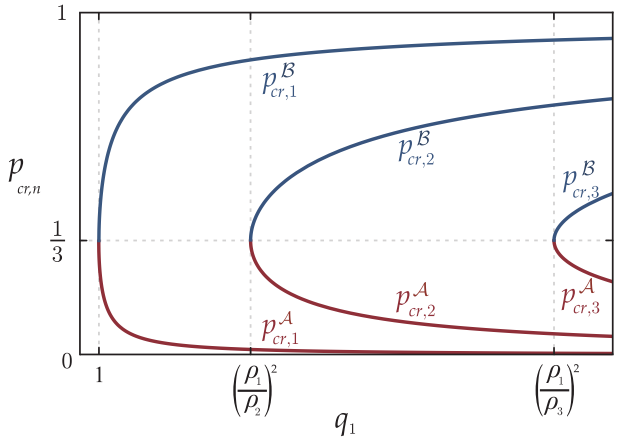

Figure 35. Dimensionless bifurcation loads $p_{cr,n}$ (*buckling* load $p^{\mathcal{A}}_{cr,n}$ and *restabilization* load $p^{\mathcal{B}}_{cr,n}$) as a function of the dimensionless relative stiffness q_1. Note that if the stiffness ratio q_1 decreases then the n-th buckling load increases while the n-th restabilization load decreases, and the number of bifurcation modes can even reduce to zero in the case of 'highly compliant systems' ($q_1 < 1$), where bifurcation does not exist.

- ◇ for fixed properties of the rod, a reduction of the spring stiffness k leads to an increase of the *buckling* load $p^{\mathcal{A}}_{cr}$ (a result agreeing with Tarnai, 1980) and to a reduction of the *restabilization* load $p^{\mathcal{B}}_{cr}$;
- ◇ differently from the behaviour observed in usual structures, the elastic systems under consideration can have a countable (finite) number of critical loads;
- ◇ 'highly compliant systems' ($q_1 < 1$) do not show any bifurcation.

6.2 Non-trivial configurations for the blade

Clamped blade Let us consider the system shown in Fig. 34 (upper part), where an inextensible elastic planar rod is forced to penetrate a sliding sleeve, restrained by an axial linear spring of stiffness k, through the application of a dead compressive load P at the other end, which is constrained by a movable clamp.

Considering only the outer part of the rod at an equilibrium configuration with $\theta(s) = 0$ for $s \in [0, l_{eq}]$ and introducing the dimensionless axial load $\lambda^2 = P/B$, the rotation field at equilibrium $\theta_{eq}(s)$ (unknown for the outer part, $s \in [l_{eq}, \bar{l}]$) is a solution of the following differential problem

In *CISM Lecture Notes No. 562*
"Extremely Deformable Structures" D. Bigoni
Ed. Springer, Wien–New York, 2015
ISBN 978-3-7091-1876-4 doi 10.1007/978-3-7091-1877-1

$$\begin{cases} \dfrac{\mathrm{d}^2\theta_{eq}(s)}{\mathrm{d}s^2} + \lambda^2 \sin\theta_{eq}(s) = 0, \qquad s \in \left(l_{eq}, \bar{l}\right) \\ \theta_{eq}\left(l_{eq}\right) = \theta_{eq}\left(\bar{l}\right) = 0, \\ \left.\dfrac{\mathrm{d}\theta_{eq}(s)}{\mathrm{d}s}\right|_{s=\frac{\bar{l}+3l_{eq}}{4}} = 0, \\ \lambda^2 = \dfrac{k}{B} l_{eq} + \dfrac{1}{2}\left[\theta'_{eq}(l_{eq})\right]^2, \end{cases} \tag{200}$$

Equation $(200)_4$ represents the equilibrium in the axial direction, revealing the presence of the configurational force $B\left[\theta'_{eq}(l_{eq})\right]^2/2$ (Bigoni et al., 2014b). For conciseness, only the first bifurcation mode will be analyzed, so that the symmetry of the problem allows us to consider only the first quarter of the outer blade, similarly to Section 2.2. The rotation at the inflection point is $\theta_{eq}\left((\bar{l}+3l_{eq})/4\right) = \theta_q$ so that, through a change of variable and the Riemann theorem, an integration of the differential problem (200) leads to the relation between the load parameter λ and the angle θ_q as follows

$$4\mathcal{K}\left(\sin\frac{\theta_q}{2}\right) = \lambda\left[\bar{l} - \lambda^2\frac{B}{k}\left(1 - 2\sin^2\frac{\theta_q}{2}\right)\right]. \tag{201}$$

The coordinates $x_1(s)$ and $x_2(s)$ of the rod's axis in the deformed configuration for $s \in \left(l_{eq}, \bar{l}\right)$ can be computed from rotation field $\theta_{eq}(s)$ by integration of equation (11) as

$$\begin{aligned} x_1(s) &= -s + \frac{2}{\lambda}E\left[\mathrm{am}\left(\lambda\left(s - l_{eq}\right), \sin\frac{\theta_q}{2}\right), \sin\frac{\theta_q}{2}\right] - l_{eq}, \\ x_2(s) &= \frac{2}{\lambda}\sin\frac{\theta_q}{2}\left[1 - \mathrm{cn}\left(\lambda\left(s - l_{eq}\right), \sin\frac{\theta_q}{2}\right)\right]. \end{aligned} \tag{202}$$

Rotationally constrained blade The differential problem governing the equilibrium of the system reported in Fig. 34 (center), where the elastic

In *CISM Lecture Notes No. 562*
"Extremely Deformable Structures" D. Bigoni
Ed. Springer, Wien–New York, 2015
ISBN 978-3-7091-1876-4 doi 10.1007/978-3-7091-1877-1

blade is constrained in rotation at its loaded end, is

$$\begin{cases} \dfrac{\mathrm{d}^2\theta_{eq}(s)}{\mathrm{d}s^2} + \lambda^2 \sin\theta_{eq}(s) = 0, \qquad s \in \left(l_{eq}, \bar{l}\right) \\ \theta_{eq}\left(l_{eq}\right) = \theta_{eq}\left(\bar{l}\right) = 0, \\ \left.\dfrac{\mathrm{d}\theta_{eq}(s)}{\mathrm{d}s}\right|_{s=\frac{\bar{l}+l_{eq}}{2}} = 0, \\ \lambda^2 = \dfrac{k}{B} l_{eq} + \dfrac{1}{2}\left[\theta'_{eq}(l_{eq})\right]^2, \end{cases} \tag{203}$$

where the rotation at the inflection point (mid-span of the outer part of the elastic rod, $s = (\bar{l}+l_{eq})/2$) is denoted with θ_m. For this system, the relation between the dimensionless load parameter λ and the rotation at the rod's mid-span θ_m is written for the first buckling mode as

$$2\mathcal{K}\left(\sin\frac{\theta_m}{2}\right) = \lambda\left[\bar{l} - \lambda^2\frac{B}{k}\left(1 - 2\sin^2\frac{\theta_m}{2}\right)\right]. \tag{204}$$

The coordinates $x_1(s)$ and $x_2(s)$ of the rod's axis in the deformed configuration can be computed from the rotation field $\theta_{eq}(s)$ through integration of equation (11) and result to be expressed by equation (202), already obtained in the previous case of clamped end.

Simply supported blade Considering the system shown in Fig. 34 (lower part), where the elastic planar rod is simply supported at its loaded end and may slide into the frictionless sliding sleeve, the rotation field $\theta(s)$ of the outer part of the rod is obtained as the solution of the following differential problem

$$\begin{cases} \dfrac{\mathrm{d}^2\theta_{eq}(s)}{\mathrm{d}s^2} + \dfrac{P}{B}\sin\theta_{eq}(s) + \dfrac{R}{B}\sin\theta_{eq}(s) = 0, \qquad s \in \left(l_{eq}, \bar{l}\right) \\ \theta_{eq}\left(l_{eq}\right) = 0, \\ \left.\dfrac{\mathrm{d}\theta_{eq}(s)}{\mathrm{d}s}\right|_{s=\bar{l}} = 0, \\ \displaystyle\int_0^{\bar{l}} \sin\theta(s)\mathrm{d}s = 0, \\ \dfrac{\sqrt{P^2+R^2}}{B} = \dfrac{k}{B} l_{eq} + \dfrac{1}{2}\left[\theta'_{eq}(l_{eq})\right]^2. \end{cases} \tag{205}$$

In *CISM Lecture Notes No. 562*
"Extremely Deformable Structures" D. Bigoni
Ed. Springer, Wien–New York, 2015
ISBN 978-3-7091-1876-4 doi 10.1007/978-3-7091-1877-1

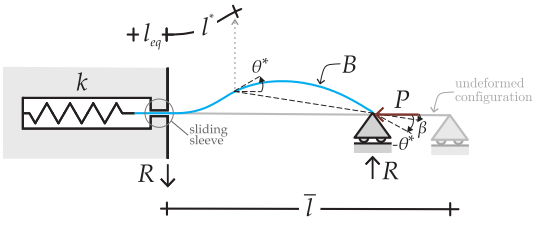

Figure 36. The penetrating blade with a simply supported end in a deformed configuration. An inflection point exists at $s = l^*$, where the rotation angle is denoted with $\theta(s = l^*) = \theta^*$. The angle β defines the inclination with respect to the horizontal direction of the resultant vector, sum of the the applied load P and of the vertical reaction of the support R.

Note that equation $(205)_5$ is the equilibrium equation in the sliding direction of the rod, where the 'Eshelby-like' force can be recognized. Introducing the dimensionless load $\gamma^2 = \sqrt{P^2 + R^2}/B$ and the angle $\psi(s) = \theta_{eq}(s) + \beta$, where β is the angle of inclination of the resultant vector sum of P and R (see Fig. 36), the differential problem (205) can be rewritten as

$$\begin{cases} \dfrac{\mathrm{d}^2\psi(s)}{\mathrm{d}s^2} + \gamma^2 \sin\psi(s) = 0, \qquad s \in \left(l_{eq}, \bar{l}\right) \\ \psi\left(l_{eq}\right) = \beta, \\ \left.\dfrac{\mathrm{d}\psi(s)}{\mathrm{d}s}\right|_{s=\bar{l}} = 0, \\ \displaystyle\int_0^{\bar{l}} \sin\left(\psi(s) - \beta\right) \mathrm{d}s = 0, \\ \dfrac{\sqrt{P^2 + R^2}}{B} = \dfrac{k}{B} l_{eq} + \dfrac{1}{2}\left[\psi'\left(l_{eq}\right)\right]^2. \end{cases} \tag{206}$$

Similarly to the antisymmetric buckling modes of a doubly clamped rod (Section 2.2), it is a standard expedient to operate the following change of variables

$$\eta = \sin\frac{\psi^*}{2}, \qquad \eta \sin\omega(s) = \sin\frac{\psi(s)}{2}, \tag{207}$$

where $\psi^* = \theta^* + \beta$. For the first bifurcation mode, integration of the differential problem (206) leads to the following relation between the dimensionless

In *CISM Lecture Notes No. 562*
"Extremely Deformable Structures" D. Bigoni
Ed. Springer, Wien–New York, 2015
ISBN 978-3-7091-1876-4 doi 10.1007/978-3-7091-1877-1

load parameter γ and the angle β

$$3\mathcal{K}(\eta) - \mathcal{K}(\eta, \omega_\beta) = \gamma \left[\bar{l} - \gamma^2 \frac{B}{k} \left(1 - 2\eta^2\right) \right], \tag{208}$$

where $\omega_\beta = \arcsin\left(\eta^{-1} \sin\left(\frac{\beta}{2}\right)\right)$. Using the dimensionless parameters (193) it is possible to rewrite equation (208) in the following form

$$pq_1 \left(1 - p\left(1 - 2\eta^2\right)\right)^2 = \left(1 - 2\sin^2\frac{\beta}{2}\right) \left[3\mathcal{K}(\eta) - \mathcal{K}(\eta, \omega_\beta)\right]^2. \tag{209}$$

The relation between the load P and the kinematic parameter θ^* can now be obtained by considering, in addition to eqn (209), the condition $(205)_4$, which provides a relation between θ^* and β, so that, similarly to equation (89), we obtain

$$\begin{aligned} 0 = &-2\eta \cos\omega_\beta \left(1 - 2\eta^2 \sin^2\omega_\beta\right) \\ &+2\eta \sin\omega_\beta \sqrt{1 - \eta^2 \sin^2\omega_\beta} \left\{3\left[2E(\eta) - K(\eta)\right] - 2E(\omega_\beta, \eta) + K(\omega_\beta, \eta)\right\}. \end{aligned} \tag{210}$$

Equations (209) and (210) are highly non-linear and determine the non-trivial solution. The relation between β and θ^* (the former contained in ω_β and the latter in η) can be numerically obtained from equation (210) and used into equation (209) to obtain the relation between P and θ^*.

Finally, the coordinates $x_1(s)$ and $x_2(s)$ of the rod's axis in the deformed configuration for $s \in \left(l_{eq}, \bar{l}\right)$ can be computed from the rotation field $\theta_{eq}(s)$ by integrating equation (11) as

In *CISM Lecture Notes No. 562*
"Extremely Deformable Structures" D. Bigoni
Ed. Springer, Wien–New York, 2015
ISBN 978-3-7091-1876-4 doi 10.1007/978-3-7091-1877-1

$$
\begin{aligned}
x_1(s) = &+\sin\beta\left[-\frac{2\eta}{\gamma}\mathrm{cn}\big(\gamma\,(s-l_{eq})+\mathcal{K}(\omega_\beta,\eta),\eta\big)+\frac{2\eta}{\gamma}\mathrm{cn}\big(\mathcal{K}(\omega_\beta,\eta),\eta\big)\right]\\
&\cos\beta\Big\{-s+\frac{2}{\gamma}\big[E\left[\mathrm{am}\left(\gamma\,(s)+\mathcal{K}(\omega_\beta,\eta),\eta\right),\eta\right]\\
&-E\left[\mathrm{am}\left(\mathcal{K}(\omega_\beta,\eta),\eta\right),\eta\right]\big]\Big\},\\
x_2(s) = &\cos\beta\left[-\frac{2\eta}{\gamma}\mathrm{cn}\big(\gamma\,(s)+\mathcal{K}(\omega_\beta,\eta),\eta\big)+\frac{2\eta}{\gamma}\mathrm{cn}\big(\mathcal{K}(\omega_\beta,\eta),\eta\big)\right]\\
&-\sin\beta\Big\{-s+\frac{2}{\gamma}\big[E\left[\mathrm{am}\left(\gamma\,(s)+\mathcal{K}(\omega_\beta,\eta),\eta\right),\eta\right]\\
&-E\left[\mathrm{am}\left(\mathcal{K}(\omega_\beta,\eta),\eta\right),\eta\right]\big]\Big\}.
\end{aligned}
\tag{211}
$$

7 The elastica arm scale

The integration of the elastica and the concept of configurational forces so far developed are now employed in the design of an innovative weighing device. It is well-known that for millennia the equal and unequal arm balance scales have been used (for instance the classic Roman balance, see Fig. 37 left), and still are used (see the overview by Robens et al., 2014), to measure weight by exploiting the equilibrium of a rigid lever, so that a deformation of the arms would merely represent an undesired effect. On the other hand, the modern digital weighting systems, inspired by the principle of the spring balance (which was invented at the end of the 17th century by R. Hooke, Fig. 37 on the right), are based on the strain of an elastic element, so that equilibrium is always satisfied and a counterweight is not needed.

A new concept is now introduced of an 'elastica arm scale', based on the exploitation of nonlinear kinematics and configurational mechanics of elastic rods, following Bosi et al. (2014). The new scale has deformable arms, so that an inflected equilibrium configuration is employed to measure weight and the scale can work both *with or without a counterweight*. In a sense, this new type of balance is a combination of a rigid arm balance with a spring balance, because equilibrium and deformation are both simultaneously exploited. The prototype of the elastica arm scale is shown on the right of Fig. 38, as a realization of the scheme reported on the left of the same figure, where an elastic rod (of total of length $\bar{l}+l^*$ and inclined at

In *CISM Lecture Notes No. 562*
"Extremely Deformable Structures" D. Bigoni
Ed. Springer, Wien–New York, 2015
ISBN 978-3-7091-1876-4 doi 10.1007/978-3-7091-1877-1

Figure 37. A steelyard based on rigid lever principle (left) and a spring balance based on deformation (right).

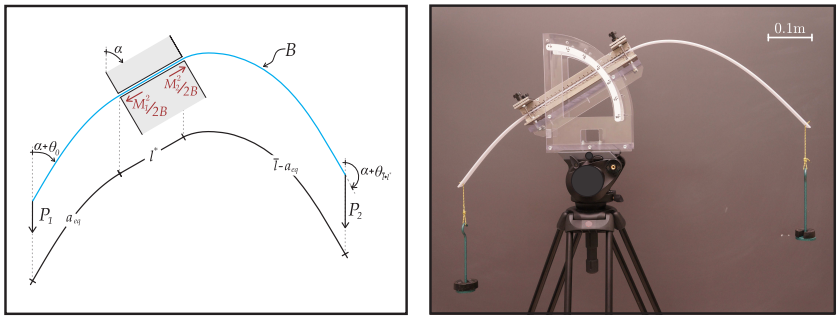

Figure 38. Scheme (left) and prototype (right) of the deformable arm scale. An elastic lamina of bending stiffness B is inserted into a sliding sleeve of length l^* inclined at an angle α with respect to the vertical direction. The length of the left part of the lamina is a_{eq}, while the length of the second is $\bar{l} - a_{eq}$.

an angle $\alpha \in [0, \pi/2]$ with respect to the vertical loads applied at its ends) is free to slide in a frictionless sleeve of length l^*. For given loads (P_1 and P_2), the scale admits an equilibrium configuration, possible by virtue of the flexural deformation of the arms.

The presence of 'Eshelby-like' forces (see section 5) at the ends of the sliding sleeve defines the nonlinear equilibrium equation in the sliding direction that can be written as

$$(P_1 + P_2)\cos\alpha + \underbrace{\frac{M_1^2 - M_2^2}{2B}}_{\text{Eshelby-like forces}} = 0, \tag{212}$$

In *CISM Lecture Notes No. 562*
"Extremely Deformable Structures" D. Bigoni
Ed. Springer, Wien–New York, 2015
ISBN 978-3-7091-1876-4 doi 10.1007/978-3-7091-1877-1

or, equivalently, but with reference to the angles at the ends of the elastic rod, as the following 'geometrical condition' of equilibrium

$$P_1 \cos(\alpha + \theta_0) + P_2 \cos(\alpha + \theta_{\bar{l}+l^*}) = 0, \tag{213}$$

representing the balance of axial thrust of the deformable scale ($0 \leq \alpha+\theta_0 \leq \alpha$ and $\pi/2 \leq \alpha + \theta_{\bar{l}+l^*} \leq \pi$). The equilibrium equations of the two arms of the scale are

$$B\theta_{eq}^{''}(s) - P_j \sin\left[\theta_{eq}(s) - (-1)^j \alpha\right] = 0, \tag{214}$$

where $j = 1$ for the left arm ($s \in [0, a_{eq}]$) and $j = 2$ for the right one ($s \in \left[a_{eq} + l^*, \bar{l} + l^*\right]$). From integration of these two differential equations we can obtain the relations between the applied loads P_1 and P_2, the kinematical parameters θ_0 and $\theta_{\bar{l}+l^*}$ and the lengths of the two arm a_{eq} and $\bar{l} - a_{eq}$ as

$$a_{eq}\sqrt{\frac{P_1}{B}} = \mathcal{K}(\kappa_1) - \mathcal{K}(m_1, \kappa_1), \qquad \left(\bar{l} - a_{eq}\right)\sqrt{\frac{P_2}{B}} = \mathcal{K}(\kappa_2) - \mathcal{K}(m_2, \kappa_2), \tag{215}$$

where $\mathcal{K}(\kappa_j)$ and $\mathcal{K}(m_j, \kappa_j)$ are respectively the complete (39) and incomplete (83) elliptic integral of the first kind, and

$$\begin{aligned}
&\kappa_1 = \sin\frac{\theta_0 + \alpha + \pi}{2}, && m_1 = \arcsin\left[\frac{\sin\dfrac{\alpha+\pi}{2}}{\kappa_1}\right],\\
&\kappa_2 = \sin\frac{\theta_{\bar{l}+l^*} + \alpha}{2}, && m_2 = \arcsin\left[\frac{\sin\dfrac{\alpha}{2}}{\kappa_2}\right],\\
&\kappa_1 \sin\phi_1(s) = \sin\frac{\theta_{eq}(s) + \alpha + \pi}{2}, && \kappa_2 \sin\phi_2(s) = \sin\frac{\theta_{eq}(s) + \alpha}{2}.
\end{aligned} \tag{216}$$

Note that, when $\alpha + \theta_{\bar{l}+l^*} = \pi/2$ the equilibrium equation (213) implies $P_1 = 0$, so that *a counterweight is not needed.*

Furthermore, when the sliding sleeve is in the vertical direction, namely $\alpha = 0°$, the equilibrium is governed by the following *purely geometrical condition*, visibly satisfied in Fig. 39,

$$P_2 \cos\left(\theta_{\bar{l}+l^*}\right) + P_1 = 0, \tag{217}$$

where the two weights have to satisfied the condition

$$0 \leq \frac{P_1}{P_2} \leq 1. \tag{218}$$

In *CISM Lecture Notes No. 562*
"Extremely Deformable Structures" D. Bigoni
Ed. Springer, Wien–New York, 2015
ISBN 978-3-7091-1876-4 doi 10.1007/978-3-7091-1877-1

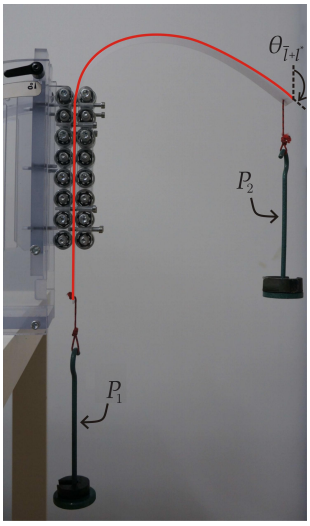

Figure 39. Example of use of the elastica arm scale when the sliding sleeve is in the vertical direction, $\alpha = 0$. The Eshelby-like force guarantees equilibrium of the elastic lamina subject to two loads $P_2 = 2\text{N}$ and $P_1 = 3\text{N}$, so that the angle $\theta_{\bar{l}+l^*}$ is equal to 131.81°.

7.1 Mode of use of the elastic scale

The following modes of use of the elastica arm scale can be envisaged.

- ◇ The easiest way to use the elastica arm scale is with reference to equation (213) and therefore measuring the two angles θ_0 and $\theta_{\bar{l}+l^*}$. In this way, assuming that P_1 and α are known, P_2 can be evaluated. Note that the knowledge of the bending stiffness B is not needed in this mode of use.
- ◇ Another mode of use of the elastica arm scale is through the measure of the length a_{eq}. Knowing P_1, B, and α, the weight P_2 can be determined in the following steps:
  - i) Equation $(215)_1$ gives θ_0;
  - ii) Equation (213) gives $\theta_{\bar{l}+l^*}$ as a function of the unknown P_2;
  - iii) Equation $(215)_2$ can be numerically solved for the unknown P_2.

Note that equations (215) define a_{eq} as a one-to-one function respectively of θ_0 (first equation) and of $\theta_{\bar{l}+l^*}$ (second equation), while equation (213) defines a unique relation between θ_0 and $\theta_{\bar{l}+l^*}$. Therefore, excluding all deformations of the elastica which would be unstable even for clamped ends,

In *CISM Lecture Notes No. 562*
"Extremely Deformable Structures" D. Bigoni
Ed. Springer, Wien–New York, 2015
ISBN 978-3-7091-1876-4 doi 10.1007/978-3-7091-1877-1

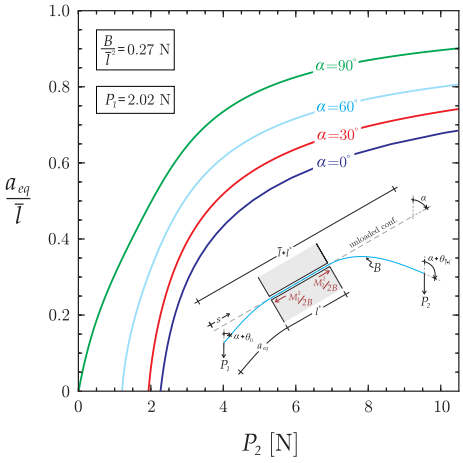

Figure 40. The elastica arm scale: equilibrium length a_{eq} versus weight P_2 for different inclinations $\alpha = \{0; 30; 60; 90\}°$. The values of the counterweight P_1 and the parameter $B/\bar{l}$ are the same adopted in the experiments reported by Bosi et al. (2014).

when the equilibrium solution of equations (215) and (213) exists, it is also unique.

The graph reported in Fig. 40 can be used in the second of the above-listed modes of use of the elastica arm scale to obtain the value of P_2 from the measured length a_{eq}. The inclination of the scale α can be adjusted to obtain a desired range of variation for the measured weight P_2 or sensitivity $\mathcal{S}$ (see Section 7.2). In fact, when α increases from 0° (vertical configuration) to 90° (horizontal configuration), the range of measure for the weight tends to increase, up to the case when all possible values of P_2 can be covered, namely $\alpha = 90°$.

7.2 Sensitivity analysis and comparisons between different scales

The performance of the elastica arm scale can be appreciated through a comparison with the steelyard (Fig. 37, left), a simple device still used nowadays. The comparison is performed through the sensitivity parameter $\mathcal{S}$, when the properties of the scales (inclination angle α, bending stiffness B, length $\bar{l}$) are varied.

Steelyard The steelyard is based on the principle of the lever with two rigid arms, so that it operates exactly as the second mode of use of the elastica arm scale, presented in Section 7.1. In this scale the equilibrium

In *CISM Lecture Notes No. 562*
"Extremely Deformable Structures" D. Bigoni
Ed. Springer, Wien–New York, 2015
ISBN 978-3-7091-1876-4 doi 10.1007/978-3-7091-1877-1

equation is guaranteed by the moment balance at the fulcrum

$$P_1 a_{eq} = P_2 \left(\bar{l} - a_{eq}\right), \tag{219}$$

where P_1 is the counterweight associated with the left arm of length a_{eq}, whereas P_2 represents the weight (to be measured) linked with the right arm of length $\bar{l} - a_{eq}$ (see also the scheme in Fig. 41). Therefore, also for the unequal balance, once the values of the counterweight P_1 and the total length of the two rigid arms $\bar{l}$ are fixed, after measuring the length a_{eq}, the value of unknown load P_2 can be obtained from the linear equation (219).

Sensitivity analysis The concept of sensitivity associated to scales allows to compare the precisions in weighing (Robens et al. (2014)). According to DIN/ISO, sensitivity is defined as the response of a measuring instrument, which may be an angle or a length, divided by the corresponding change in the stimulus, that is in our case the weight to be evaluated. For the considered scale, the sensitivity $\mathcal{S}$ is defined as the ratio between the observed variation of a_{eq} and the corresponding variation of the measured weight P_2 for a fixed value of the counterweight P_1,

$$\mathcal{S} = \frac{\partial a_{eq}}{\partial P_2}. \tag{220}$$

For the steelyard, taking into account the equilibrium equation (219), the sensitivity can be evaluated as

$$\mathcal{S}_{\text{steelyard}} = \frac{P_1 \bar{l}}{\left(P_1 + P_2\right)^2}, \tag{221}$$

while the sensitivity $\mathcal{S}$ of the elastica arm scale can be evaluated only numerically due to the non-linearity of the equilibrium equations (215) and (213).

Comparison between the steelyard and the elastica arm scale A comparison between the unequal arm balance and the elastica arm scale is reported in Fig. 41, where the equilibrium length a_{eq} as a function of the unknown weight P_2 is shown on the left, while the sensitivity $\mathcal{S}$, representing the tangent to the curve on the left, is shown on the right. From Fig. 41 (left), it can be noted that, while the steelyard can measure every value of the weight P_2, for the elastica arm scale there is a minimum value for the weight P_2 that can be measured, except in the case when the device is in the horizontal position ($\alpha = 90°$). On the other hand, the sensitivity

In *CISM Lecture Notes No. 562*
"Extremely Deformable Structures" D. Bigoni
Ed. Springer, Wien–New York, 2015
ISBN 978-3-7091-1876-4 doi 10.1007/978-3-7091-1877-1

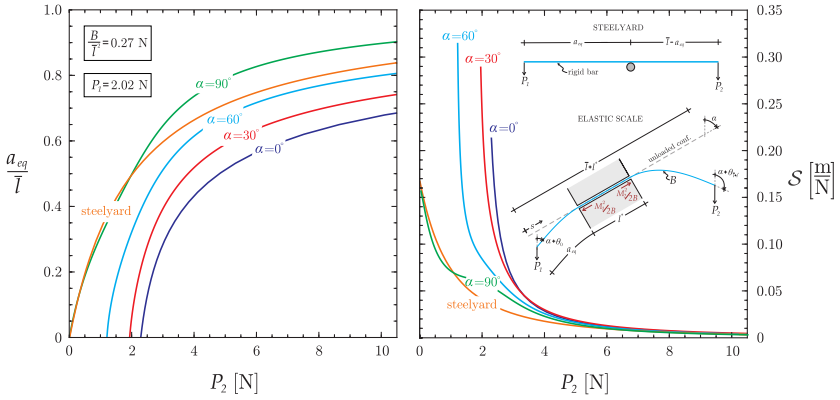

Figure 41. Comparison between the performances of a steelyard and of the elastica arm scale for different inclinations $\alpha = \{0°; 30°; 60°; 90°\}$: equilibrium length a_{eq} (left) and sensitivity $\mathcal{S}$ (right) are reported versus the weight to be measured P_2. The values of the counterweight P_1 and the parameter $B/\bar{l}^2$ have been assumed fixed and equal to the same values adopted in the experiments performed by Bosi et al. (2014).

analysis shows that the inclined elastica arm scale ($\alpha \neq 0$) can measure weights with a precision higher than that observed with the steelyard. In fact, once P_2 is fixed, the sensitivity $\mathcal{S}$ increases at increasing inclination towards the vertical configuration ($\alpha = 0°$), where possible effects due to friction are also considerably reduced.

Comparison between different elastica arm scales Finally, a comparison between elastica arm scales with two different values for $B/\bar{l}^2$ each with different inclinations α is shown in Fig. 42. The figure shows that a decrease (increase) in the parameter $B/\bar{l}^2$ leads to an increase (decrease) in both the range of measured weights P_2 and of sensitivity $\mathcal{S}$. Therefore, a more accurate device can be realized either by reducing the rod's bending stiffness (at fixed length $\bar{l}$) or by increasing the length $\bar{l}$ (at fixed bending stiffness B).

A proof-of-concept device showing how the elastica arm balance works was realized by Bosi et al. (2014), movies of the experiments can be found at http://ssmg.unitn.it/elasticscale.html.

7.3 A perspective view on configurational forces

Configurational or Eshelby-like forces emerge in a mechanical system when the possibility arises of a change in configuration with a consequent

In *CISM Lecture Notes No. 562*
"Extremely Deformable Structures" D. Bigoni
Ed. Springer, Wien–New York, 2015
ISBN 978-3-7091-1876-4 doi 10.1007/978-3-7091-1877-1

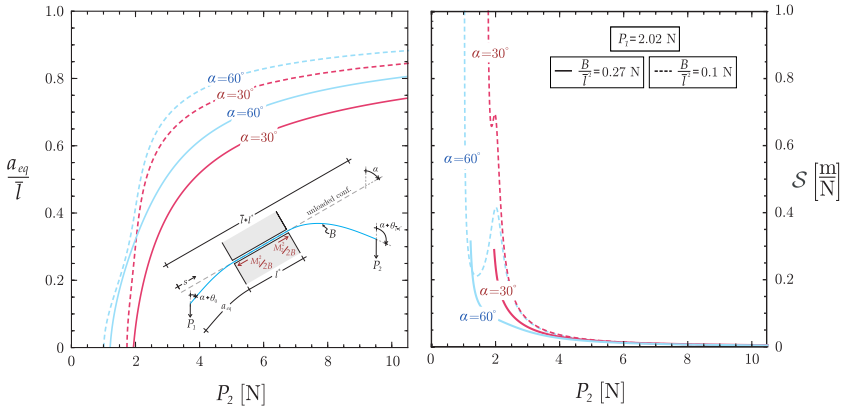

Figure 42. Comparison between two elastica arm scales differing in the parameter B/l^2 for two different inclinations $\alpha = \{30°; 60°\}$: equilibrium length a_{eq} (left) and sensitivity $\mathcal{S}$ (right) are reported versus the weight to be measured P_2.

release of elastic energy. These forces are therefore more widespread than the few simple structural examples shown above. For instance, configurational forces have been revealed under torsion (Bigoni et al., 2014c) and the same forces are responsible for snake locomotion; in fact the sliding sleeve used in the above structural systems can be viewed as a frictionless, narrow channel in which an elastic rod can move. Our results show that motion along this channel can be induced even when the applied forces are orthogonal to it, which is the essence of the locomotion strategy employed by a snake, which exploits lateral friction to generate a constraint (similar to the channel) and releases bending energy to generate a propulsive force, see Gray (1974), Gray and Lissmann (1950) and Gray (1953).

8 A concluding remark

The study of the Euler's planar elastica is useful from many points of view: it represents a nice introduction to the complex behaviour of nonlinear mechanical systems and provides an important tool in the design of flexible mechanisms such as in the emergent field of soft robotics. Indeed, we have used this tool to create elastic structures capable of displaying new mechanical behaviour, such as tensile instability, configurational forces, restabilization of the trivial path, and an innovative measuring device.

In a world where machines drive blind researchers along unknown and often false directions, our structures have been sketched on a piece of pa-

In *CISM Lecture Notes No. 562*
"Extremely Deformable Structures" D. Bigoni
Ed. Springer, Wien–New York, 2015
ISBN 978-3-7091-1876-4 doi 10.1007/978-3-7091-1877-1

per and solved usually by hand calculations, sometimes with the help of a numerical solver, before the development of experiments. The solutions have guided the design of prototypes capable of giving evidence to phenomena first discovered with the 'paper solution'. The evidence was usually so closely following predictions that we found our experiments loving our theory.

Acknowledgements Financial support of the FP7-PEOPLE-IDEAS-ERC-2013-ADG-340561-INSTABILITIES is gratefully acknowledged.

Bibliography

L.I. Balabukh, M.N. Vulfson, B.V. Mukoseev and Ya G. Panovko (1970). On work done by reaction forces of moving supports. *Research on Theory of Constructions*, Moscow. **18**, 190-200.

D. Bigoni and L. Deseri (2011). *Recent Progress in the Mechanics of Defects*. Springer.

D. Bigoni (2012). *Nonlinear Solid Mechanics. Bifurcation theory and material instability*. Cambridge University Press.

D. Bigoni, D. Misseroni, G. Noselli and D. Zaccaria (2012). Effects of the constraints curvature on structural instability. *Proc. Roy. Soc. A*, **468**, 2191-2209.

D. Bigoni, D. Misseroni, G. Noselli and D. Zaccaria (2014a) Surprising instabilities of simple elastic structures. In *Nonlinear Physical Systems - Spectral Analysis, Stability and Bifurcations, Kirillov, N. and Pelinovsky, D.E. Eds., Wiley*, 1-14; ISBN: 978-1-84821-420-0.

D. Bigoni, F. Bosi, F. Dal Corso and D. Misseroni (2014b). Instability of a penetrating blade. *J. Mech. Phys. Solids*, **64**, 411-425.

D. Bigoni, F. Dal Corso, D. Misseroni and F. Bosi (2014c). Torsional locomotion. *Proc. Roy. Soc. A*, **470** (2171), 20140599.

D. Bigoni, F. Dal Corso, F. Bosi and D. Misseroni (2015). Eshelby-like forces acting on elastic structures: theoretical and experimental proof. *Mech. Materials*, **80**, 368-374.

F. Bosi, D. Misseroni, F. Dal Corso and D. Bigoni (2014). An Elastica Arm Scale. *Proc. Roy. Soc. A*, **470** (2169), 20140232.

A. Broman (1970). *Introduction to Partial Differential Equations: From Fourier Series to Boundary-Value Problems*. Addison-Wesley, London.

P.F. Byrd and M.D. Friedman (1954). *Handbook of elliptic integrals for engineers and scientists*. Springer-Verlag, Berlin.

R. Courant and D. Hilbert (1962). *Methods of Mathematical Physics*. J. Wiley and Sons, New York.

In *CISM Lecture Notes No. 562*
"Extremely Deformable Structures" D. Bigoni
Ed. Springer, Wien–New York, 2015
ISBN 978-3-7091-1876-4 doi 10.1007/978-3-7091-1877-1

C. Dascalu, G.A. Maugin and C. Stolz (2010). *Defect and Material Mechanics*. Springer.

G. Domokos (1994). Global description of elastic bars. *Z. Angew. Math. Mech.*, **74**, T289-T291.

J.D. Eshelby (1956). The continuum theory of lattice defects. *Solid State Phys.*, **3** (C), 79-144.

V.I. Feodosyev (1977). *Selected Problems and Questions in Strength of Materials*. MIR, Moscow.

A. Gajewski and R. Palej (1974). Stability and shape optimization of an elastically clamped bar under tension (in Polish). *Rozprawy Inzynierskie - Engineering Transactions*, **22**, 265-279.

Gray, J. (1946) The mechanism of locomotion in snakes. J. Exp. Biol. 23, 101-120.

Gray, J. and Lissmann H.W. (1950) The kinetics of locomotion of the grass-snake. J. Exp. Biol. 26, 354-367.

Gray, J. (1953) How animals move. Cambridge University Press.

M.E. Gurtin. (2000). *Configurational forces as basic concept of continuum physics*. Springer.

K.A. Hoffman, R.S. Manning and R.C. Paffenroth (2002). Calculation of the stability index in parameter-dependent calculus of variations problems: buckling of a twisted elastic strut. *SIAM J. Appl. Dyn. Syst.*, **1** (1), 115-145.

R. Kienzler and G. Herrmann (2000). *Mechanics in Material Space*. Springer.

V.M. Kuznetsov and S.V. Levyakov (1999). Secondary loss of stability of an euler rod. *J. Appl. Mech. Tech. Phy.*, **40** (6), 1161-1162.

V.M. Kuznetsov and S.V. Levyakov (2002). Complete solution of the stability problem for elastica of Euler's column. *Int. J. Non-Linear Mech.*, **37** (6), 1003-1009.

H. Lamb (1928). *Statics*. Cambridge University Press.

S.V. Levyakov and V.M. Kuznetsov (2010). Stability analysis of planar equilibrium configurations of elastic rods subjected to end loads. *Acta Mech.*, **211**, 73-87.

A.E.H. Love (1927). *A treatise on the mathematical theory of elasticity*. Cambridge University Press.

J.H. Maddocks (1984). Stability of nonlinear elastic rods. *Arch. Rat. Mech. Analysis*, **85** (4), 311-354.

C. Majidi (2007). Remarks on formulating an adhesion problem using Euler's elastica. *Mech. Res. Comm.*, **34** (1), 85-90.

C. Majidi, O.M. O'Reilly and J.A. Williams (2012). On the stability of a rod adhering to a rigid surface: Shear-induced stable adhesion and the instability of peeling. *J. Mech. Phys. Solids*, **60** (5), 827-843.

In *CISM Lecture Notes No. 562*
"Extremely Deformable Structures" D. Bigoni
Ed. Springer, Wien–New York, 2015
ISBN 978-3-7091-1876-4 doi 10.1007/978-3-7091-1877-1

R.S. Manning, K.A. Rogers and J.H. Maddocks (1984). Isoperimetric conjugate points with application to the stability of DNA minicircles. *Proc. Roy. Soc. A*, **454** (1980), 3047-3074.

R.S. Manning (2009). Conjugate points revisited and Neumann-Neumann problems. *SIAM Review*, **51** (1), 193-212.

R.S. Manning (2014). A catalogue of stable equilibria of planar extensible or inextensible elastic rods for all possible dirichlet boundary conditions. *J. Elast.*, **115** (2), 105-130.

G.A. Maugin (1993). *Material Inhomogeneities in Elasticity*, Applied Mathematics and Mathematical Computation. Springer, London.

G.A. Maugin (2011). *Configurational forces: Thermodynamics, physics, mathematics and numerics*. Taylor and Francis Ltd, New York.

Y. Mikata (2007). Complete solution of elastica for a clamped-hinged beam, and its applications to a carbon nanotube. *Acta Mech.*, **190**, 133-150.

O.M. O'Reilly and D.M. Peters (2011). On Stability Analysis of Three Classical Buckling Problems for the Elastic Strut. *J. Elast.*, **105**, 117-136.

O.M. O'Reilly and D.M. Peters (2012). Nonlinear stability criteria for tree-like structures composed of branched elastic rods. *Proc. Roy. Soc. A*, **468**, 206-226.

M. Potier-Ferry (1987). Foundations of elastic postbuckling theory. *Buckling and Post-Bucklings*, Lecture Notes in Physics, Springer Berlin Heidelberg, **288**, 1-82.

E.L. Reiss (1969). Column buckling: An elementary example of bifurcation. *Bifurcation theory and nonlinear eigenvalue problems*. W.A. Benjamin Inc., New York, 1-16.

E. Robens, S.A.A. Jayaweera and S. Kiefer (2014). *Balances. Instruments, Manufacturers, History*. Springer Berlin Heidelberg.

J. Tarnai (1980). Destabilizing effect of additional restraint on elastic bar structures. *Int. J. Mech. Sci.*, **22** (6), 379-390.

N.M. Temme (1996). *Special functions*. John Wiley and Sons, New York.

S.P. Timoshenko and J.M. Gere (1961). *Theory of elastic stability*. McGraw-Hill, New York.

B. Van Brunt (2005). *The calculus of variations*. Springer.

M.A. Vaz and D.F.C. Silva (2003). Post-buckling analysis of slender elastic rods subjected to terminal forces. *Int. J. Nonlinear Mech.*, **38**, 483-492.

C.Y. Wang (1997). Post-buckling of a clamped-simply supported elastica. *Int. J. Nonlinear Mech.*, **32** (6), 1115-1122.

D. Zaccaria, D. Bigoni, G. Noselli and D. Misseroni (2011). Structures buckling under tensile dead load. *Proc. R. Soc.A*, **467**, 1686-1700.

H. Ziegler (1977). Principles of Structural Stability. *Birkhauser Verlag, Basel und Stuttgart*.